ZIKA VIRUS PATHOGENESIS AT SITES OF VECTOR-INDEPENDENT TRANSMISSION AND A FORAY INTO APPLIED SEROPREVALENCE

Cesar Augusto Lopez

A dissertation submitted to the faculty at the University of North Carolina at Chapel Hill in partial fulfillment of the requirements for the degree of Doctor of Philosophy in the Department of Microbiology & Immunology

Chapel Hill
2021

Approved by:

Helen M. Lazear

Aravinda M. de Silva

Stanley M. Lemon

Toni Darville

Ralph S. Baric

ABSTRACT

Cesar Augusto Lopez: Zika virus pathogenesis at sites of vector-independent transmission and a foray into applied seroprevalence
(Under the direction of Helen M. Lazear)

Zika virus (ZIKV) recently emerged in 2016 spread by mosquito-borne, sexual, and congenital transmission. During the course of this work, severe acute respiratory syndrome coronavirus 2 (SARS-CoV-2) also emerged and has been one of the most significant causes of mortality in 2020 as a result of the disease it causes, coronavirus disease 2019 (COVID-19).

Because ZIKV causes placental damage, I set out to establish in collaboration with Tulika Singh in Dr. Sallie Permar's laboratory whether antibody transfer is preserved during gestational ZIKV infection. I found that approximately half of our small 20-person cohort had serologic evidence of ZIKV infection during gestation and that ZIKV infection does not impair transfer of ZIKV and DENV-neutralizing antibodies. One individual had prolonged infection during gestation, and I showed that an IgM isolated from this individual potently neutralizes ZIKV and can protect mice from severe disease.

I also investigated ZIKV replication in the vagina of wild-type (WT) mice. Typically, ZIKV infections in the laboratory are performed in mice deficient in IFN-αβ signaling because these mice are permissive to disseminated infection following

inoculation by footpad. I found that ZIKV infection in the vagina is regulated by progesterone but not IFN-αβ signaling. I also found that progesterone-induced susceptibility to ZIKV is unlikely to be due to decreased epithelial integrity, changes in leukocyte numbers in vaginal tissue, or dampened antiviral signaling in the vagina.

Finally, I coordinated a multi-site effort to measure SARS-CoV-2 seroprevalence over a 6-month time frame. We found that Latinx and underinsured individuals were at greatest risk of infection. Also, SARS-CoV-2 neutralizing antibody titers for individuals without respiratory symptoms were lower than for those with symptoms or COVID-19 diagnosis, supporting that asymptomatic infections may result in lower neutralizing titers.

My results support that transplacental antibody transfer is not solely a result of placental damage. They also support that progesterone regulates some aspect of viral susceptibility independent of the interferon response. My results also emphasize that those at risk of systemic racism also may be at greatest risk of infection of emerging viruses that are driven by transmission in close quarters.

ACKNOWLEDGEMENTS

It was serendipity that I was seeking a mentor and laboratory to be my home for my PhD training at the same time that Helen Lazear was starting her laboratory. I thank her for taking a chance and taking me on before we even had a full set of pipettes. Her mentorship has been vital to my success and her patience when positive data were hard to come by allowed me to pursue science at its best with rigor and integrity. I wish all graduate students could have experienced as great of a mentor because there hasn't been a single moment where I've felt desperate to move on—it truly has been a great partnership. I am also thankful to my committee, Drs. Aravinda de Silva, Toni Darville, Stan Lemon, and Ralph Baric for their guidance. You've been incredible sources of information and the time you've taken to meet with me to discuss the myriad directions this project could have gone did not go unappreciated.

Many thanks also go to the members of the Lazear lab who have helped shape an amazing work environment from the ground up. In particular, I want to highlight Melissa Mattocks's amazing and irreplaceable skill in performing 20 jobs at the same time. I look forward to seeing where the students I've mentored go in their careers as well. Viren Baharani, with whom I worked the longest, has a bright future ahead of him.

The nature of science, particularly during outbreaks, requires excellent collaborators and to all of you I'm thankful.

A special thanks go to my friends, in particular my closest friends Carly, Osaki, Vincent for their encouragement, late night runs for tea and donuts, and mutual support.

Our friendships have persisted despite time and distance because you are truly special to me.

Most importantly, I'd never have gotten to where I am without my family. My parents have sacrificed on careers and even their homes for us. I hope we do them proud, because there is no material way to pay them back for everything they've done. My siblings Erik and Vanessa have been sources of brilliance, encouragement, and love. And finally, the greatest and most significant support in recent years has been my fiancée Samantha. You've been a grounding force for me when I've felt adrift and my love and gratitude for you is immeasurable.

Lastly, I want to recognize that this work was carried out on land of the Eno, Occaneechi, Shakori, and Sissipahaw peoples and is now occupied by the University of North Carolina at Chapel Hill.

TABLE OF CONTENTS

LIST OF FIGURES

LIST OF TABLES

LIST OF ABBREVIATIONS

ACE-2 – angiotensin converting enzyme 2

ADE – antibody dependent enhancement

BHM – Bayesian hierarchical model

CCR5 – C-C chemokine receptor 5

CI – confidence interval/credible interval

CMV – cytomegalovirus

COVID-19 – coronavirus disease of 2019

CP – convalescent plasma

CXCR4 – C-X-C chemokine receptor 4

CZS – congenital Zika syndrome

DENV – dengue virus

DI – domain I

DII – domain II

DIII – domain III

DMPA – depot medroxyprogesterone acetate

DNA – deoxyribonucleic acid

dpi – days post infection

E – envelope protein

ELISA – enzyme linked immunosorbent assay

EMR – electronic medical record

ER – endoplasmic reticulum

FBS – fetal bovine serum

FcRn – neonatal Fc receptor

Fc – fragment crystallizable

FFA – focus forming assay

FFU – focus forming unit

FRNT-50 – 50% focus reduction neutralization titer

H&E – hematoxylin and eosin

HAV – hepatitis A virus

HbO-HA – *Haemophilus influenzae* type B oligosaccharide-conjugated to human serum albumin

HIV-1 – human immunodeficiency virus-1

HSV – herpes simplex virus

ICD-10 – international classification of diseases 10^{th} revision

IFIT1 – Interferon-induced protein with tetratricopeptide repeats 1

IFN – interferon

IFNAR1 – interferon alpha receptor 1

IFNLR1 – interferon lambda receptor 1

IgA – immunoglobulin A

IgG – immunoglobulin G

IgM – immunoglobulin M

iLN – iliac lymph node

IRB – institutional review board

ISG – interferon stimulated gene

JEV – Japanese encephalitis virus

LFRT – lower female reproductive tract

M – membrane protein

MAC-ELISA – IgM antibody capture enzyme linked immunosorbent assay

MERS-CoV – Middle East respiratory syndrome coronavirus

MOI – multiplicity of infection

N – nucleocapsid protein

NK – natural killer cell

NTD – N terminal domain

OD – optical density

PBMC – peripheral blood mononuclear cell

PCR – polymerase chain reaction

pI:C – polyinosinic:polycytidylic acid

PIV – penis-in-vagina

pr – precursor protein

prM – precursor membrane protein

PRR – pattern recognition receptor

RBD – receptor binding domain

RNA – ribonucleic acid

RT-PCR – reverse transcription polymerase chain reaction

RUBV – rubella virus

S – spike protein

SARS-CoV – severe acute respiratory syndrome coronavirus

SARS-CoV-2 – severe acute respiratory syndrome coronavirus 2

SPOV – Spondweni virus

STAT2 – signal transducer and activator of transcription 2

STING – stimulator of interferon genes

TB –tuberculosis

TORCH – *Toxoplasmosis,* other, rubella, cytomegalovirus, herpes simplex/human immunodeficiency virus

UFRT – upper female reproductive tract

USUV – Usutu virus

UV – ultraviolet

VDRL – venereal disease research laboratory test

WHO – World Health Organization

WT – wild-type

ZIKV – Zika virus

CHAPTER 1 – INTRODUCTION

1.1 Summary

Flaviviruses are significant causes of human disease. Most recently, Zika virus (ZIKV) has emerged in areas that were already endemic for the related flavivirus dengue virus (DENV). Uniquely among flaviviruses, ZIKV can be transmitted sexually and congenitally in addition to the more typical arthropod-borne transmission. During the course of this work, severe acute respiratory syndrome coronavirus 2 (SARS-CoV-2) also emerged and has been one of the most significant causes of mortality in 2020 despite having only emerged a little over a year ago.

1.2 Zika virus emergence

Prior to 2014, ZIKV was one of many arboviruses poised for broader emergence known only to cause little more than mild febrile illness[1–5]. ZIKV had previously only caused sporadic infections within the geographic range of the *Aedes aegypti* mosquito vector it shares with related flaviviruses such as DENV and Spondweni virus (SPOV). But in 2013-2014 ZIKV began to emerge as a cause of serious human disease when it caused an increase in acute ascending paralysis cases that were consistent with Guillain-Barre syndrome observed in an outbreak in French Polynesia[6,7].

ZIKV emerged within the next two years in a massive outbreak across the Americas with almost 600,000 clinically suspected cases although it has been estimated that millions were infected[8–10]. The Latin American ZIKV pandemic revealed that ZIKV

infection during pregnancy could cause microcephaly, arthrogryposis, intrauterine growth restriction and other congenital defects now established to be caused by congenital ZIKV infection[11–13]. ZIKV also caused increased rates of Guillain-Barre syndrome in Latin America during this outbreak[14]. This outbreak also confirmed the ability of ZIKV to spread via sexual transmission in addition to mosquito-borne transmission, although one case of ZIKV sexual transmission had been reported previously following infection in Africa indicating that sexual transmission was not a new property of ZIKV[15–19].

1.3 ZIKV Antibody response

Myeloid cells are an important target for flavivirus infection[20–22]. Flavivirus proteins are first translated as a single polyprotein in replication centers on the endoplasmic reticulum (ER)[23,24]. This polyprotein contains multiple transmembrane regions, and is cleaved into different proteins by both host and viral proteases[25]. The envelope protein (E) is cleaved from the membrane protein (M) by host signal peptidase but remains membrane-anchored. The E protein forms the surface of the virus once viral RNA protected by capsid proteins bud into the ER. Most enveloped viruses do not have regular icosahedral symmetry, as proteins embedded in the envelope are usually fewer in number and able to diffuse laterally within the membrane. However, the surface of flaviviruses consists of 180 interlocking E proteins forming 90 dimers in a herringbone pattern embedded in the membrane derived from the ER[24,26]. The flavivirus precursor membrane (prM) protein protects the fusion loop present on the E protein, preventing its insertion into membranes during virion assembly. The pr peptide is cleaved from M by host furin enzymes during virion maturation but this cleavage process is thought to be

inefficient in cell culture, leaving a mixture of particles that are mostly mature with E proteins ready to rearrange and expose the fusion loop following a low pH trigger, and particles that are only partially mature and have the fusion loop protected by pr. However, recent evidence from DENV isolated from patient sera suggests that though DENV grown in the laboratory is a mix of mature and immature particles, DENV particles in humans are mostly mature[27]. The presence of the pr peptide affects antibody binding and therefore can affect neutralization, antibody dependent enhancement of infection (ADE), and protection from disease.

Flavivirus infections, including ZIKV, induce a potent neutralizing antibody response targeting the E protein. The E protein is divided into Domains I, II, and III (DI, DII, DIII). The fusion loop on one E protein is located at the tip of DII near DIII of its paired E protein (Figure 1.1). The lateral ridge of DIII is thought to be important for cellular attachment[28,29]. Antibodies to the fusion loop are commonly isolated after infection, and the high degree of conservation in the fusion loop region between flaviviruses means that these antibodies are likely to cross-react among viruses[30–34]. Some of the most potently neutralizing human antibodies against ZIKV target either the lateral ridge of DIII[34–37] or across E proteins within or between 2-3 dimers[38,39]. No human antibodies targeting the pr peptide on the surface of the ZIKV particle have been reported.

1.4 Flavivirus antibody cross-reactivity & enhancement of infection

Flaviviruses have historically been classified into serogroups, such that if immune sera raised against one virus neutralizes another virus they were placed into the same serogroup[40–42]. This cross-neutralization is due to extensive antigenic cross-reactivity

between flaviviruses. One of the greatest diagnostic challenges during the 2015-2016 ZIKV pandemic was the high degree of antibody cross-reactivity between the newly introduced ZIKV and DENV, which was already endemic to the Americas. In some regions, by age 18 over 95% of individuals had serologic evidence of prior DENV infection[43]. ZIKV and mild DENV infections are difficult to distinguish clinically, and the antibody response to the two is highly cross-reactive due in large part to conserved regions near the flavivirus fusion loop. ZIKV is in the same serogroup as Spondweni virus (SPOV) separate from DENV so these cross-reactive antibodies have only limited cross-neutralizing activity in cell culture and do not appear to provide long-term protection against the other virus. Similarly, prior infection with one of the four viruses within the DENV serogroup does not confer protective immunity to the other three, but does generate cross-reactive non-neutralizing antibodies. These cross-reactive antibodies bind to virions from another DENV serotype and facilitate DENV infection of myeloid cells via Fcγ receptors, a process termed antibody-dependent enhancement (ADE). ADE results in higher viremia and increased risk of severe dengue, including hemorrhagic fever and shock. Antibodies can worsen disease caused by various viruses due to immunopathology[44–46], but in the case of DENV, the worsened disease is thought to result from increased viral replication. It is possible to demonstrate ADE in cell culture with a wide variety of viruses from different families[47–52], but in humans, only with DENV is enhancement of viral infection demonstrated to be directly associated with worsened disease[53].

Given the established role of cross-reactive non-neutralizing antibodies exacerbating DENV disease via ADE, at the beginning of the ZIKV pandemic it was a

reasonable hypothesis that ZIKV infection might be enhanced by cross-reactive DENV antibodies. Other flaviviruses are easily enhanced in cell culture[54–56] and in mice[57] by cross-reactive antibodies from heterologous flaviviruses, or even by neutralizing antibodies that are sufficiently diluted. Thus it is no surprise that ZIKV infection also can be enhanced by sera and antibodies from heterologous flaviviruses in laboratory assays[58]. Likewise, heterologous cross-reactive antibodies worsen ZIKV-induced fetal pathology in mice[59]. There however remains no evidence to date that any flavivirus besides DENV undergoes ADE of infection in primates. If anything, cross-reactive antibodies may offer transient cross-protection soon after infection[60] though despite the high seroprevalence of DENV in communities affected in the 2015-2016 ZIKV epidemic[43,61], this cross-protection was clearly not sufficient to prevent the high force of ZIKV infection. Consistent with the hypothesis that DENV is uniquely capable of antibody-enhanced infection in primates, prior ZIKV exposure elevates risk of severe DENV[62].

1.5 ZIKV placental pathology

The 2015-2016 Latin American ZIKV outbreak was large enough to observe rare outcomes including congenital infection. The types of pathogens capable of causing congenital disease in humans varies widely (viruses, bacteria, and parasites), but only a select few pathogens are able to do so. The types of congenital disease they can cause and the mechanism by which they cause disease can be the result of direct infection of the fetus, as is the case with *Toxoplasma gondii*, which can cause brain calcifications in the developing fetus. Others, like *Plasmodium falciparum*, cause intrauterine growth restriction by causing placental insufficiency.

Though ZIKV is the first arbovirus demonstrated to cause significant congenital disease in humans, it is not the only one capable of congenital infection in mammals. Among bunyaviruses, the mosquito-borne Rift Valley fever virus and midge-borne Schmallenberg virus cause spontaneous abortions in ruminants[63,64], and the flavivirus Japanese encephalitis virus (JEV) can cause abortions in swine[65]. In humans, there have been isolated cases of spontaneous abortion following JEV infection[66] and congenital defects following West Nile virus (WNV) infection[67] but these do not appear to be common outcomes of JEV or WNV infection.

Gestational DENV infection may also be associated with elevated maternal mortality, pregnancy complications, premature birth, and low infant birth weight [68–72], but these adverse outcomes may result from the severity of DENV infection on the mother, such as inflammatory responses and cytokine storm. ZIKV not only causes intrauterine growth restriction, but also is neurotropic within the developing fetus even if the mother only has mild or no symptoms. ZIKV infection of neural progenitor cells can result in microcephaly, lissencephaly, arthrogryposis, cortical atrophy, sensorineural hearing loss, and ocular defects[13,73–79]. In the years that come, we may also come to find that congenital ZIKV infection affects development after gestation resulting in other long term cognitive deficits that have not been characterized. ZIKV infection in pregnancy can result in prolonged viremia, suggesting that the placenta may be an active site of viral replication and seeding virus back into circulation within the infected gestational parent[78,80–82]. The placenta is an organ that develops during pregnancy from fetal cells and anchors into the uterine wall with cytotrophoblast cells extending from placental villi. These villi are bathed in blood originating from endometrial arteries. It is across these

villi that oxygen and macromolecule exchange such as transplacental IgG transfer occurs, providing the fetus with passive immune protection that persists for a few months after delivery[83–87]. These villi consist of cytotrophoblasts and a multinucleated syncytiotrophoblast layer that is resistant to infection by all pathogens tested[88–90]. The syncytiotrophoblasts are also the site of transplacental IgG transfer via the neonatal Fc receptor (FcRn)[91]. This transfer occurs after binding of IgG to FcRn in acidified endosomes, where it is rerouted from degradative pathways and released at the basolateral membrane. Hofbauer cells, specialized placental macrophages, also are present within the villi and aid the development of vasculature as well as serving as a second line of immune surveillance past the syncytiotrophoblasts[92–95].

ZIKV infects cells within the placenta such as Hofbauer macrophages and villous trophoblasts and thus infects the placenta itself [74,96–98]. Placental damage such as necrosis, calcifications, fibrosis, and Hofbauer cell hyperplasia have been observed after gestational ZIKV infection in humans[74,97,98]. It seems likely that the placental damage observed during ZIKV infection results from infected placental cell types as well as inflammatory immunopathology mediated by antiviral interferon (IFN) signaling[99,100]. Damage to the likely derives from multiple factors such as ZIKV infection of fetal neurons, virus-induced immunopathology, and placental insufficiency resulting from ZIKV damage to the placenta[101,102].

The placental pathology associated with congenial ZIKV infection (e.g. calcification, inflammation, and hypoxia) also is associated with gestational malaria[103–106]. Vascular changes to the placenta during gestational malaria are thought to result in hypoxia, and also result in hampered transplacental transfer of IgG from mother to fetus

during gestation[107–109]. Human immunodeficiency virus 1 (HIV-1) is also thought to impair transplacental IgG transfer, though the mechanism is poorly understood[110,111]. IgG transferred to the fetus during gestation are critical for neonatal health, and thus it was important to determine whether ZIKV similarly decreases transplacental IgG transfer like malaria or if like DENV it does not affect IgG transfer[112,113]. This serious knowledge gap was something I sought to tackle in my research.

1.7 ZIKV infection in reproductive tracts

Most sexually transmitted ZIKV cases appear to be unidirectional following penis-in-vagina (PIV) sex, presumably after exposure to infectious seminal fluids from a penetrative partner who recently returned from a region with an active outbreak. However, there are isolated cases implicating oral sex[114], anal sex[115], or where the source of infectious virus was vaginal mucus or menstrual blood[116]. Mouse models have also demonstrated that an infected male can infect a female, but the opposite did not occur[117]. The testes are the site of spermatogenesis and can become productively infected by ZIKV in animal models and human explants[118–123], and sperm cells themselves may contain ZIKV antigens[124]. However, viral shedding in semen and sexual transmission have also been reported from vasectomized individuals[16,125,126] and has been confirmed in animal models[117], indicating that the testes are not the sole source of ZIKV in semen. Accessory glands in the male reproductive tract potentially could be other sources of ZIKV in semen and ZIKV infection of the prostate been observed in animal models and human explants[122,127].

Following ejaculation, ZIKV is thought to infect a variety of cells in the vagina including epithelial and immune cells[128,129]. From here, the virus is able to disseminate

and cause viremia, producing similar symptoms as mosquito-borne transmission[130], including congenital Zika syndrome[131]. In non-human primates, vaginal infection can also result in viremia and fetal transmission[132,133].

In mice deficient in type I interferon (IFN-αβ) signaling, ZIKV inoculated into the vagina disseminates through the entire mouse similar to infection via footpad inoculation[129,134,135]. This infection can then result in fetal pathology in pregnant mice[99,135,136], though there is strong evidence that fetal pathology is also driven by immunopathology[99,137,138]. There is also a report of fetal pathology and possible viral transmission to fetuses in wild-type mice resulting from vaginal inoculation, despite the lack of systemic infection[135]. This suggests the possibility for ascending infection that bypasses the placenta entirely. The related flavivirus SPOV can only be found rarely in the semen of infected mice, and can also cause fetal pathology[139,140]. Nonetheless, surveillance of SPOV should consider the possibility that it could also be sexually transmitted in humans

Of note, studies evaluating ZIKV pathogenesis are typically performed in mice deficient in IFN-αβ signaling because these mice are permissive to disseminated infection following inoculation by footpad[134]. In wild-type mice, ZIKV inoculated via footpad does not cause disease or more than a very transient viremia. This is because ZIKV is able to inhibit and target STAT2 in humans but not murine STAT2[141], preventing IFN-αβ signaling in infected cells. These same mice are the ones typically used in vaginal infection models.

1.8 Antiviral mechanisms in the vagina

The vagina is a unique tissue that has to respond to sexually transmitted pathogens while also maintaining a degree of immune homeostasis so as to not mount a pathologic immune response against its own microbiome, microabrasions resulting from sexual intercourse, or foreign antigens in the form of sperm and semen.

The mucosal environment of the vagina contains specialized immune mechanisms not typically encountered by mosquito-borne viruses. One example of this is interactions with mucins, which are large molecular weight proteins covered in glycosylations [142,143]. IgG is secreted into vaginal mucus from the systemic circulation and is the predominant immunoglobulin in the vagina[144–147]. Individual IgG molecules bind to mucins only transiently and with low affinity[148–151]. However, IgG-opsonized particles can be immobilized by the additive effects of multiple IgG-mucin interactions[152]. This immobilizing activity of IgG is independent of virus neutralization, meaning that the particles can remain infectious but are physically trapped in mucus and prevented from accessing host cells. By this mechanism, non-neutralizing antibodies can contribute to protection against viruses in the vagina[153].

Innate immune cells present in the vagina that contribute to defense against pathogens include dendritic cells, natural killer (NK) cells, and neutrophils[154]. Neutrophils and NK cells in particular have been highlighted for their roles in responding to herpes simplex virus (HSV) infections[155–157]. T cells outnumber B cells as the adaptive immune cells in the vagina[158], but ZIKV-specific IgG are thought to be the predominant adaptive immune mechanism by which the vagina is protected from a second ZIKV infection in mice[159]. Prior to the emergence of ZIKV there was little reason

to study the immune cells that respond to arbovirus infections in the vagina, so little is known about the role they play on the first ZIKV infection.

Like at many other barrier sites, antiviral signaling in the vagina includes a role for type III interferons (IFN-λ) in addition to IFN-αβ and type II IFN (IFN-γ) involved in systemic antiviral responses[160]. IFN-λ signals through different receptors on the cell surface but activates many of the same signaling pathways and transcriptional programs as IFN-αβ. Despite the similarities, IFN-λ can also perform unique restriction of viruses independent of other IFN signaling pathways[161]. IFN-λ restricts HSV infection in the vagina[162] and may also play a role in restricting ZIKV infection in the vagina of ovariectomized mice, a model where the hormonal state is tightly controlled by hormone replacement[129].

1.9 Hormonal control of antiviral state in the vagina

Antiviral mechanisms within the vagina are under control of hormones such as sex hormones. In place of the 4-week-long menstrual cycle in humans, mice instead have an estrous cycle that lasts 4-5 days. In mice the longest phase of the estrous cycle is diestrus, characterized by high levels of progesterone and low levels of estrogen[163–165]. Estrogen rises thereafter, resulting in ovulation and bringing mice from proestrus to estrus where estrogen levels decline while progesterone remains low. The estrus phase is also when mice are sexually receptive. Estrus gives way to metestrus as progesterone begins to rise, and estrogen continues to trend downwards. Diestrus occurs once estrogen is again at its lowest.

The quality of vaginal mucus changes throughout different stages of the human menstrual cycle and murine estrous cycle or following treatment with sex hormones.

These changes include the concentration of secreted antibodies[166–170]. Vaginal epithelium is thicker at hormonal stages where progesterone is low [128,171–173]. Neutrophils are increased in the vagina when estrogen signaling is low as in diestrus in mice, or when estrogen signaling is disrupted[172]. Likewise, the vaginal epithelium also becomes more permeable to immune cells and microbiota following administration of exogenous progesterone[172], though the relative numbers of immune cells in the vagina might not change in the absence of disease or infection.

Regardless, exogenous progesterone may induce local changes to leukocytes already present in the vagina which may increase HIV infection risk by increasing expression of HIV coreceptors, CXCR4 and CCR5[174–176]. Exogenous progesterone treatment is also a required component of HSV and *Chlamydia* murine infection models and is required for the inflammation observed in response to these pathogens[177,178]. The precise mechanism by which progesterone is required for these infection models remains unknown but it may be due to a combination of thinned epithelium, increased permeability, and increased inflammatory infiltrate. Systemically, progesterone may also skew the immune response away from a Th1 type response and towards a Th2 response[179–181].

Non-pregnant mouse models for vaginal ZIKV infection tend to all treat with progesterone, following in the footsteps of HSV and *Chlamydia* infection models[128,135,159,170,177,178,182,183]. Tang et al. showed that after treatment with exogenous hormones, ZIKV preferentially infects mice in diestrus-like phase compared to an estrus-like phase[128]. Similarly, Caine et al. demonstrated that exogenous estradiol in ovariectomized mice is sufficient to protect even *Ifnar1*$^{-/-}$ mice from vaginal infection[129].

Khan et al. have speculated that as with HSV, the susceptibility of progesterone-treated mice to vaginal ZIKV infection may be the result of thinned epithelium[183]. They also find potentially small decreases in RNA virus pattern recognition receptors in the lower reproductive tract (cervix and vagina) at baseline, and speculate that this may be the reason vaginal infection with ZIKV is possible even in wild-type mice that are typically not susceptible to ZIKV infection. However, this does not explain why progesterone is required for ZIKV infection in the vagina, which I chose to study.

1.10 SARS-CoV-2 Emergence

Emerging viral infections continue to be a present and future threat. ZIKV was not the only viral infection to emerge and cause a pandemic during the course of this dissertation research. A cluster of pneumonia cases identified and reported to the WHO in late December 2019 in Hubei province in China was publicly identified weeks later as being caused by a novel β-coronavirus, severe acute respiratory syndrome coronavirus 2 or SARS-CoV-2[184–186]. Like other β-coronaviruses that have caused recent outbreaks of human disease, SARS-CoV-2 emerged as a zoonosis, though the details remain unclear[187,188]. The most similar sequenced viruses have been identified from horseshoe bats[185,189], and there has been speculation that pangolins served as intermediate hosts[190].

Aggressive containment measures in China were instituted too late after the outbreak had already spread among the population of Hubei. As of March 31, 2021, nearly 3 million deaths have resulted from almost 130 million cases around the globe[191]. The earliest virologically confirmed case in the United States presented in mid-January in Seattle, Washington and resulted in significant community transmission[192193]. Though

later it was revealed that there were likely multiple initial introductions of SARS-CoV-2 into the United States[194].

Deaths from coronavirus disease 2019 (COVID-19), the disease caused by SARS-CoV-2, largely result from respiratory disease and inappropriate vascular coagulation following infection of epithelial cells and endothelial cells in the lungs and vasculature[195]. Mortality is strongly associated with age and various comorbidities[196,197]. Additionally, the burden of COVID-19 mortality in the United States has been amplified by systemic racism[198]. For example, COVID-19 case and hospitalization rates among Black, Latinx and Indigenous populations in the US are 2.5-4.5 times higher than those in white populations[199].

1.11 SARS-CoV-2 Antibody response

Like flaviviruses, coronaviruses are enveloped positive-sense RNA viruses, though coronavirus genomes are substantially larger (~30kb compared to ~10kb for flaviviruses). Coronaviruses replicate in vesicles associated with the ER and then bud into the Golgi complex and ER-Golgi intermediate compartments, encasing the genome bound to nucleocapsid proteins (N)[200,201]. Budding requires the interaction of both the transmembrane proteins membrane (M) and envelope (E)[202]. Roughly 25 homotrimers of spike (S) proteins stud the surface of each viral particle[203–205]. The S protein is cleaved into two subunits, S1 and S2. S1 contains the receptor binding domain (RBD), which lies flat on top of the trimer and only flips upwards to expose the receptor binding site to engage with the entry receptor (ACE2 in the case of SARS-CoV-2)[206,207].

β-coronavirus infections can induce antibodies against all of these structural proteins, though antibodies to M and E are far fewer and less important[208]. There may

be some cross-reactivity between antibodies targeting N of SARS-CoV-2 and SARS-CoV, and N-binding antibodies may not correlate as well as S- or RBD-binding antibodies with potent neutralization titers[185,209]. S-targeting antibodies dominate the neutralizing antibody response for the other two most recently emerged β-coronaviruses, SARS-CoV and Middle East respiratory syndrome coronavirus (MERS-CoV)[210–212]. In particular, the RBD appears to be a vulnerable target for protective neutralizing antibodies and thus also is the target of therapeutic antibodies and vaccine immunogens[213]. The duration of protective immunity to these recently emerged β-coronaviruses remains unknown. SARS-CoV antibody titers may decay after 2-3 years[214,215]. For SARS-CoV-2, for at least 8 months after symptomatic infection there still appear to be substantial amounts of neutralizing antibodies with only a small amount of decay as expected for convalescence[216]. Of note, mild infections may result in lower SARS-CoV-2 antibody titers and conversely, severe disease correlates with increased antibody titers[217].

1.12 SARS-CoV-2 prevalence

Due to factors including asymptomatic spread, disparities in healthcare access, and bottlenecks in diagnostic testing, there have been substantial issues obtaining accurate counts of SARS-CoV-2 infections. Knowing the true number of infections is essential to understanding rates of morbidity and mortality, the role of asymptomatic transmission, the effect of public health interventions, and differences in burden of disease among demographic groups. Serological testing offers a complementary method to PCR testing for evaluating the spread of SARS-CoV-2 and can be deployed efficiently at the population level[218]. Most seroprevalence studies employ an assay that

detects N-targeting IgG developed for diagnosing symptomatic infections in clinical practice. As a result, N-based assays may have decreased sensitivity among mild or subclinical infections[219,220].

Immediately in the wake of the first outbreaks in China, Iran, France, and Italy, SARS-CoV-2 seroprevalence ranged from as low as 7% in Milan, Italy up to almost 26% in Oise, France[221–224]. In New York City, seroprevalence may have been as high as 20% following the initial outbreak in Spring 2020[225]. There is significant regional variation in seroprevalence estimates in the United States, because many outbreaks have been localized as well as the above discussed limitations. In North Carolina, Barzin et al found an estimated seroprevalence of 0.7 – 0.8%, and another study of 177,919 remnant clinical laboratory samples from routine screening (3,817 from NC) from July 27-September 24, 2020 found an estimated seroprevalence of 2.5 – 6.8%[226,227]. Many seroprevalence studies are limited by sampling methodology that is not reflective of the general population[228]. Additionally, although serologic tests have imperfect sensitivity and specificity, few studies have incorporated this assay uncertainty into the subsequent analysis and propagated that uncertainty through the estimated seroprevalence. An example of propagating assay uncertainty into seroprevalence analysis is an estimate from Switzerland using a state-of-the-art Bayesian inference model[229]. Briefly, a Bayesian inference framework assumes that (1) the probability that a particular seroprevalence is true given the validation and study data is proportional to (2) the validation and study data given a particular seroprevalence[230–232]. The most likely seroprevalence estimates that fit the data can then be determined by algorithmically sampling numbers to form probability distributions

of the most likely seroprevalence, sensitivity, and specificity. However, this more rigorous analysis is more complex than other methods that simply approximate seroprevalence by subtracting the false positive rate and adding a false negative rate, an equation referred to as the Rogan-Gladen estimate for seroprevalence[226,233]. These approaches are required because at low seroprevalence (such as SARS-CoV-2 early in this outbreak), false positives can comprise a high proportion of the small number of positive samples, thus overestimating seroprevalence unless adjusted for false positives. The opposite is true at high seroprevalence (as is the case for DENV or ZIKV in Latin America), where false negatives comprise a high proportion of the small number of negative samples.

Morbidity, mortality, and case rates disproportionately affect Black, Latinx, and Indigenous populations in the United States[198,199,234]. In addition, structural and occupational factors previously identified as drivers of race and ethnic disparities in health and COVID-19 include unequal labor market opportunities and higher representation in essential work positions that lack job security, access to infection prevention control, benefits, and sick leave[235–240].

1.13 Conclusions & Objectives

Flaviviruses that cause human disease are typically arthropod-borne and induce potent antibody responses after natural infection and vaccination. The degree of cross-reactivity between the newly emerged ZIKV and the related flavivirus DENV complicated serodiagnostics during the 2015-2016 outbreak. Despite the significant number of flaviviruses that cause human disease and long history of flavivirus research, the new and unanticipated clinical outcomes and transmission mechanisms for ZIKV

mean that significant questions are still left unanswered. The placental pathology observed in ZIKV disease is similar to that observed for other congenital infections. Because these other congenital infections cause decreased antibody transfer presumably via placental damage, we investigated whether ZIKV similarly impairs transplacental antibody transfer during gestational ZIKV infection. This investigation into ZIKV and DENV cross-reactive antibody transfer further led to questions in whether antibodies play a role in prevention of vaginal ZIKV infection, because there also remain many questions in whether antiviral mechanisms in the vagina may also protect against flaviviruses. In the course of investigating these mechanisms in non-immunocompromised mice thought to be less susceptible to ZIKV infections, it became apparent that ZIKV susceptibility in the vagina may be different than systemic susceptibility and is regulated by the sex hormone progesterone. Further defining the mechanism by which progesterone regulates susceptibility to ZIKV infection may have implications for other flaviviruses that may also be sexually transmitted but have not yet emerged as significant human pathogens, such as SPOV.

While conducting these investigations into the emerging ZIKV, another virus, SARS-CoV-2, emerged and became one of the most common causes of death in 2020. The expertise gained in antibody responses to viruses was leveraged to study the rate of SARS-CoV-2 seropositivity in central North Carolina. Previously published estimates have focused on asymptomatic infections using an assay that may not be sensitive for capturing asymptomatic or subclinical infections, and also suffer from undersampling of populations hardest struck by the SARS-CoV-2 pandemic.

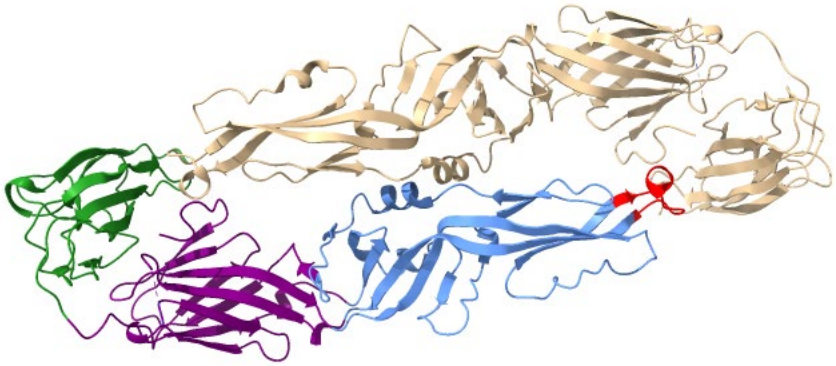

Figure 1.1 Zika virus E dimer structure. Two ZIKV E proteins in complex, PDB# 5JHM[33]. Note the multicolored E protein antiparallel to the E protein in gold. Purple=DI, blue =DII, green=DIII, red=fusion loop.

CHAPTER 2 – GESTATIONAL ZIKV DOES NOT AFFECT TRANSPLACENTAL TRANSFER OF IGG[1]

2.1 Summary

Zika virus (ZIKV) is a newly-identified infectious cause of congenital disease. Transplacental transfer of maternal IgG to the fetus plays an important role in preventing many neonatal infections. However, antibody transfer can also have negative consequences, such as mediating enhancement of dengue virus (DENV) infections in early life, or trafficking of virus immune complexes to the fetal compartment. ZIKV infection produces placental pathology which could lead to impaired IgG transfer efficiency as occurs in other maternal infections, such as HIV-1 and malaria. In this study, we investigated whether ZIKV infection in the gestational parent during pregnancy impairs transplacental transfer of IgG. We enrolled pregnant individuals with fever or rash in a prospective cohort in Vitoria, Brazil during the recent ZIKV epidemic. ZIKV- and DENV-specific IgG, ZIKV and DENV neutralizing antibodies, and routine vaccine antigen-specific IgG were measured in gestational parental samples collected around delivery and in 20 paired cord blood samples. We concluded

[1]The work presented in this chapter has been published as either Collins MH, McGowan E, Jadi R, Young E, Lopez CA, Baric RS, Lazear HM, de Silva AM. Lack of Durable Cross-Neutralizing Antibodies Against Zika Virus from Dengue Virus Infection. Emerg Infect Dis 2017; 23: 773–81 or as Singh T, Lopez CA, Giuberti C, Dennis ML, Itell HL, Heimsath HJ, Webster HS, Roark HK, Merçon de Vargas PR, Hall A, Corey RG, Swamy GK, Dietze R, Lazear HM, Permar SR. Efficient transplacental IgG transfer in women infected with Zika virus during pregnancy. PLoS Negl Trop Dis 2019; 13: e0007648. I performed all mouse infection experiments, virus purification and preparation, neutralization assays, sample categorization, and ZIKV qRT-PCR assays on placental samples.

that 8 of these individuals had a history of ZIKV infection and 12 were ZIKV-uninfected. The magnitude of flavivirus-specific IgG, neutralizing antibody, and vaccine-elicited IgG were highly correlated between gestational parent and infant cord blood plasma in both ZIKV-infected and -uninfected pregnancies. Moreover, there was no difference in the magnitude of flavivirus-specific IgG levels in plasma between gestational parent/infant dyads regardless of ZIKV infection status. Our data suggests that ZIKV infection in the gestational parent during pregnancy does not impair the efficiency of transplacental transfer of flavivirus-specific, functional, or vaccine-elicited IgG. These findings have implications for the neonatal outcomes of ZIKV infection in gestational parents during pregnancy and optimal administration of antibody-based ZIKV vaccines and therapeutics.

2.2 Introduction

The emergence of Zika virus (ZIKV) in the Americas in 2015 revealed that ZIKV could be congenitally transmitted and cause fetal neurological damage[11,75,241]. Neurodevelopmental defects associated with congenital Zika syndrome (CZS) include microcephaly, arthrogryposis, motor and cognitive impairment, as well as vision and hearing loss[12]. ZIKV is the first example of a teratogenic vector-borne disease in humans. Initial estimates during the epidemic detected a 42% rate of fetal or neonatal abnormalities in symptomatic ZIKV-infected pregnant individuals[75]. A recent meta-analysis estimated that after adjusting for the baseline rate of all-cause congenital disease, 13% of first trimester ZIKV infections result in congenital disease, with risk decreasing later in gestation[242]. ZIKV is likely to be a re-emerging and ongoing cause of congenital infections.

Transplacental transfer of IgG during pregnancy provides passive immunity to the fetus and is critical to protecting newborns against infections[83]. Immunization during pregnancy can boost levels of protective IgG transferred to the fetus, providing a valuable tool for reducing neonatal morbidity. For example, tetanus immunization of pregnant individuals, or those that could become pregnant, resulted in a 94% reduction in neonatal tetanus mortality rates[84]. Moreover, gestational parent influenza vaccination and the magnitude of vaccination-derived antibodies are associated with protection of infants from influenza illness[85–87]. These benefits have led to the recommendation of providing diphtheria, tetanus, pertussis combined vaccines and influenza vaccines routinely during pregnancy[243,244]. Therefore, transplacental transfer of IgG is an important feature of vaccination-induced and natural immunity that may be leveraged for protection against neonatal pathogens.

Humoral immunity plays an important role in protection against flavivirus infections[245–247]. ZIKV-neutralizing antibodies likely provide durable protection against re-infection, therefore eliciting robust antibody responses is a key goal of ZIKV vaccine development[248]. Given the severe consequences of ZIKV disease in neonates, an ideal ZIKV vaccine would not only prevent infection in vaccine recipients but also protect fetuses from ZIKV congenital transmission. One way to protect fetuses could be transplacental transfer of ZIKV vaccine-elicited IgG. Due to the key role of antibody transfer in newborn health, it is important to delineate the quantity and function of IgG transferred during pregnancy in the context of infections during gestation.

However, the degree of cross-reactivity in the antibody responses between DENV and ZIKV may lead to risks in early life for DENV disease enhancement in infants through

transplacental transfer of flavivirus antibodies[112,249–252]. This risk is known to be mediated by antibodies generated from a prior DENV infection that can enhance DENV viremia and disease and ZIKV antibodies may have the potential to similarly enhance DENV infection[53,253,254]. Timing of past flavivirus infection also influences this risk as cross-neutralization of DENV and ZIKV is restricted to early convalescence, and antibody populations become more virus-specific over time [255,256]. While DENV-specific IgG are efficiently transferred in healthy pregnancies, waning flavivirus-specific IgG levels acquired from the gestational parent throughout the first year of life lead to increased risk for severe DENV infection in infants [112,257–259]. The available data suggest that DENV immunity provides modest and transient protection against ZIKV[60,260], highlighting the need to better understand the impact of cross-reactive antibodies in flavivirus disease. Antibody-dependent transfer of ZIKV across the placenta, antibody-mediated enhancement of DENV disease in infants, and antibody-mediated protection of fetuses and newborns are all dependent on intact transplacental IgG transfer.

IgG transfer during gestation occurs at placental villus trees in contact with parental blood[91]. In healthy pregnancies, IgG is transferred efficiently such that IgG concentrations in infant cord blood are often equivalent to or higher than the gestational parent's levels at delivery [83,261]. Many factors contribute to efficient transplacental IgG transfer via FcRn, such as IgG subclass, antibody avidity, gestational stage, and hypergammaglobulinemia [91,262,263], and transfer can be impeded by placental pathology. Additionally, other Fcγ receptors may also play a supporting role in transfer of IgG across the placenta[264].

Gestational infection with DENV, a closely related flavivirus, leads to increased risk of mortality, pregnancy complications, premature birth, and low infant birth weight, as well

as placental damage[68–72]. Yet, DENV infection in pregnancy does not impair transplacental IgG transfer in normal birth weight infants[113]. ZIKV infection in pregnancy can result in prolonged viremia, suggesting a viral reservoir in an immune privileged site, potentially the placenta[78,80–82]. Gestational malaria and HIV-1 infection have been established to differentially impact transfer of IgG subpopulations specific to routine pediatric vaccines[110,265], which may be dependent on distinct Fc characteristics of each IgG population[266]. Gestational HIV-1 infection and placental damage due to malaria infection are two clinical settings associated with impaired IgG transfer[107–111]. Gestational ZIKV infection can result in similar placental damage[97,99,267,268]. While prior studies show efficient transfer of recently boosted flavivirus antibodies after the ZIKV epidemic[269], we further examined whether pre-existing IgG subpopulations relevant to newborn health are efficiently transferred following gestational ZIKV infection.

To investigate whether ZIKV infection in the gestational parent during pregnancy impairs transplacental transfer of IgG specific to flaviviruses and common vaccine antigens, we enrolled a prospective cohort of 26 pregnant individuals from Vitória, Brazil, who presented with fever and rash symptoms consistent with ZIKV infection during the recent Brazilian ZIKV epidemic. Of these, 20 paired plasma samples from gestational parents and infant cord blood samples were collected from delivery and used to define the efficiency of transplacental IgG transfer. Of these, we classified 8 gestational parents as ZIKV-infected based on viral RNA detection and/or neutralization serology, and 12 gestational parents as ZIKV-uninfected. Comparing ZIKV-infected and uninfected groups, we detected no difference in transfer efficiency of IgG targeting ZIKV, DENV, or routine vaccine antigens. These findings indicate that the magnitude of IgG transferred across

the placenta was not deficient at the time of birth in the setting of gestational ZIKV infection. Sustained transplacental transfer with ZIKV infection in the gestational parent during pregnancy indicates that ZIKV exposure in utero should not impact protection mediated by gestational parent antibodies during early life, yet indicates potential risks of severe primary DENV infection in ZIKV-exposed infants in endemic regions. This passive antibody transfer in pregnancy is an important consideration for flavivirus vaccine and therapeutic development efforts.

2.3 Materials and methods

Study population and design

Positive control sera were collected in North Carolina from residents who had possible DENV or ZIKV infection based on a combined history of symptoms and travel. Serum samples were assigned arbitrary identification numbers beginning with “DT”. All donations were collected in compliance with the University of North Carolina (UNC) Institutional Review Board (IRB) (protocol 08–0895). Infection history of these samples was determined on the basis of neutralizing antibodies to DENV serotypes and ZIKV, such that if the highest 50% focus reduction neutralization titer (FRNT-50) was >4-fold higher than for the other viruses, it was defined as a primary infection with that virus. Otherwise, it was defined as a secondary DENV or both ZIKV and DENV infection history, depending on whether ZIKV was within a 4-fold range of the highest FRNT-50 titer.

The study enrolled 26 pregnant individuals living in Southeast Brazil, but from which only 20 delivery samples were collected. All enrollees presented with fever and/or rash during the ZIKV epidemic in 2016. Two groups of gestational parent-infant pairs are included in this observational study: one group with ZIKV infection during pregnancy, and

the other group without ZIKV infection during pregnancy. Therefore, pregnant individuals with rash or fever but without ZIKV infection served as a comparator group for those with ZIKV infection and symptomology. Participants in this study were enrolled from July 2016 to October 2017 in the city of Vitória, which is the capital of the State of Espírito Santo. There are 4 million inhabitants and 50,000 births per year in Espírito Santo with the majority living in the metropolitan region of Vitória[270,271]. This region has had endemic DENV circulation for the past two decades[272] so it was expected that many participants would have been exposed to DENV previously and be seropositive for DENV. The first clinically suspected cases of ZIKV infection in Brazil were described in May 2015, and six months later (November 2015) the first autochthonous ZIKV case was confirmed in Espírito Santo[273–275]. In the months preceding our enrollment, there was a ZIKV incidence of 3,100 cases per 100,000 inhabitants, and a DENV incidence of 901 cases per 100,000 inhabitants in Espírito Santo[272]. In this timeframe, 77 CZS cases were reported to the State Health Department, including cases of microcephaly, defects of the central nervous system suggestive of congenital infection, or stillbirths[272]. Since this region reflected key features of flavivirus co-endemic settings and had ongoing ZIKV transmission, it was considered representative of regions with a burden of ZIKV disease and appropriate for study of ZIKV immunity during pregnancy.

Recruitment

The enrollment field site is based in the city of Vitória at the the Núcleo de Doenças Infecciosas (NDI), at the Universidade Federal do Espírito Santo. During our study, suspected ZIKV infection was considered a reportable condition to the State Health Department for all patients seen at public or private clinics within the state.

Within a week of a case reported by a physician to the State Health Department, a staff member reported notifications of pregnant suspected ZIKV cases within the State to NDI. Thus the recruitment strategy relied on passive surveillance systems, and no active recruitment was conducted in the community. Upon referral, staff at the NDI contacted pregnant suspected ZIKV cases within the Vitória metropolitan area by phone regarding interest in participating in this study. If interested, pregnant suspected ZIKV cases were invited to the NDI for written informed consent and first recorded visit in our study at the time of enrollment.

Enrollment and follow-up

At the initial visit for study enrollment, four inclusion criteria were confirmed: 1) currently pregnant; 2) rash or fever consistent with ZIKV infection; 3) patient was a minimum of 18 years of age; 4) willingness to participate in study through provision of written informed consent. No exclusion criteria were defined. During the enrollment visit, a clinical history and physical evaluation were performed by a licensed physician, and blood and urine were collected. The following demographic information was collected at enrollment: age, municipality, date of birth, last menstrual date, recall of prior DENV disease, family members or neighbors with symptoms of ZIKV infection, use of insect repellant, prior vaccination for yellow fever virus, sexual activity in the 10 days before symptoms of ZIKV infection, symptoms of ZIKV infection in sexual partners, partner's use of insect repellent, and use of drugs, tobacco, or alcohol during pregnancy. Any clinical records and ultrasounds during the pregnancy before symptoms of ZIKV infection also were collected. All participants were referred for additional prenatal clinical care consultations and ultrasounds. Transportation to the NDI research site for every

visit, as well as all recommended consultations with obstetrician-gynecologists and ultrasounds were funded by the study. For each participant, gestational ages at the time of symptoms and delivery were calculated based on the last menstrual period date and confirmed by ultrasound (performed at 9-22 weeks).

After the enrollment visit, all participants were followed up weekly for up to four weeks, and monthly visits thereafter until delivery. Though follow-up of the gestational parents and infants in this study is ongoing, the present report only includes samples through delivery. At every visit, a standardized questionnaire was administered in the form of a semi-structured interview by a trained research staff member at NDI. Through this questionnaire we collected information on the presence and duration of symptoms related to ZIKV infection.

At the time of delivery, gestational parent blood and urine, infant cord blood, and placenta were collected. Newborn head circumference was measured by a nurse prior to hospital discharge, and reported to study staff. Head circumferences were converted to z score for the corresponding gestational age using the Newborn Cross-Sectional Study of the INTERGROWTH-21st Project standards. Microcephaly was defined per WHO and INTERGROWTH-21st guidelines as a z score lower than -1.88, which is the 3rd percentile of newborns at each gestational age[276,277].

Sample collection

Blood samples were collected into heparin or EDTA tubes, stored at room temperature up to six hours, and centrifuged at 1300 x G for 10 minutes to obtain plasma. Infant umbilical cord blood was collected by clamping the cord, cutting it, and

draining blood into sterile collection tubes. Urine samples were collected mid-stream in a sterile screw-top container and stored at -80°C. Plasma samples were stored at -80°C, then shipped to Duke University on dry ice.

Ethics statement

This prospective cohort study was approved by the Institutional Review Board of Hospital Cassiano Antonio Moraes, Brazilian National Research Ethics Committee (CEP/CONEP Registration number: 52841716.0.0000.5071), and Duke University Medical Center Institutional Review Board (Pro00100218). Individuals meeting enrollment criteria who provided written informed consent were included.

RT-PCR assay for ZIKV detection

Viral RNA was extracted from 140µL of plasma and urine using QIAmp Viral RNA Mini Kit (Qiagen). Previously described RT-PCR primers and probes specific for ZIKV were used for clinical diagnosis: ZIKV1086, ZIKV 1162c, and ZIKV1107-FAM [278]. For this one-step RT-PCR reaction, 5µL of RNA was combined with 500nM primers, 250nM probe and nucleotides in a total volume of 20µL, including SuperScriptIII RT and Platinum Taq DNA polymerase Mix (Invitrogen). The negative controls were serum from a 30-year old asymptomatic subject in Vitoria collected in 2016, and PCR grade water (no template control). The positive control was supernatant from ZIKV-infected Vero cells. Samples and controls were tested in duplicate, and ZIKV positivity was indicated by detection of amplification at <38 cycles in both duplicate wells on the Applied Biosystems 7500 Fast platform.

ZIKV IgM antibody capture enzyme-linked immunosorbent assay (MAC-ELISA)

The CDC MAC-ELISA (IgM antibody capture enzyme linked immunosorbent assay) was adapted and used to detect IgM specific for ZIKV in parental and cord blood plasma [279]. Briefly, 96-well high-binding ELISA plates were coated with 20 µg/ml of mouse anti-human IgM (Sigma #I0759) overnight at 4°C. Plates were blocked for 30 minutes at room temperature with 5% milk in 0.5% TBST, and then samples were added at a 1:40 dilution in quadruplicate for 1 hour at 37°C. Antigen (ZIKV H/PF/2013 grown in C6/36 cells), or C6/36 conditioned media as a negative control, was added at a 1:40 dilution overnight at 4°C. Then, an HRP-conjugated pan-flavivirus antibody (6B6C-1) was added for 1 hour at 37°C, followed by TMB substrate. Plates were incubated for 20 minutes, upon which 1N H_2SO_4 was added to stop the reaction. A positive result required that the absorbance for a particular plasma was >3-fold higher than the absorbance for that same plasma on C6/36 conditioned media. Samples run on each plate also include a confirmed ZIKV IgM positive and negative sample.

Cell culture and virus stocks

Vero-81 cells were grown in Dulbecco's Modified Eagle Media (Gibco 11965092) supplemented with 5% heat-inactivated fetal bovine serum (Cellgro, Cat#35-016-CV) and L-alanyl-L-glutamine (Thermofisher, GlutaMAX Cat#35050079). Viruses used for the focus reduction neutralization test were DENV1 (WestPac74), DENV2 (S-16803), DENV3 (CH54389), DENV4 (TVP-360), obtained from Dr. Aravinda de Silva, University of North Carolina at Chapel Hill, ZIKV (H/PF/2013), obtained from the United States Centers for Disease Control and Prevention (Division of Vector-borne Diseases, Fort Collins, CO), ZIKV (MR766) and ZIKV (DAKAR 41525) obtained from the World

Reference Center for Emerging Viruses and Arboviruses (WRCEVA), University of Texas Medical Branch, Galveston, TX, USA. DAKAR 41525 in the laboratory and publication was previously incorrectly identified as DAKAR 41519 due most likely to a mislabeled tube received from WRCEVA but was later correctly identified through deep sequencing[280]. For the detection of virion binding antibodies, the following viruses from BEI were used: ZIKV (PRVABC59), DENV1 (Hawaii), DENV2 (New Guinea C), DENV3 (Philippines), and DENV4 (H241). Virus stocks were grown in Vero-81 cells supplemented with 2% heat-inactivated fetal bovine serum and 10mM HEPES (Corning, Cat#25-060-CI).

Placental sampling and examination

Placenta samples were available from 11 ZIKV-infected and 8 ZIKV-uninfected subjects out of 26 individuals total in the cohort. Fragments were collected from the whole placenta up to 24 hours after delivery. Three sets of full thickness samples of placental parenchyma were obtained in every case and histology performed as previously described [281]. For the histological analysis, sections were fixed in 4% formaldehyde phosphate buffered solution, paraffin embedded and 5µm sections were stained with hematoxylin and eosin. Histological sections were examined specifically for villous lesions by a pathologist. Villitis was diagnosed if inflammatory exudate was present in the trophoblast or in the villous stroma and was categorized by Knox & Fox and Redline criteria[282,283]. Placentas were assessed as low-grade villitis if fewer than 10 villi were involved per focus, and high-grade if more than 10 villi were involved per focus [282].

Focus reduction neutralization test

We used previously described methods for FRNT-50 in a 96 well plate[256]. Briefly, serial 5-fold dilutions of heat-inactivated plasma were added to 50-80 focus forming units of either DENV or ZIKV and incubated for 1 hour at 37°C, then transferred to a confluent plate of Vero-81 cells and incubated for 1 hour at 37°C. Then an overlay of 1% methylcellulose was added. Cells were fixed with 2% paraformaldehyde and stained with 1 µg/mL of E60 mouse monoclonal antibody targeting the conserved flavivirus fusion loop[284], then detected with an anti-mouse IgG horseradish peroxidase conjugate and True Blue substrate (KPL). FRNT-50 values were calculated with the sigmoidal dose-response (variable slope) curve in Prism 7 (GraphPad), constraining values between 0 and 100% relative infection. A valid FRNT-50 curve required an R^2 >0.75, hill slope absolute value >0.5, and had to reach at least 50% relative infection within the range of the plasma dilutions in the assay.

Detection of virion binding IgG

High-binding 96-well ELISA plates (Greiner) were coated with 30 ng/well of 4G2 antibody (clone D1-4G2-4-15) in carbonate buffer, pH 9.6 overnight at 4°C. Plates were blocked in Tris-buffered saline containing 0.05% Tween-20 and 5% normal goat serum for 1 hour at 37°C, followed by an incubation with either ZIKV, DENV1, DENV2, DENV3 or DENV4 for 1 hour at 37°C. Plasma was tested at a 1:25 starting dilution in 8 serial 3-fold, 5-fold, or 10-fold dilutions, incubating for 1 hour at 37°C. Horseradish peroxidase-conjugated goat anti-human IgG antibody (Jackson ImmunoResearch Laboratories, Inc; 109-035-008) was used at a 1: 5,000 dilution, followed by the addition of SureBlue reserve TMB substrate followed by stop solution (KPL). Optical densities (OD) were

detected at 450 nm (Perkin Elmer, Victor). ED_{50} values were calculated with the sigmoidal dose-response (variable slope) curve in Prism 7 (GraphPad), which uses a least squares fit. An ED_{50} value was considered valid if the OD at plasma dilution 1:25 was two (2SD) or three (3SD) standard deviations above the mean OD observed for 11 plasma samples from healthy U.S. subjects (2SD OD cut-offs: DENV-1 = 0.406, DENV-2 = 0.648, DENV3 = 0.906, and DENV-4 = 0.885; 3SD OD cut-off: ZIKV = 0.596). Software generated ED_{50} values from curves with an OD at 1:25 plasma dilution below this cut-off were considered non-binding and plotted at the limit of detection.

Determination of transplacental transfer of IgG against routine pediatric vaccines

IgG binding to antigens from pediatric vaccines that are used routinely in Brazil was tested using a customized binding antibody multiplex assay on the Luminex platform as previously described[285]. Pediatric vaccine antigens used for screening included: hepatitis B virus surface antigen (antigenic combination: adw), rubella virus capsid (AbCam), *Bordetella pertussis* toxin and *Corynebacterium diphtheriae* toxin (Sigma-Aldrich), *Haemophilus influenzae* type B oligosaccharide-conjugated to human serum albumin (HbO-HA) and tetanus toxoid (Reagent Proteins). Antibody binding was detected with mouse anti-human IgG-PE (Southern BioTech) and the fluorescent output was measured on a Bio-Plex 200 system (Bio-Rad Laboratories). Antibody concentrations in µg or International Units per mL were interpolated from corresponding sigmoidal curves of serially diluted WHO international reference sera (National Institute of Biological Standards and Control, Potters Bar, UK; NIBSC code numbers: 07/164, 09/222, 06/140, TE-3, 10/262, RUBI-1-94). The efficiency of transplacental IgG transfer was calculated for each gestational parent-infant pair by dividing the concentration of

infant pediatric vaccine-specific IgG by the concentration of gestational parent vaccine-elicited IgG.

Screening for neonatal TORCH pathogens

Data on *Toxoplasma*, rubella, and syphilis serological status was extracted from the gestational parent's prenatal visit clinical records. All tests were performed by State Health Department or clinical laboratories using commercially available kits approved by the Brazilian Health Regulatory Agency (ANVISA), as per the manufacturer's instructions. Chemiluminescent microparticle immunoassay kits were used for detection of *Toxoplasma* IgM and IgG, as well as rubella virus IgG. Syphilis serostatus was assessed using a Venereal Disease Research Laboratory test, which is a nontreponemal test. Congenital CMV infection was evaluated using quantitative PCR of infant cord blood. To pellet CMV from plasma, 200 µL of infant cord blood was transferred to a high g-force micro-centrifuge tube and spun in an S45A fixed angle rotor at 30,000 rpm, 4°C, for 3 hours in a Sorvall Discovery M120 Ultracentrifuge. Then the supernatant was removed and the pellet re-suspended in 200 µL of 1x PBS. DNA was extracted using the Roche High Pure Viral Nucleic Acid Kit according to the manufacturer's protocol. To quantify and detect CMV DNA, extracted DNA from each sample was amplified in six replicates. For this reaction, 5 µL of DNA was added to 15 µL SYBR Select Master Mix with (ThermoFisher Scientific), 5 µL of water, and 300 nM primers designed to amplify the immediate-early 1 (IE1) gene of CMV (Integrated DNA Technologies). IE1 Forward Primer (20 bp): CAA GCG GCC TCT GAT AAC CA. IE1 Reverse Primer (24 bp): ACT AGG AGA GCA GAC TCT CAG AGG. For the negative control, PCR grade water was used as a substitute for extracted DNA in the reaction with in four replicate wells. A 10-

fold, 7 series dilution of plasmid with the amplification region was serially diluted starting at $1x10^8$ copies/mL to generate a standard curve for quantitation of CMV DNA in each sample. The lowest dilution on the standard that could be reliably amplified across replicates was considered as the threshold for positivity (250 viral DNA copies/mL).

Definition of ZIKV infection

As ZIKV viremia is transient, RT-PCR does not reliably detect ZIKV infection beyond 10-14 days from exposure[286]. Therefore, we combined a RT-PCR diagnostic with serological approaches based on gestational parent delivery plasma FRNT-50 titer (FRNT-50) against ZIKV and DENV (types 1-4). “Primary ZIKV” infection (no prior DENV or ZIKV infection) was defined as either i) a high ZIKV FRNT-50 (>300) and a low DENV1-4 FRNT-50 (<300), or ii) a low ZIKV FRNT-50 titer that is still >25 and at least one DENV FRNT-50 >25, suggesting only a weak transient cross-neutralizing response between ZIKV and DENV. A history of both ZIKV and DENV (“DENV+ZIKV”) was defined as high ZIKV FRNT-50 (>300), and at least one DENV FRNT-50>300. DENV immunity only (no ZIKV immunity) was classified as low ZIKV FRNT-50 (<300), but DENV FRNT-50 >25. Thus, we defined ZIKV infection as “primary” or “secondary” ZIKV based on serological evidence of prior DENV exposure, whereas the ZIKV-uninfected group includes subjects naïve to both ZIKV and DENV or those exposed to only DENV.

Since infection with one DENV serotype results in neutralizing activity only against that same serotype[287], and a subsequent infection with a different serotype results in broad DENV cross-neutralizing activity, we designed criteria to differentiate primary and secondary DENV infections based on whether the second-highest DENV FRNT-50 was within four-fold of the highest DENV FRNT-50. To further account for serological cross-

reactivity from recently infected subjects in assessing ZIKV infection status, we confirmed DENV-negative status by RT-PCR where acute samples were available. Sera with FRNT-50 values below the limit of detection for all five viruses were classified as ZIKV and DENV naïve. This definition is based on the assumption that a dominant ZIKV neutralization response at delivery was attributable to the recent symptomatic illness during pregnancy and not a prior ZIKV infection, given the recency of ZIKV introduction to the region during the period of enrollment; this assumption will not be valid for future studies in the same region. RT-PCR results from a plasma sample collected <7 days after symptom onset that were discordant with the serological assessment were repeated.

Statistical Analysis and Power.

Statistical analysis was performed using SAS (version 9.4) and Prism software (GraphPad; version 7). Serological responses are presented as a magnitude of flavivirus binding IgG (ED50), neutralizing (FRNT-50), and vaccine antigen binding IgG (μg/mL or IU/mL). The percent IgG transferred from gestational parent to infant describes the transplacental transfer efficiency, and is calculated as the ratio of the magnitude of infant cord blood IgG binding level (measured as ED50 or μg/ml) to the gestational parent IgG binding level. Note that this percent transfer ratio is specific to each antigen tested. Data are presented as dot plots of percent transfer for each gestational parent-infant pair in the ZIKV-infected group as compared to the ZIKV-uninfected group. Scatter plots are used to display the relationship and distribution of the gestational parent IgG level as compared to the infant IgG level, by antigen.

With a sample size of 26 gestational parents and 20 infant samples, this study is powered to reject the null hypothesis (no correlation between parental and infant antibody

responses), at an alpha of 0.05 with a power of 0.89 for neutralizing titer correlations, and 0.99 for correlations of IgG binding to flaviviruses or vaccine antigens. Therefore, this study is adequately powered to detect associations between gestational parent and infant antibody measures. For Wilcoxon Rank tests comparing IgG transfer efficiency between ZIKV-infected and uninfected gestational parent-infant pairs, this study is powered to assess significant differences between ZIKV-infected and uninfected groups in flavivirus IgG binding at an alpha of 0.05 (power = 0.93), but not for vaccine antigen IgG (power = 0.15) and neutralizing IgG (power = 0.48). This is due to differences in the extent of variability in measures by assay type.

Due to the small size of this cohort, a Gaussian distribution could not be inferred and therefore non-parametric statistical tests were applied. To compare IgG binding between ZIKV-infected and -uninfected groups, the Wilcoxon Signed and Exact Wilcoxon Rank Sum tests were applied. For correction of multiple comparisons, the Bonferroni correction was applied. Data were not stratified beyond the ZIKV infection status exposure group. The Kendall Tau test was used to evaluate correlations between parental and infant responses with the alpha level of significance set to 0.05.

Staining and sorting ZIKV-reactive B cells.

Peripheral blood mononuclear cells (PBMCs) were thawed and stained with 1 x 10^6 PFU of freshly thawed UV-inactivated ZIKV labelled with AF488. B cells were gated as CD14-/CD16-/CD3-/CD19+ and memory B cells were gated with an additional IgD-/CD27. ZIKV-reactive cells were defined by those that bound to the UV-inactivated and AF488-labeled ZIKV.

Culturing B cells in vitro and EBV transformation to generate B cell lines.

Cells were suspended and sorted by limiting dilution at a calculated concentration of 1-2 cells/well into 96-well round-bottom tissue culture plates in the presence of mouse CD40 ligand-expressing cells (3,000 cells/well). Cell culture supernatants were harvested on day 14 and assessed for secretion of any immunoglobulin by total IgG, IgM, and IgA ELISAs. Wells with detectable Ig were further evaluated for ZIKV-reactivity with a virion binding ELISA. The median IgG concentration of the cultures at the end of stimulation was 163 ng/ml (total IgG concentration range: 1.1- 1357 ng/ml; n=85), the median IgM concentration was 299 ng/mL (total IgM concentration range: 5.4 - 1304 ng/mL; n=20), and the median IgA concentration was 138 ng/mL (total IgA concentration range: 0.6 – 561 ng/mL; n=10).

Isolation of V(D)J immunoglobulin regions.

RNA from select positive cultures was extracted using standard procedures recommended by the manufacturer (Qiagen RNeasy Minikit), and the V_H and V_L genes were amplified[288]. The first round V_H PCR products were pooled for heavy chain second round nested PCR. Samples of second round PCR products were analyzed on 2% agarose gels. Positive wells were purified and sequenced by Genewiz. Sequencing results were analyzed by Clonalyst software to obtain needed Ig classification information[289]. When more than one heavy- or light-chain pair was obtained from a single culture, the clonal pairs were identified from sorted single B cells of the respective cultures by using the same procedure described above. All available antibody pairs were processed to overlapping PCR and transient transfection for further analysis as reported before[288].

Production of recombinant antibodies.

Recombinant IgG and Fab were synthesized as previously described[290]. Isolated DH1017 V_H and V_L Ig genes were cloned into pcDNA3.1(+) plasmid gene expression cassettes containing the CMV promoter and either the IgG heavy- and light-chain constant regions or to generate Fab, a partial heavy-chain constant region up to the V_H hinge region (GenScript). Plasmids were transformed into MAX Efficiency DHα Competent Cells and amplified by Plasmid Plus kit (Qiagen). Heavy chain plasmids were co-transfected with appropriate light chain plasmids at an equal ratio in Expi 293i cells (Invitrogen). Supernatant containing antibody was harvested and filtered, and co-incubated with a Protein A affinity resin (Thermo Fisher Scientific) for IgG antibody or LambdaFabSelect Agarose Beads (GE Healthcare Life Sciences) at 4°C on a rotating shaker overnight. The bead and supernatant mixture was then column purified. Purified antibody concentration was determined by Nanodrop and product was evaluated by reducing and nonreducing SDS-polyacrylamide gel electrophoresis and Coomassie Blue staining.

Mouse infections

All mouse husbandry and experiments were performed with approval of the University of North Carolina at Chapel Hill's Institutional Animal Care and Use Committee. Five to six-week old *Ifnar1*$^{-/-}$ mice were infected with 1000 FFU of ZIKV H/PF/2013. One day before and one day after inoculation, 100µg of either the ZIKV-neutralizing antibody CDH1017.IgM or non-ZIKV binding antibody 119-4-G11 were administered intravenously via retro-orbital injection. Serum was separated at 8000 rpm for 5 minutes and stored at -80°C ready for RNA extraction with the Qiagen viral RNA minikit. ZIKV genomes were

then quantified by Taqman one-step qRT-PCR on a CFX96 Touch real-time PCR detection system (BioRad) and were reported on a $\log_{10}$ scale measured against standard curves from a ZIKV A-plasmid as previously described[291].

2.4 Results

Neutralization assays can differentiate flavivirus infection history

Early in the course of the ZIKV outbreak in Latin America, diagnosis of ZIKV was challenging because viremia is only transient and the antibody response between DENV and ZIKV is so cross-reactive that they are indistinguishable via most binding assays against the E protein. Given the significant degree of antigenic cross-reactivity between DENV and ZIKV, we evaluated to what extent sera against one virus would also cross-neutralize the other because neutralization assays have more specificity between viruses and can even be used to distinguish between different DENV serotypes which are also strongly cross-reactive on most antibody binding assays[62,256,292–294]. We tested whether convalescent DENV immune sera, or sera collected from 4 individuals who traveled in 2015 to Brazil and were classified on the basis of serology of having both ZIKV and DENV exposure, could neutralize the prototype ZIKV strain MR766 (Uganda 1947, non-glycosylated variant Figure 2.1A)[291]. Most convalescent sera from individuals exposed only to DENV did not cross-neutralize ZIKV. Those who did neutralized ZIKV less well than convalescent sera from individuals exposed to ZIKV or both DENV and ZIKV.

Additionally, to determine whether the neutralization profiles of these sera are similar for more recent ZIKV strains, we compared the neutralization of a subset of these sera to two historic African lineage ZIKV strains (MR766 and DAKAR 41525 and two contemporary Asian lineage ZIKV strains (H/PF/2013 and PRVABC59) (Figure 2.1B-C).

The secondary DENV serum sample poorly neutralized these 4 ZIKV strains, but all were neutralized well by sera after prior ZIKV exposure. Historic and contemporary ZIKV strains display similar neutralization profiles.

Almost half of the study cohort is ZIKV seropositive

Pregnant individuals aged 18 to 39 years were enrolled based on symptoms suggestive of ZIKV infection, such as rash, arthralgia, and fever (Table 2.1). Nearly all enrolled participants (24/26) were from the Vitoria metropolitan area. All subjects were tested for common congenital “TORCH” pathogens where samples were available (Table 2.2). These data indicated no recent *Toxoplasma* infections (no gestational parent IgM detected), high IgG seropositivity to rubella virus (consistent with widespread MMR vaccination), and no evidence for syphilis infection. Testing of infant cord blood for CMV DNA found one case of congenital CMV transmission in the ZIKV-uninfected group. One subject (B1_0037) exhibited prolonged viremia, which was detected in serum by RT-PCR up to 42 days post symptoms.

ZIKV testing by RT-PCR was performed in serum and urine, collected between 2 and 15 days post symptom onset in 22 out of 26 individuals (Table 2.3) As expected, most were DENV seropositive, regardless of ZIKV infection status. The remaining individuals were referred for enrollment only after the resolution of symptoms, at 36 to 217 days since symptoms, and thus their negative ZIKV RT-PCR results were inconclusive. All individuals with acute samples available were negative for DENV by RT-PCR at enrollment, and one (B1_0035) was positive for chikungunya virusby RT-PCR (Table 2.3).

Because ZIKV viremia typically is detected only in the acute phase of infection (≤14 days after exposure), and because of the possibility of a false positive RT-PCR ZIKV test, we used serology to classify gestational parent ZIKV exposure as well as prior DENV infection history. Since detection of ZIKV-binding antibodies by ELISA does not distinguish ZIKV exposure from other flaviviruses, and this region has high DENV seroprevalence, we determined the FRNT-50 of all gestational parent plasma samples collected at delivery, which ranged from 39 to 217 days following onset of ZIKV symptoms. With the knowledge that ZIKV as well as DENV-recovered individuals do not have extensive cross-neutralizing antibodies against the virus to which they were not exposed, we designed an algorithm to define ZIKV and DENV exposure history. The algorithm is described in the methods and displayed in Figure 2.2. By these definitions, 11 out of 26 individuals had serological evidence of ZIKV infection, only 2 of which were DENV naïve, indicating a primary ZIKV infection (Table 2.4). Two out of 26 individuals were naïve for both ZIKV and DENV, and the rest had serological evidence of DENV infection with no ZIKV infection. Though one individual classified as ZIKV naïve (Primary DENV) by serology (B1_0009) had a positive RT-PCR result at initial presentation, subsequent RT-PCR testing of stored plasma was negative, suggesting that the initial result was a false positive. Of note, when tested we tested the samples classified as likely ZIKV exposed, two (B1_0002 and B1_0037) were ZIKV IgM positive at delivery, suggesting that these individuals had a recent ZIKV infection.

IgG transfer is maintained in the context of ZIKV infection of the gestational parent during pregnancy.

At birth, all infants born to ZIKV negative gestational parents were assessed to be healthy. Of the 11 infants born to gestational parents with serological evidence of ZIKV infection, one infant (born to B1_0001) presented with microcephaly at birth, with a head circumference below 3rd percentile based on WHO International Standards, and neurologic abnormalities including cortical-subcortical calcifications, dysgenesis of the corpus callosum, pachygyria, and colpocephaly upon transfontanellar ultrasound and CT scan[295]. Delivery cord blood sample was not available for this infant.

Lymphohistiocytic chronic villitis (inflammatory lesions in the placenta with an infiltrate of lymphocytes and macrophages)[296], was observed in the placentas of 5 of 11 (45%) ZIKV-infected gestational parents (Table 2.5 and Figure 2.3). The villitis was focal, involving less than 10 villi per focus, consistent with mild, low grade chronic villitis[282,283]. One placenta (B1_0004) demonstrated mild necrosis in the villitis focus and two placentas (B1_0004 and B1_0014) demonstrated small focal avascular villi with stromal fibrosis, consistent with fetal artery thrombosis in the absence of any other abnormality. In contrast, no vilitis was observed in any of the 8 ZIKV-uninfected subjects. We tested frozen placental samples from 8 ZIKV-positive individuals by qRT-PCR but did not detect ZIKV RNA.

To determine if ZIKV infection during pregnancy disrupts transplacental transfer of flavivirus-specific IgG, we compared the magnitude of flavivirus-specific antibody binding responses in gestational parent plasma at delivery and infant cord blood plasma by virion capture ELISA in 20 gestational parent-infant pairs with delivery samples available. For

those gestational parents with ZIKV infection, IgG binding to ZIKV, DENV1, DENV2, DENV3, and DENV4 virions was not significantly different between gestational parent plasma and paired infant cord blood from delivery (Wilcoxon Signed Rank Test; Bonferroni adjusted P >0.05 for all viruses tested). The efficiency of transplacental transfer of flavivirus-specific IgG was calculated as the ratio of the magnitude of infant cord blood antibody binding response to the gestational parent response, expressed as a transfer efficiency percentage (Figure 2.4). For those with paired parental and infant samples available, we compared the flavivirus-specific IgG transfer efficiencies in ZIKV-infected (n=8) and uninfected (n= 12) individuals, and found no significant difference in the transplacental transfer efficiency of flavivirus-specific IgG between the groups (Exact Wilcoxon Rank Sum Test; Bonferroni adjusted P > 0.05 for all viruses tested), indicating that ZIKV infection during pregnancy did not disrupt transplacental transfer of flavivirus-specific IgG.

As expected, in the virion capture ELISA we observed significant cross-reactive binding to ZIKV from individuals who were defined as ZIKV-uninfected based on neutralizing antibody titers. These ZIKV-uninfected subjects also demonstrated transfer of ZIKV-binding (cross-reactive, non-neutralizing) IgG. No ZIKV-specific IgG were detected from 2 ZIKV/DENV naïve individuals or in 2 DENV seropositive individuals and therefore percent IgG transfer could not be calculated for these subjects. Of the 8 DENV seropositive subjects with ZIKV-reactive IgG transferred to cord blood, 5 were seropositive for multiple DENV serotypes (B1_0016, B1_0024, B1_0026, B1_0033, and B1_0034), and 2 were seropositive for only a single DENV serotype (B1_0009 and

B1_0011), indicating that ZIKV cross-reactive IgG can be transferred to the fetus in the case of primary or secondary DENV exposure history.

Importantly, we also assessed whether there was efficient transplacental transfer of flavivirus neutralizing IgG in ZIKV-infected pregnant individuals. The DENV FRNT-50 of paired parental and cord blood plasma also were positively correlated, suggesting that functional gestational parent IgG were transferred efficiently to the fetus (Figure 2.5).

To assess whether ZIKV infection during pregnancy impacts transplacental transfer of IgG against vaccine antigens, we measured the magnitude of IgG binding against a panel of standard vaccine antigens from hepatitis B virus, rubella virus, *Haemophilus influenzae* type B, *Corynebacterium diphtheriae, Bordetella pertussis*, and *Clostridium tetani*. There were no significant differences in the magnitude of vaccine-specific IgG in gestational parent plasma and infant cord blood from delivery, in both ZIKV-infected and uninfected individuals (Wilcoxon Signed Rank Test, $P > 0.05$ for all vaccine antigens). We observed strong positive correlations in the concentration of vaccine-specific IgG between gestational parent plasma and infant cord blood for all vaccine antigens tested, indicating efficient placental transfer of vaccine-specific IgG levels regardless of ZIKV infection status (Figure 2.6). Based on the protective vaccine-specific IgG levels established by the WHO, infants born to individuals who had protective levels of vaccine-specific IgG and ZIKV infection during pregnancy, received similarly protective IgG levels as infants born to ZIKV-naïve individuals[297].

Kinetics of ZIKV IgG binding over the course of pregnancy

ZIKV infection during pregnancy has been associated with prolonged viremia in humans and non-human primates[78,298–300], and one individual in our study (B1_0037)

exhibited prolonged viremia, with plasma testing positive for ZIKV RNA up to 42 days post onset of symptoms (Figure 2.7A). We compared ZIKV neutralization titers between patient B1_0037 and the two other ZIKV-infected individuals from the cohort for whom sequential serum and urine samples were available for analysis (B1_0014 and B1_0030). B1_0030 only tested positive for ZIKV in urine by RT-PCR at the first 2 visits (within 18 days of symptoms), and B1_0014 tested ZIKV-negative by RT-PCR but was classified as ZIKV-infected by serology. These individuals have different flavivirus exposure histories as B1_0014 had prior exposure to DENV, and B1_0030 had a primary ZIKV infection. All three subjects sustained high levels of ZIKV-neutralizing titers throughout pregnancy. Monoclonal antibodies were isolated from B1_0037 after viremia subsided.

We evaluated the ZIKV-neutralizing activity of 4 antibodies that bound ZIKV by ELISA: 1 IgM and 3 IgG. We determined that two IgG were non-neutralizing, one IgG was weakly neutralizing (119-4-D6, FRNT50 = 770ng/ml), and the IgM was potently neutralizing (DH1017.IgM, 6.6ng/ml) (Figure 2.7B). IgM are pentavalent (10 Fab compared to 2 Fab for IgG) so the potency of DH1017.IgM could result from the pentavalent IgM having 5 times as many Fab regions on a single molecule compared to IgG, or additional features of the IgM could contribute to avidity for the epitope and thus neutralization. To distinguish these possibilities, the Fab sequence of DH1017.IgM was expressed on an IgG backbone and we measured ZIKV neutralizing activity. We would expect pentavalency to result in DH1017.IgM being 5-fold more potent than DH1017.IgG when assessed on a molecular basis. Instead, we found that DH1017.IgG had 40-fold less potent neutralization than DH1017.IgM by molarity (Figure 2.7C), suggesting that additional properties of the IgM antibody contribute to its potent neutralizing activity.

Both human and mouse IgG are stabilized in circulation in mice by FcRn[301]. However, human IgM does not interact with FcRn and is thus less stable in circulation. IgM also is not transported into the fetal circulation by FcRn, meaning that ZIKV-neutralizing IgM potentially could be administered to pregnant individuals to restrict parental infection without the risk of passively transferred antibodies conferring enhanced DENV infection in infants. To determine whether this potently ZIKV-neutralizing IgM is able to protect against infection and disease in mice, we infected *Ifnar1*$^{-/-}$ mice with ZIKV by subcutaneous inoculation in the footpad and treated them intravenously one day before and one day after inoculation with either DH1017.IgM or a control IgM that does not bind ZIKV but was isolated from the same patient. We found that DH1017.IgM protected against ZIKV infection as measured by viremia, as well as mortality (Figure 2.7D).

2.5 Discussion

Transplacental transfer of IgG provides passive immunity to fetuses, which is critical to protecting newborns in their first months of life[83]. However, conditions and infections during pregnancy may disrupt IgG transfer via mechanisms including placental impairment and inflammatory responses[302]. Moreover, viral antigenic complexity and natural history of infection shapes the IgG populations elicited, which have different propensities to be transferred across the placenta by FcRn[302,303]. Thus, we investigated the impact of gestational infection with ZIKV on transplacental IgG transfer in 20 gestational parent-infant pairs from a prospective cohort in Vitoria, Brazil. We assessed transfer of key IgG populations, including ZIKV and DENV binding and neutralizing IgG, as well as IgG specific to routine vaccine antigens.

For all flavivirus and vaccine antigens tested, we found that gestational parent and infant binding IgG levels were highly correlated in both ZIKV-infected and -uninfected groups. Also, there were no significant differences in the magnitude of flavivirus-binding IgG levels between gestational parents and infants among those parents with gestational ZIKV infection. Moreover, DENV neutralization and binding IgG levels were highly correlated between gestational parent-infant pairs regardless of gestational ZIKV infection. Outliers from these linear trends were shifted such that the magnitude of infant IgG neutralization was greater than that of the gestational parent neutralizing titer, indicating efficient IgG transfer. This positive association of gestational parent and infant IgG levels represents active transfer that is not solely dependent on the magnitude of the type-specific IgG in gestational parent plasma. Also, the substantially overlapping ranges in antibody levels between gestational parents and infants suggests no biologically relevant differences in transplacental transfer of flavivirus binding and neutralizing IgG, or of vaccine specific IgG after ZIKV infection in pregnancy. As different viral antigen-specific IgG subpopulations may be differentially impaired in placental transfer due to other infections and conditions during pregnancy[266,304], we tested IgG transfer of non-flavivirus antibodies that are specific to diverse vaccine antigens. IgG elicited by routine pediatric and boosted parental vaccines were also transferred efficiently despite gestational ZIKV infection. Cumulatively, these data indicate no evidence of impairment in the transplacental IgG transfer at the time of birth after gestational ZIKV infection, as compared to individuals with fever and rash during pregnancy without ZIKV infection.

Our study corroborates recent findings demonstrating efficient transfer of neutralizing antibodies against ZIKV, DENV3, and DENV4 in pairs of gestational parents

and infants from the Northeast of Brazil in 2016[269]. Specifically, Castanha et al found that newborns with the outcome of microcephaly, some of whom were exposed to ZIKV in utero, had no evidence of impaired transfer of neutralizing antibodies at birth as compared to controls without microcephaly[269]. Our work complements the finding from that case-control study through a prospective cohort design, in which we identified individuals with ZIKV infection during pregnancy and followed up until birth to quantify impact on transplacental IgG transfer. This prospective design adds a temporality to the association between ZIKV infection and neutralizing IgG transfer observed earlier[269]. Moreover, our study represents a geographically distinct site in Southeast Brazil, with lower ZIKV prevalence. Another recently published study with 3 serologically confirmed gestational ZIKV infections found similar levels of ZIKV-binding IgG in both gestational parent and cord blood, corroborating our findings that transplacental IgG transfer is preserved in the context of gestational ZIKV infection[305]. Altogether, this work strengthens the body of evidence indicating that transplacental IgG transfer is sustained during ZIKV infection in pregnancy.

This study further aimed to complement existing evidence of placental pathology caused by ZIKV infection, and determine whether this could have a role in the transplacental transfer of humoral immunity. Previous observations of impaired transplacental IgG transfer in the setting of gestational HIV and malaria infection generally have been noted in conjunction with identifiable placental pathology[110,302]. Although we did not detect ZIKV RNA in placentas from our study, another study identified ZIKV RNA in 54% of placentas from 44 ZIKV-infected individuals[268]. We found that 5 of 11 ZIKV-infected individuals in our cohort had chronic placental villitis, higher than the 5-15%

expected for term placentas[306]. Notably, this pathology is similar to that described in placental infection with CMV, rubella virus, or *Toxoplasma gondii*[296]. In contrast, no villitis was observed in the 8 placentas assessed from ZIKV-uninfected gestational parents, suggesting that the observed villitis may result from ZIKV infection in pregnancy. To assess the impact of ZIKV-associated placental pathology on IgG transfer, subgroups of ZIKV-infected subjects with noted placental pathology would have to be compared to a ZIKV-infected subgroup without placental pathology. However, our limited sample size of 8 ZIKV-infected individuals with paired infant samples precludes formal comparison.

We found that despite disruption of placental architecture in nearly half the ZIKV-infected individuals in the cohort, transplacental transfer of flavivirus-binding and -neutralizing IgG was sustained. This finding is relevant to future studies of vaccine-elicited fetal protection against ZIKV, as animal studies demonstrate neutralizing antibodies as correlates of protection against ZIKV infection[307,308]. Transfer of flavivirus-neutralizing antibody is relevant because neutralization titers are known to correlate with vaccine protection against other flaviviruses, including Japanese encephalitis virus, yellow fever virus, and tick-borne encephalitis virus[309–312].

In ZIKV-infected individuals with serial plasma collection during their pregnancies, ZIKV-specific IgG levels were sustained throughout gestation after peak response within 3 weeks of symptoms. These kinetics suggest that transfer of flavivirus-specific IgG to the fetus should readily occur throughout the 2nd and 3rd trimester of pregnancy following ZIKV infection. While it is possible that ZIKV infection during pregnancy could result in a transient disruption of transplacental IgG transfer that is restored by the time of birth, our

goal was to evaluate levels of IgG present at delivery as these transferred IgG have the potential to modulate protection or disease risk in infants[59,83–86,313,314].

There are several implications of the findings in our study. Efficient transfer of ZIKV-neutralizing IgG could transfer protective humoral immunity despite infection during pregnancy. Notably, transfer of protective levels of vaccine-specific IgG to boost passive immunity in the newborn is a key goal of immunizing gestational parents [315] and our findings suggest that ZIKV infection during pregnancy does not impair this protective mechanism. With candidate ZIKV vaccines or therapeutics, this may be one mode of conferring passive immunity to the fetus and reducing the burden of congenital and neonatal ZIKV infection. However, transfer of cross-reactive non-neutralizing DENV-binding antibodies may pose a risk as antibodies from primary DENV infection can enhance secondary DENV infection, leading to more severe disease in infants as parental antibody titers wane[53,257].

Limitations of this study include the small sample size of only 20 gestational parent-infant pairs with delivery samples available, but two other studies of small cohorts similarly found that antibody transfer is maintained in the wake of ZIKV infection during pregnancy in the gestational parent[269,305]. Though each study suffers independently from small sample size, together they suggest that antibody transfer is maintained despite gestational ZIKV infection even in the presence of placental inflammation.

Another limitation of our study is the challenge of determining whether subjects were truly exposed to ZIKV during pregnancy, as symptoms could have resulted from other infections and/or ZIKV infection could have occurred prior to pregnancy. Since viremia may have subsided by the time of study enrollment, we developed an algorithm

to define ZIKV infection serologically, even in the context of cross-reactive antibodies from prior DENV infection. This algorithm and ZIKV case definition were based on the rational assumption that ZIKV seropositivity resulted from a recent infection (i.e. during pregnancy) due to the timing of our study relative to the introduction of ZIKV into Brazil. This assumption will not apply in future studies, since the high force of infection during the 2015-2017 outbreak and the potential for subsequent endemic transmission mean many individuals will already be ZIKV seropositive before pregnancy. Moreover, this study reflects the findings in a symptomatic pregnancy cohort, whereas the majority of ZIKV infections are asymptomatic[316–318].

ZIKV infection during pregnancy can result in prolonged viremia , as was the case for one of the individuals in this study who displayed persistent viremia for 1 month while most ZIKV infections are typically viremic for <2 weeks. To our knowledge, no ZIKV-neutralizing IgM have been previously isolated and no flavivirus-neutralizing IgM have been isolated. It may have been easier to do so in the case of DH1017.IgM because of the prolonged viremia in this individual. The binding epitope of this IgM is still under investigation by Tulika Singh, in collaboration with Dr. Richard Kuhn, Purdue University; defining this epitope and comparing it to epitopes targeted by other potently neutralizing ZIKV MAbs may provide insight into the development of neutralizing IgG that make up the convalescent antibody response to natural ZIKV infection. This particular monoclonal antibody also could be the basis of prophylactic protection against ZIKV infection in pregnant individuals, as it also appears to protect mice from severe disease. One concern of other ZIKV monoclonal antibody therapies for pregnant individuals is that DENV disease in infants could be made more severe by ZIKV antibodies acquired via

transplacental antibody transfer[60]. IgG can be engineered with Fc modifications to prevent or decrease FcRn-mediated binding transfer either by mutating residues at the interface of the FcRn-IgG interface or by introducing steric inhibition of the interaction[319,320]. DH1017.IgM would however not require such modification as IgM are natively not transported across the placenta. Additionally, it will not bind the Fcγ receptors implicated in ADE of DENV. Perhaps most importantly, DH1017.IgM displays particularly potent ZIKV neutralization, more than would be expected from a simple 5-fold increase of the DH1017.IgG.

In summary, this study demonstrates efficient transplacental transfer of IgG specific to diverse flaviviruses and routine vaccine antigens following ZIKV infection during pregnancy in a unique prospective cohort of gestational parent-infant pairs from the Latin American ZIKV outbreak. Transplacental transfer of ZIKV-specific IgG in pregnancy may contribute to protection of the fetus from congenital Zika syndrome and the infant from ZIKV infection. However, efficiently transferred IgG might mediate adverse effects in infants including increased risk of severe DENV in infancy, as well as potentially mediating FcRn-dependent transfer of ZIKV immune complexes into the fetal compartment. The relationship between efficient parental IgG transfer and reduced or enhanced congenital infection or disease remains to be further elucidated. Delineating ZIKV-specific IgG levels and function that favor fetal and neonatal protection will be key for guiding a strategic timeline for pediatric vaccine boosts, timing of vaccine administration during pregnancy, and dosing of antibody therapies targeted for pregnancy. Longitudinal investigations of neonatal immunity, in the context of transplacental transfer of flavivirus antibodies will be a valuable area of investigation to

define serological mediators of risk or protection for infants. Given the uncertain benefits or risks of efficient transfer of flavivirus IgG, ZIKV and DENV vaccine strategies will need to carefully consider the timing and type of vaccination and boosting.

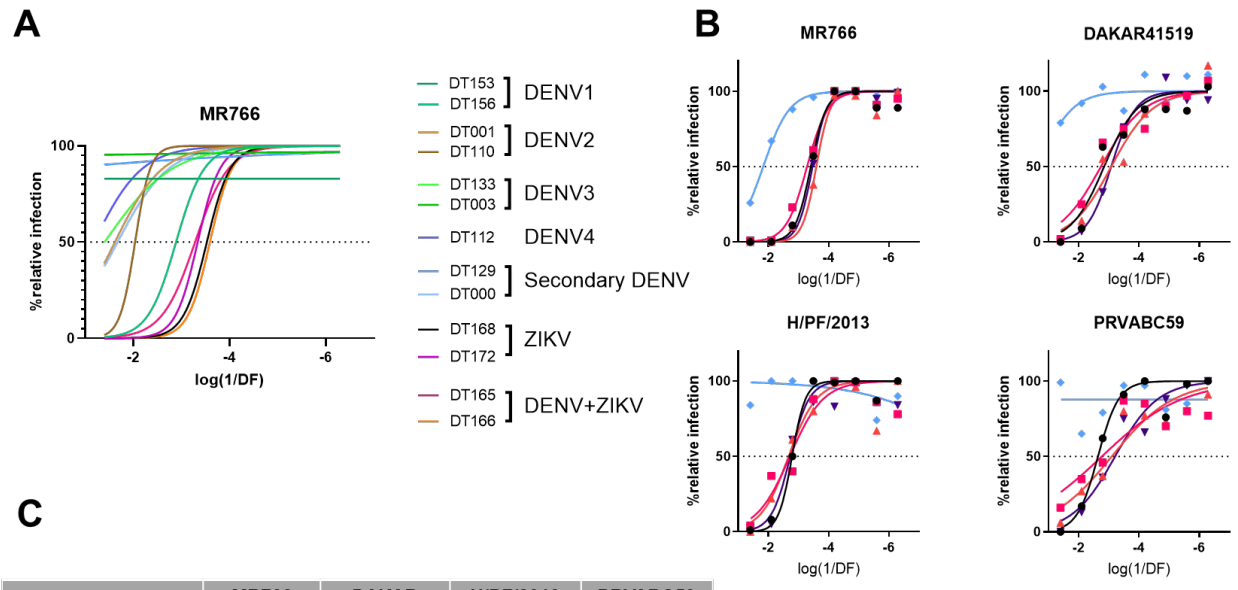

	MR766	DAKAR 41525	H/PF/2013	PRVABC59
DT168 ZIKV	2546	700	609	436
DT172 ZIKV	2898	1197	531	1606
DT165 ZIKV+DENV	1918	547	516	ND
DT166 ZIKV+DENV	3889	1203	469	ND
DT145 DENV+DENV	67	<25	<25	<25

Figure 2.1 ZIKV strains are serologically distinct from DENV by neutralization assay **A.** Immune sera from North Carolina individuals with travel history to DENV-endemic regions was tested for neutralization of ZIKV strain MR766 via serial dilution. Samples were previously classified as either a single DENV infection with 1 of 4 serotypes, multiple DENV infections (secondary DENV), ZIKV exposure alone, or both ZIKV and DENV exposure history. **B.** Neutralization curves for 4 Zika virus strains, including African lineage (MR766 and DAKAR41525) and Asian lineage (H/PF/2013 and PRVABC59) strains. **C.** Table of FRNT-50 values from B. ND=not determinable because the neutralization curves did not pass quality control criteria.

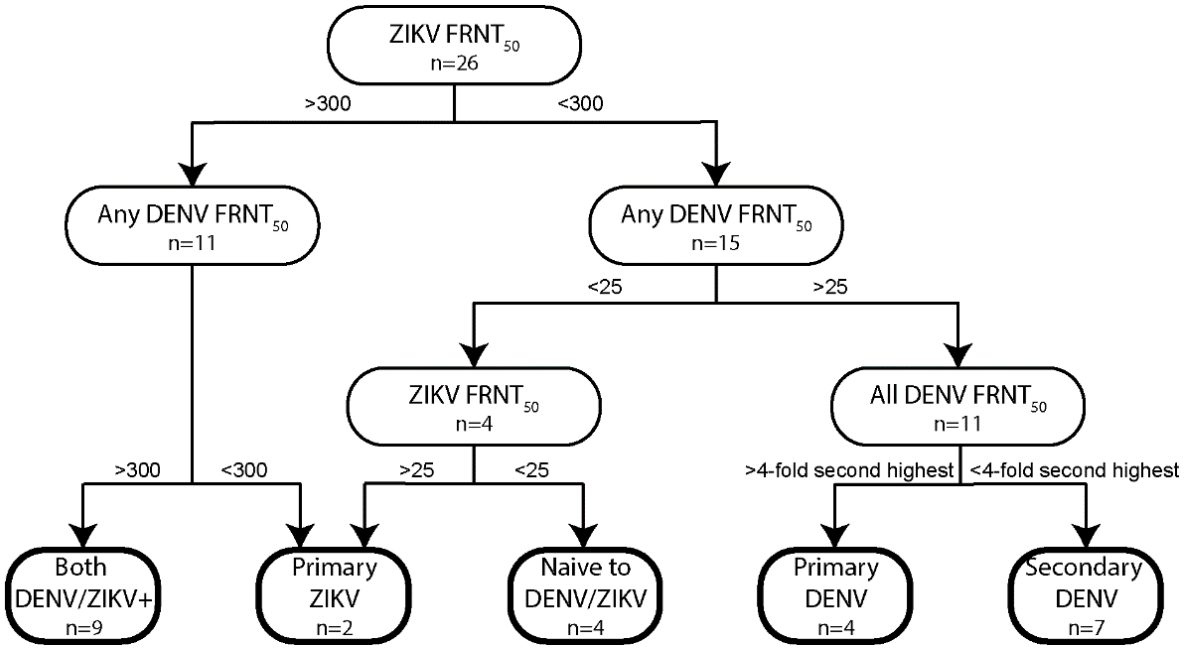

Figure 2.2 Algorithm used to categorize flavivirus exposure history according to ZIKV and DENV FRNT-50 titers. Gestational parent plasma were tested by FRNT-50 against 5 viruses (ZIKV and 4 DENV serotypes) and FRNT-50 titers used to infer flavivirus exposure history. All samples were anti-flavivirus IgM negative, reducing the likelihood of cross-reactivity resulting from recent infections.

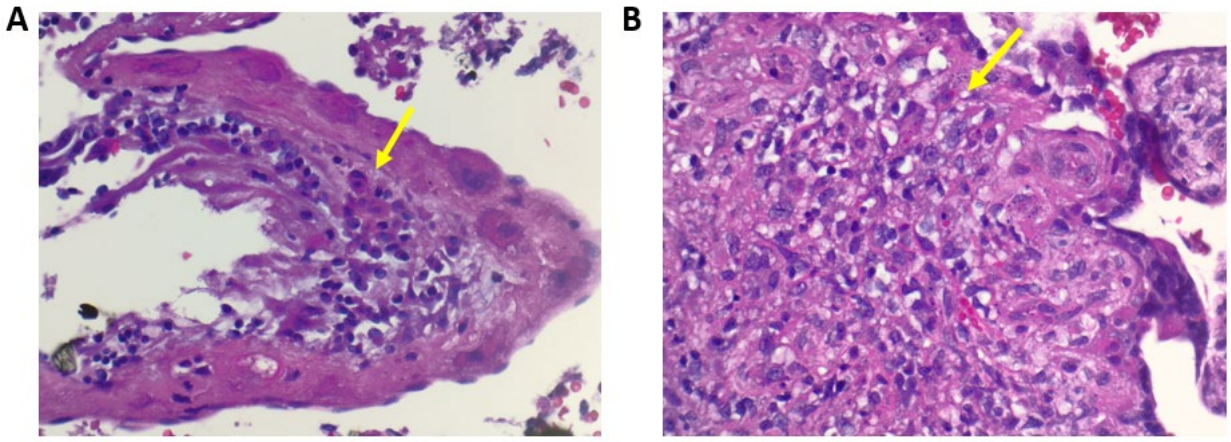

Figure 2.3 Histology of the placenta from a ZIKV-infected pregnant individual. Placental tissue from subject B1_0004 was stained with hematoxylin and eosin. Lymphocytes and macrophages are present in the chorionic villi (**A**-100X, **B**-400X). The arrow indicates inflammatory cells within a villus.

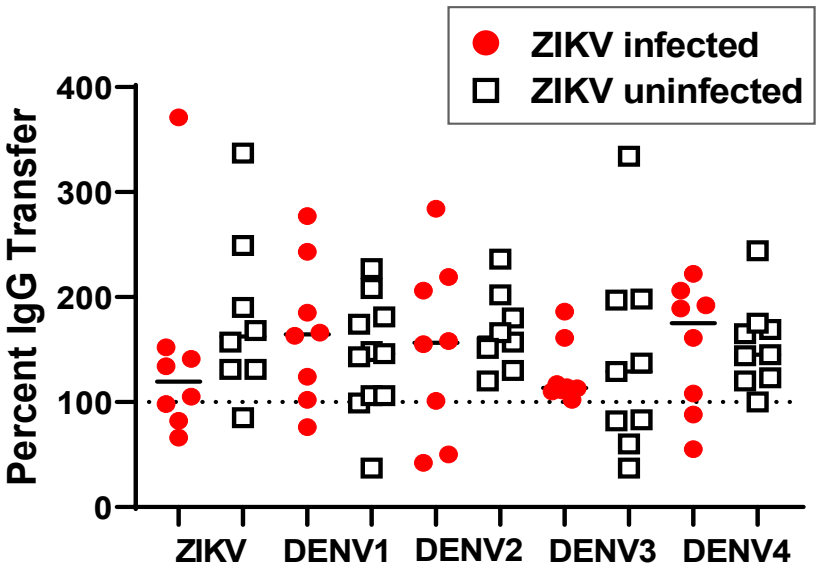

Figure 2.4 Efficient transplacental transfer of flavivirus-specific IgG. Plasma antibody binding to ZIKV, DENV1, DENV2, DENV3, and DENV4 was measured via a virion capture ELISA using serial dilutions of gestational parent plasma and infant cord blood collected at delivery. The dilution at 50% of maximal binding (ED50) was calculated and the infant ED50 was assessed as a percentage of the parental ED50 to yield percent transfer. Dotted line indicates 100% transfer and the solid line indicates the median. No significant differences in percent transfer were found in comparing ZIKV-infected and uninfected individuals for the all viruses tested by Exact Wilcoxon Rank Sum Test; Bonferroni adjusted $P > 0.05$ for all viruses tested.

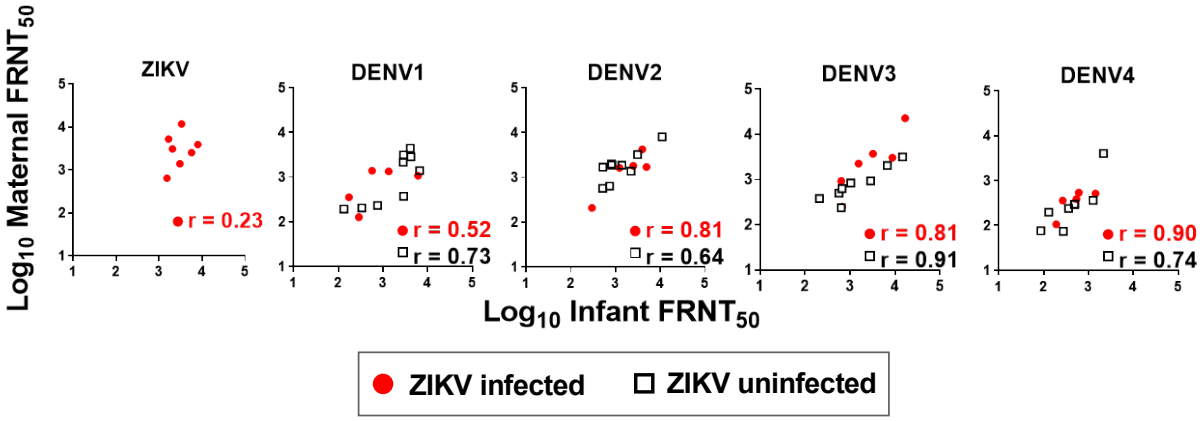

Figure 2.5 Gestational ZIKV infection does not disrupt transplacental transfer of DENV neutralizing IgG. Kendall Tau correlation of focus neutralization reduction titer-50 (FRNT-50) for gestational parent plasma and infant cord blood, separated by parental ZIKV serostatus. All correlations are $P<0.05$, except ZIKV-infected gestational parent DENV1 ($P<0.09$) and ZIKV ($P<0.45$).

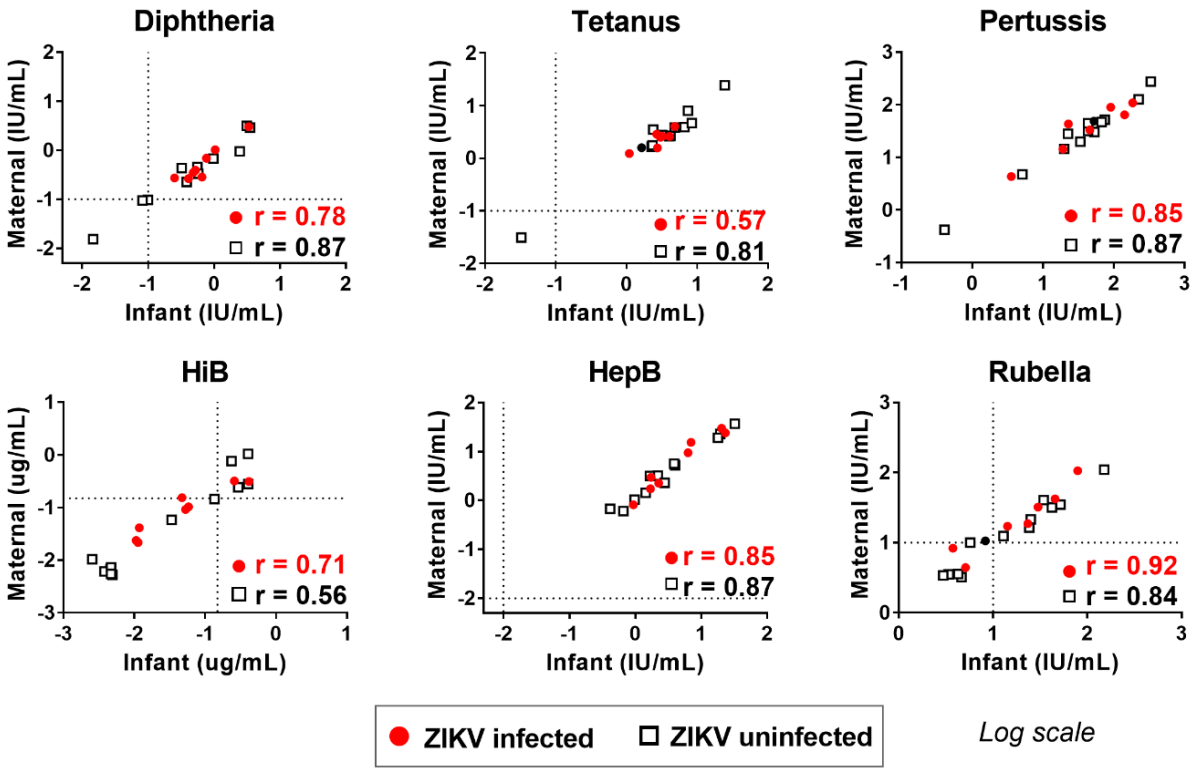

Figure 2.6 Gestational parent and infant vaccine-elicited IgG levels are highly correlated regardless of gestational parent ZIKV infection status. IgG response to vaccine antigens in infant cord blood plasma and gestational parent plasma collected at delivery were measured via a binding antibody multiplex assay. Concentrations of vaccine-elicited IgG responses were calculated from reference sera standards as International Units (IU)/mL or µg/mL. ZIKV-infected (n=8) and uninfected (n=12) subjects are indicated in red and black respectively, and dotted lines denote WHO established protective IgG levels. Kendall Tau correlations were performed for each ZIKV infection group, with $p<0.05$ for all.

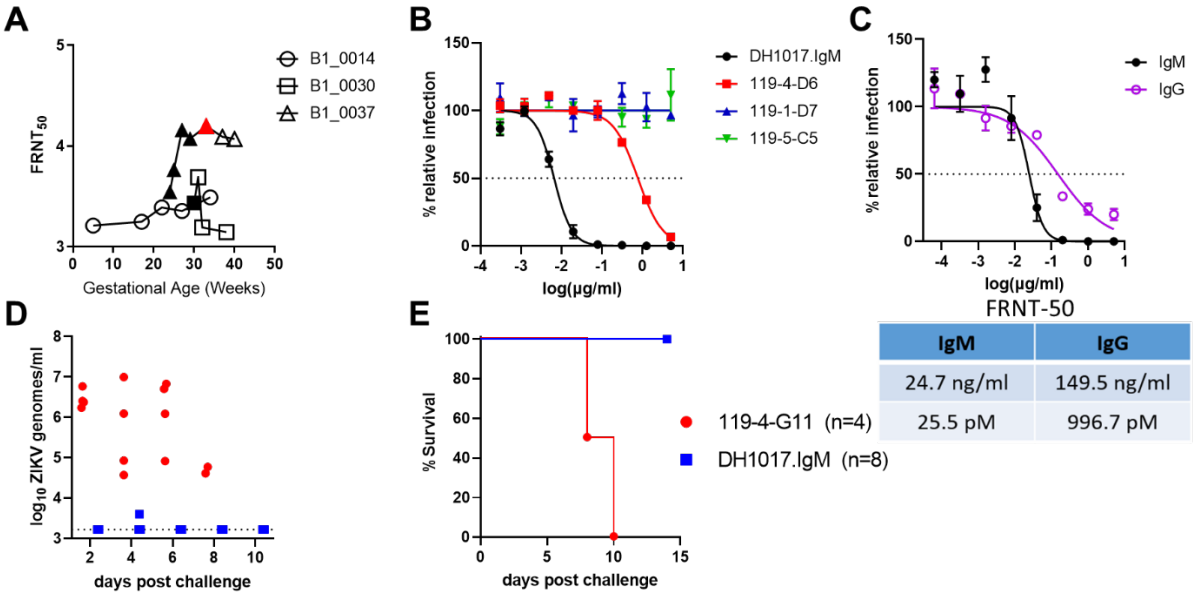

Figure 2.7 A ZIKV-targeting IgM monoclonal antibody isolated from a pregnant individual protects against ZIKV infection in mice. A. ZIKV focus reduction neutralization titers from serial samples during gestation for each of three individuals (Filled symbols = time points when ZIKV viremia was detected by RT-PCR, Red = blood draw from which PBMCs were isolated from which to generate monoclonal antibodies). **B**. ZIKV neutralization curves of 4 monoclonal antibodies isolated from B1_0037. **C**. ZIKV neutralization curves and FRNT50 values for DH1017 on the native IgM and cloned IgG backbone. **D. and E.** Five week old *Ifnar1*$^{-/-}$ mice were then infected with 1000 FFU of ZIKV strain H/PF/2013 by footpad inoculation on day 0. On day -1 and 1, they were administered intravenously 100µg of either DH1017.IgM or a control IgM, 119-4-G11. Viral RNA was extracted from serum collected every 2 days in and ZIKV RNA measured by qRT-PCR **(D)** and survival was tracked for 14 days in **(E).**

	ZIKV PCR+ (n=9)	ZIKV PCR- (n=13)	ZIKV PCR ND (n=4)	Total (n=26)
	9/26	13/26	4/26	26/26
Proportion of individuals symptomatic in each gestational trimester				
First	3/9	3/13	2/4	8/26
Second	4/9	7/13	2/4	13/26
Third	2/9	3/13	0/4	5/26
Percent with symptoms				
Rash	8/9	13/13	3/4	24/26
Arthralgia	5/9	4/13	3/4	12/26
Fever	3/9	5/13	3/4	11/26
Conjunctivitis	4/9	4/13	3/4	11/26
Myalgia	5/9	4/13	1/4	10/26
Headache	4/9	7/13	3/4	14/26
Retro-orbital pain	2/9	4/13	2/4	8/26
Lymphadenopathy	1/9	1/13	0/4	2/26

Table 2.1 Symptomatology of patient cohort. Symptoms were collected by survey at the time of enrollment as well as a blood draw for ZIKV RT-PCR. ZIKV=Zika virus, RT-PCR= reverse-transcription polymerase chain reaction, ND=not done.

	ZIKV-infected	ZIKV-uninfected	Unavailable
***Toxoplasma* IgM**	0/8	0/9	3/20
***Toxoplasma* IgG**	3/8	7/10	2/20
Rubella IgG	6/7	9/9	4/20
Cord blood CMV viremia	0/7	1/11	2/20
Syphilis VDRL	0/8	0/10	2/26

Table 2.2 Clinical results of prenatal screening for TORCH infections. Clinical test results for Toxoplasma antibodies, rubella IgG, and venereal disease research laboratory (VDRL) test for syphilis from pregnant individuals. Also included is whether cytomegalovirus (CMV) viremia was present in cord blood collected at delivery. Proportion of individuals with positive test results are reported as the numerator, whereas the denominator is the number of the total samples tested.

ID	Age	Gestational Age (days) at symptom onset	Trimester of Infection	Days between first sample collection and symptom onset	ZIKV serum RT-PCR Results	DENV serum RT-PCR Results
B1_0001	38	73	1	4	+	N/A
B1_0002	29	97	2	4	+	N/A
B1_0003	28	66	1	7	-	N/A
B1_0004	21	94	2	4	+	N/A
B1_0005	26	31	1	3	+	N/A
B1_0006	22	68	1	217	-	N/A
B1_0007	29	78	1	210	-	N/A
B1_0008	22	95	2	2	+	N/A
B1_0009	31	40	1	4	+	N/A
B1_0011	26	232	3	5	-	-
B1_0014	19	27	1	4	-	-
B1_0015	34	117	2	8	-	N/A
B1_0016	35	99	2	90	-	N/A
B1_0019	28	157	2	15	-	N/A
B1_0021	30	75	1	3	-	N/A
B1_0023	18	167	2	7	-	N/A
B1_0024	30	136	2	36	-	N/A
B1_0026	31	224	3	12	-	N/A
B1_0027	23	179	2	14	-	-
B1_0030	20	203	3	2	+	N/A
B1_0031	39	257	3	4	+	N/A
B1_0033	19	174	2	9	-	-
B1_0034	28	173	2	2	-	N/A
B1_0035	32	176	2	3	-	-
B1_0037	19	159	2	4	+	N/A
B1_0039	29	225	3	4	-	N/A

Table 2.3 Timeline of infection. Age of each pregnant individual, trimester of symptom onset (rash, fever), and PCR results for both ZIKV and DENV. N/A=Not available

Sample ID	Classification	Days since symptoms	$FRNT_{50}$					ZIKV RT-PCR
			ZIKV	DENV1	DENV2	DENV3	DENV4	
B1_0015	Naïve	NA	<25	<25	<25	<25	<25	-
B1_0019	Naïve	75	<25	<25	<25	<25	<25	-
B1_0021	Naïve	213	<25	<25	<25	<25	<25	-
B1_0039	Naïve	35	<25	<25	<25	<25	<25	-
B1_0008	Primary ZIKV	184	3918	126	209	251	106	+
B1_0030	Primary ZIKV	77	1399	<25	<25	<25	<25	+
B1_0001	DENV+ZIKV	193	10858	898	597	1270	491	+
B1_0002	DENV+ZIKV	173	14959	1524	666	5571	502	+
B1_0004	DENV+ZIKV	164	2533	1348	1818	3047	537	+
B1_0005	DENV+ZIKV	217	5213	1379	4218	2270	359	+
B1_0007	DENV+ZIKV	208	5503	1371	2511	822	353	-
B1_0014	DENV+ZIKV	210	3095	354	1625	930	388	-
B1_0031[a]	DENV+ZIKV	94	1610	2723	2492	10521	1510	+
B1_0027	DENV+ZIKV	91	654	1079	1711	3730	513	-
B1_0037	DENV+ZIKV	117	11764	2141	8019	22873	4029	+
B1_0009[b]	Primary DENV2	240	<25	205	1887	238	240	+
B1_0035	Primary DENV2	114	107	68	1201	106	68	-
B1_0011	Primary DENV3	39	<25	374	640	3172	362	-
B1_0006	Primary DENV3	211	<25	89	308	4735	82	-
B1_0003	Secondary DENV	217	<25	797	122	304	72	-
B1_0016	Secondary DENV	172	<25	232	3222	2051	74	-
B1_0023	Secondary DENV	92	<25	4417	1693	380	<25	-
B1_0024	Secondary DENV	146	<25	1395	1362	505	299	-
B1_0026	Secondary DENV	46	<25	2848	1876	635	292	-
B1_0033	Secondary DENV	91	220	3123	1996	843	197	-
B1_0034	Secondary DENV	111	<25	193	568	939	76	-

[a] FRNT-50 based on maternal plasma 3 months after delivery
[b] Likely false positive ZIKV RT-PCR result

Table 2.4 ZIKV and DENV serotype specific humoral immune profile. Serologic classification of maternal flavivirus infection history was determined by focus reduction neutralization titer 50% (FRNT-50) against ZIKV and DENV in plasma taken at delivery. ZIKV RT-PCR performed on serum collected at enrollment. NA=Not Available

Subject		Placental Histology Findings
ZIKV infected		
B1_0001		Villitis was not observed
B1_0002		Villitis was not observed
B1_0004		Villitis was observed in two foci, consistent with mild, low grade, chronic villitis of unknown etiology, occurrence of stromal fibrosis and occurrence of necrosis
B1_0005		Villitis was not observed
B1_0007		Villitis was not observed
B1_0008		Villitis was not observed
B1_0031		Villitis was not observed
B1_0027		Villitis was observed in two foci, consistent with mild, low grade, chronic villitis of unknown etiology
B1_0030		Villitis was observed in one focus, consistent with mild, low grade, chronic villitis of unknown etiology
B1_0014		Villitis was observed in two foci, consistent with mild, low grade, chronic villitis of unknown etiology and occurrence of stromal fibrosis
B1_0037		Villitis was observed in one focus, consistent with mild, low grade, chronic villitis of unknown etiology
ZIKV uninfected		
B1_0003		Villitis was not observed
B1_0009		Villitis was not observed
B1_0033		Villitis was not observed
B1_0026		Villitis was not observed
B1_0023		Villitis was not observed
B1_0016		Villitis was not observed
B1_0034		Villitis was not observed
B1_0015		Villitis was not observed

Table 2.5 Placental Pathology: In 5 of 11 ZIKV-infected cases, focal villitis was observed as defined by less than 10 villi per focus.

CHAPTER 3 – PROGESTERONE CONTROLS SUSCEPTIBILITY TO ZIKA VIRUS INFECTION IN THE VAGINA OF MICE[2]

3.1 Summary

The unique ability of Zika virus (ZIKV) to be spread via vector-borne as well as sexual transmission raised many questions about cellular tropism, as well as innate and adaptive immune control. The skin has been studied as the inoculation site for flaviviruses but the vagina contains many unique immune mechanisms which had not previously been investigated with regards to flaviviruses. Mucins and antibody complexes provide an additional barrier before viruses can access the vaginal epithelium and interferon-λ (IFN-λ) can restrict viral infections at epithelial barriers. ZIKV generally replicates poorly in wild-type mice due to an inability to antagonize interferon signaling in mice, so ZIKV pathogenesis studies typically employ *Ifnar1*$^{-/-}$ mice or otherwise ablate type I interferon (IFN-αβ) signaling. Yet in this study, we confirmed previous reports that ZIKV can infect wild-type mice intravaginally even when these mice are not susceptible to systemic infection. In contrast to a previous report, we did not find that IFN-λ signaling restricts intravaginal ZIKV infection in contrast with a previous report. Rather, progesterone appears to control whether ZIKV infection can proceed in either wild-type or IFN-αβ-signaling deficient mice. The mechanism by which progesterone makes mice susceptible does not appear to be due to a DMPA-induced

[2]The work presented in this chapter will be published as Lopez CA, Dulson SJ, Carbaugh DL, Lazear HM. Progesterone regulates Zika virus infection in the vagina. Manuscript in progress.
I performed all mouse infections, neutralization assays, virus purification, and growth curves.

thinned weaker epithelium being more susceptible to a tear resulting from the instillation because vaginal abrasion did not render mice susceptible to vaginal infection in the absence of progesterone treatment. We considered that progesterone might modulate the vaginal immune milieu, but found that exogenous progesterone did not diminish IFN-stimulated gene expression or change leukocyte populations in vaginal tissue. Our data suggest that progesterone regulates antiviral immunity in the vagina, though the mechanism remains to be determined.

3.2 Introduction

The unprecedented size of the 2015-2016 Zika virus pandemic in the Americas (millions of people infected[8–10]) revealed new disease manifestations and transmission mechanisms[11]. This ZIKV outbreak was associated with cases of microcephaly and a constellation of other congenital defects now established to be caused by congenital ZIKV infection[11–13]. This outbreak also confirmed the ability of ZIKV to spread via sexual transmission in addition to mosquito-borne transmission, although ZIKV sexual transmission had been reported previously following infection in Africa[16–19]. Flaviviruses are transmitted to humans by arthropod vectors (mosquitoes and ticks), and ZIKV is the first example of a flavivirus that spreads between humans via sexual transmission [321–323]. The best evidence that ZIKV is sexually transmitted is travel-associated cases in the United States, Europe, and elsewhere, wherein women without mosquito exposure became infected after their male partners returned from ZIKV-endemic areas[15,17,114,323–327]. Of ZIKV cases acquired within the continental United States since 2016, close to 20% were acquired through presumed sexual transmission[328]. Of 5,483 travel-associated ZIKV cases in the US since 2015, 52 resulted in confirmed transmission to a

sexual partner. Though this represents only 1% of ZIKV cases in the US with forward sexual transmission, this is likely an underestimate of the rate at which ZIKV-infected men transmit to their partners, since ~80% of ZIKV infections are asymptomatic[317] and screening was focused on symptomatic women with travel-related exposure. The first report of ZIKV sexual transmission pre-dates the 2015-2016 epidemic and resulted from ZIKV infection in Africa[323], suggesting that sexual transmission is a general property of ZIKV, not a new trait coincident with its emergence in the Americas. The ability of ZIKV to spread via sexual transmission in addition to mosquito-borne transmission expands the geographic range over which ZIKV transmission can occur, could change the epidemiology of ZIKV even in areas with mosquito-borne transmission, and has the potential to produce distinct pathologic outcomes if congenital infection occurs via an ascending route rather than a hematogenous transplacental route. Thus, it is important to understand the antiviral mechanisms that ZIKV may encounter in the vagina that are distinct from antiviral mechanisms present at the skin following mosquito inoculation.

The mucosal environment of the vagina contains specialized mechanisms not typically encountered by mosquito-borne viruses. For example, antibodies at mucosal surfaces can access additional protective mechanisms not available to antibodies in the circulation. In mice, prior ZIKV infection protects against vaginal ZIKV infection and is largely antibody-mediated despite low levels of ZIKV IgG in vaginal mucus[159]. This protective effect of low IgG concentrations in the vagina is in contrast to mosquito-borne transmission, where protection requires virus neutralization[42]. A single IgG molecule has transient interactions with mucins, but multiple IgG molecules bound to the same particle (e.g. a virus) can immobilize that particle through the combined affinity of

multiple IgG-mucin interactions[148–151]. The antibody response after DENV infection includes antibodies that bind to ZIKV virions (cross-reactive) but do not render those virions non-infectious (non-neutralizing)[250,251,256]. If ZIKV is trapped by antibody-mucin complexes, cross-reactive antibodies could provide additional protection against sexual transmission of ZIKV in DENV endemic regions.

ZIKV replication is restricted by the IFN response in mice because ZIKV is unable to antagonize mouse STAT2 and STING[141,329]. Thus, mouse models of ZIKV pathogenesis typically employ mice lacking IFN-αβ signaling, usually through genetic loss of the IFN-αβ receptor (*Ifnar1*$^{-/-}$) alone or in combination with the IFN-γ receptor[128,134], or by treatment of wild-type (WT) mice with an IFNAR1-blocking monoclonal antibody (MAR1-5A3)[129]. Treatment with MAR1-5A3 results in increased ZIKV viremia (with higher antibody doses producing higher viremia) but does not elicit the weight loss and lethality observed in *Ifnar1*$^{-/-}$ mice[134], implying that partial loss of IFNAR1 activity may allow sufficient ZIKV replication to study pathogenic phenotypes.

Antiviral signaling in the vagina includes a role for type III interferons (IFN-λ) in addition to the type I and II IFNs involved in systemic antiviral responses[160]. IFN-λ signals through a different receptor on the cell surface but activates many of the same signaling pathways and transcriptional responses as IFN-αβ. Despite the similarities, IFN-λ can also perform unique restriction of viruses independent of other IFN signaling pathways[161]. IFN-λ restricts HSV infection in the vagina[162] and may also play a role in restricting ZIKV infection in the vagina of ovariectomized mice in a model where the hormonal state is tightly controlled by hormone replacement[129].

The ZIKV mouse vaginal infection model includes pre-treating mice with progesterone and is based on the infection models for other sexually transmitted pathogens such as herpes simplex virus (HSV) and *Chlamydia muridarum*[177,178]. The mechanism by which progesterone makes mice susceptible to ZIKV remains unknown, but it has been hypothesized to be due to a combination of increased inflammatory infiltrate that may be susceptible to ZIKV infection, thinned epithelium, or deficiencies in antiviral signaling due to decreased expression of antiviral sensing genes[128,183].

Many studies have evaluated ZIKV vaginal infection in mouse models, but these typically have used mice lacking IFN-αβ signaling, the same models that are used to study ZIKV pathogenesis by footpad and other inoculation routes because these mice are permissive to disseminated infection including fetal pathology with either footpad or intravaginal inoculation[99,128,129,134,135,330]. Here we first use that model to study whether there is a role for mucus-IgG trapping of virions. However, we then move into a WT mouse infection model under the assumption that they are less susceptible to ZIKV infection. We show that although WT mice largely are resistant to ZIKV infection via footpad inoculation, vaginal inoculation results in productive local ZIKV replication equivalent to that found in *Ifnar1*$^{-/-}$ mice. In contrast to previous work by others, we did not find that IFN-λ signaling restricts intravaginal ZIKV infection. We further show that permissiveness to vaginal ZIKV replication is determined by hormonal status, even in mice lacking IFN-αβ signaling, suggesting that hormone variation can regulate susceptibility to viral infection in the vagina independently from the IFN-dependent restriction of systemic ZIKV infection. Additionally, we show that pregnancy, another high progesterone state, is also sufficient for vaginal ZIKV infection in wild-type mice.

The mechanism by which progesterone makes mice susceptible to vaginal ZIKV infection does not appear to be due to thinned or weaker epithelium as vaginal abrasion did not render mice susceptible to vaginal infection in the absence of progesterone treatment. We considered that progesterone might modulate the vaginal immune milieu, but found that exogenous progesterone did not diminish IFN-stimulated gene expression or change leukocyte populations in vaginal tissue. Our data suggest that progesterone regulates antiviral immunity in the vagina, though the mechanism remains to be determined.

3.3 Materials and methods

Cells and viruses

Vero cells were maintained in Dulbecco's modified Eagle Media (DMEM) supplemented with 5% heat-inactivated fetal bovine serum (FBS) and L-glutamine at 37°C with 5% CO_2. ZIKV strain H/PF/2013 was obtained from the U.S. Centers for Disease Control and Prevention[331]. Spondweni virus (SPOV) strain SA AR 94 and Usutu virus (USUV) strain SA AR 1776 were obtained from the World Reference Center for Emerging Viruses and Arboviruses[332,333]. DENV3 WHO reference strain (CH54389) was provided by Dr. Aravinda de Silva (UNC)[334,335], and RUBV strain M33 was obtained from Dr. Michael Rossmann (Purdue University)[336]. Liver homogenate from HAV infected mice was provided by Dr. Stanley Lemon (UNC)[337].

Flavivirus and RUBV stocks were grown in Vero cells in DMEM supplemented with 2% FBS and HEPES and titered by focus forming assay (FFA)[338]. Virus was serially diluted in duplicate in DMEM supplemented with 2% FBS and HEPES and added to confluent Vero cells in 96 well plates for 1-3 hours at 37°C with 5% CO_2 before

being overlaid with 1% methylcellulose in minimum essential Eagle medium (MEM) supplemented with 2% FBS, HEPES, and penicillin and streptomycin. Cells were then incubated for 40-45 hours at 37°C with 5% CO_2 before being fixed with 2% paraformaldehyde for 1 hour at room temperature. Cells were then rinsed with 0.05% Tween-20 in PBS and then incubated for 2 hours at room temperature or overnight at 4°C with 1µg/mL mE60, which recognizes the conserved flavivirus fusion loop[284]. in a saponin buffer to permeabilize the cells. Following another rinse, cells were then incubated in a 1:5000 dilution of a horseradish peroxidase (HRP) conjugated goat anti-mouse IgG (Sigma). Titration of RUBV was performed similarly but with a polyclonal anti-RUBV goat IgG at 1:4000 (LifeSpan BioSciences, LS-C103273) and a HRP conjugated anti-goat IgG at 1:5000(Sigma). Color was then developed for 30 minutes in TrueBlue substrate (KPL). Foci were quantified with a CTL Immunospot Analyzer.

UV-inactivated ZIKV was generated by placing 200µL ZIKV H/PF/2013 at 1 x 10^6 FFU/mL in a petri dish and exposing to UV light at 0.9999 J/cm^2 for 10 minutes at room temperature. Mock-inactivated ZIKV was generated similarly, but placed under light in a biosafety cabinet instead of UV-light. Inactivation was confirmed by amplifying UV- and mock-treated virus stocks on Vero cells for 4 days and then titering by FFA.

Fluorophore-labeled ZIKV and imaging in mucus

ZIKV was grown in C6/36 cells at 28°C in DMEM supplemented with 2%FBS and HEPES at an MOI of 0.01. Supernatant was collected at day 4, 6, and 8, stored at 4°C and replaced with fresh media. Virus supernatant was then concentrated using 100 kD Centricon Plus-70 filters (UFC710008), then centrifuged through a continuous 15-60% sucrose gradient for 17 hours at 17,000 x g at 4°C. The most concentrated fractions

were determined by measuring the quantity of viral genomes by qRT-PCR and infectious particles by FFA. Purified virus was then labeled with a succinimidyl ester dye, Alexa Fluor 555 (Cat# A20009) according to manufacturer instructions.

Vaginal mucus collection

Vaginal mucus was collected under the approval of University of North Carolina (UNC) Institutional Review Board (IRB) #10-1817. Local North Carolina volunteers self-collected vaginal mucus by inserting a disposable menstrual cup for 60 seconds and placing the cup into a 50mL conical which was then centrifuged at 230 x g. Mucus was then collected and stored at 4°C and used within 3 days. All samples were confirmed to have pH <4.5 and were negative for bacterial vaginosis by microscopic inspection.

Imaging of ZIKV particles in vaginal mucus

ZIKV was mixed with 5 μg/ml of monoclonal IgG and incubated for 15 minutes at room temperature. Particles were visualized with an inverted epifluorescence microscope (AxioObserver D1, Zeiss). Particle paths were tracked with MetaMorph software. At least 150 particles were tracked for each vaginal mucus sample at each antibody condition.

Antibodies used in mucus experiments

HSV-targeting mouse monoclonal antibodies MC14 and DL11 were obtained courtesy of Dr. Gary Cohen (University of Pennsylvania)[339,340]. ZIKV-targeting mouse monoclonal antibodies were obtained courtesy of Dr. Michael Diamond (Washington University in St. Louis)[34] and produced from hybridomas by the UNC Protein Expression Core Facility.

Mouse infections

All mouse husbandry and experiments were performed with approval of the University of North Carolina at Chapel Hill's Institutional Animal Care and Use Committee. All mice used were on a C57BL/6J background, except BALB/cJ mice used for HSV infections. *Ifnar1*$^{-/-}$ mice were originally obtained from Dr. Jason Whitmire (UNC) and were bred on site. WT mice were either bred on site or purchased from Jackson Laboratory. BALB/cJ mice were also purchased form Jackson Laboratory Unless otherwise indicated, 5-10 week old female mice were subcutaneously injected with 2mg depot medroxyprogesterone acetate (DMPA)[128,182,183] obtained via the UNC pharmacy, diluted in 100µl of PBS. 5 days later, mice were challenged with 1000 FFU of virus in 5µL via vaginal instillation or 50µl via footpad. Vaginal abrasion was accomplished by scrubbing the vagina of isoflurane-anesthetized mice with an interdental brush[341] (GUM Proxabrush Go-Betweens tight-sized cleaners) a total of 10 combined full rotations and insertions. For experiments where mice were vaginally infected with virus-antibody complexes, we premixed equal volumes of 1000 FFU ZIKV or HSV and IgG at a concentration of 5µg/mL for 1 hour at 37°C. The virus-antibody mixture was then inoculated by vaginal instillation in 20µL.

Vaginal washes were collected in a total of 100 µl by twice pipetting 50 µl of PBS with 0.4x protease inhibitor (cOmplete, EDTA-free) into the vagina and collecting immediately, every 2 days after infection. Blood was collected into serum blood collection tubes (BD) days 2 and 6 after infection via submandibular bleed with a 5 mm Goldenrod lancet or via terminal bleed cardiac puncture. Serum was separated at 8000 rpm for 5 minutes. Tissues were collected from mice after euthanasia by isoflurane

overdose, cardiac bleed, and perfusion with 5-10 mL PBS. Tissues, vaginal washes, and serum were stored at -80°C until RNA extraction.

For experiments where we investigated the responsiveness of tissues to immunogenic RNA, we first treated 5-6 week old mice with either PBS or 2mg DMPA subcutaneously. Four days later, mice were treated with 50 µg polyinosinic:polycytidylic acid (pI:C), low molecular weight (Invivogen, TLRL-Picw) either intraperitoneally in 100µL or intravaginally in 20µL.

Generation of IFN-λ receptor knock out mice

Mice with a floxed allele of the IFN-λ receptor (*Ifnlr1*$^{f/f}$) were received from Dr. Herbert Virgin (Washington University in St. Louis). *Ifnlr1*$^{f/f}$ mice were crossed with mice expressing Cre recombinase under the β-actin promoter (Jackson Labs # 019099, obtained from Dr. Jenny Ting, UNC) to generate *Ifnlr1*$^{f/f}$ mice with ubiquitous Cre recombinase expression from a hemizygous Cre allele (resulting in *Ifnlr1*$^{-/-}$). These mice were then crossed with *Ifnlr1*$^{f/f}$ mice to generate litters in which 50% of pups lacked IFN-λ signaling (*Ifnlr1*$^{-/-}$, Cre+) and 50% retained it (*Ifnrl1*$^{+/-}$, Cre-). Females were used for vaginal infection experiments which were conducted in a blinded manner, as genotyping for *Cre* and *Ifnlr1* was performed after the experiment was completed.

Mice were genotyped from DNA extracted from tails. The actin-Cre allele was amplified with forward primer Cre-3 (GCGGTCTGGCAGTAAAAACTATC) and reverse primer Cre-4 (GTGAAACAGCATTGCTGTCACTT) at 94°C for 3 minutes followed by 35 cycles of 94°C for 15 seconds, 62°C for 20 seconds, and 68°C for 1 minute. The floxed *Ifnlr*$^{-/-}$ allele was amplified with forward primer Ifnlr1F1 (AGGGAAGCCAAGGGGATGGC) and two reverse primers Ifnlr1R1

(AGTGCCTGCTGAGGACCAGGA) and Ifnlr1R3 (GGCTCTGGACCTACGCGCTG) at 94°C for 3 minutes followed by 35 cycles of 94°C for 15 seconds, 60°C for 20 seconds, and 68°C for 1 minute. Amplicons were then run on 2% agarose gels.

Quantifying RNA and neutralization titers

RNA from vaginal washes and serum was extracted with the Qiagen viral RNA minikit. RNA from tissues was extracted with the Qiagen RNeasy minikit after homogenization in a MagNA Lyser instrument (Roche Life Science) with zirconia beads (BioSpec) in 600µl PBS followed by incubation at room temperature for 10 minutes in an equal volume RLT buffer for lysis. Viral genomes were quantified by Taqman one-step qRT-PCR on a CFX96 Touch real-time PCR detection system (BioRad) and were reported on a $\log_{10}$ scale measured against standard curves from either a ZIKV A-plasmid as previously described[291], or from 400 bp gBlock double stranded DNA fragments (Integrated DNA Technologies, IDT). ZIKV RNA was quantified as previously published[278,291] and other viruses with the gBlocks and primers in Tables 3.1 and 3.2.

RNA from tissues was quantified after extraction as above with the primers in Table 3.2. To quantitate the expression of *Ifit1* in each tissue, the difference in Ct values between *Ifit1* and *ActB* as a housekeeping gene was calculated for each tissue sample and plotted as -ΔCt.

Neutralization assays were performed by FFA as previously described[342]. Virus was first diluted to 50 focus-forming units per well and incubated with serial dilutions of heat-inactivated serum from mice (inactivated at 56°C for 30 minutes) in DMEM supplemented with 2% FBS and HEPES. The virus-antibody mixtures were then incubated at 37°C in 5% CO_2 for 1 hour before being added to Vero cells and proceeding

with the FFA protocol as above. Neutralization data was quantified by determining the number of foci at a given dilution of naïve mouse serum and determining the percentage of foci present at that same dilution of sera from infected animals. Neutralization curves were generated in Graphpad Prism with the log (inhibitor) vs response curve function with variable slope, setting the lower and upper bounds of relative infectious particles to 0% and 100%. A valid FRNT-50 curve required an R^2 >0.75, hill slope absolute value >0.5, and had to reach at least 50% relative infection within the range of the serum dilutions in the assay.

In situ hybridization

Tissues were collected from euthanized mice after exsanguination cardiac puncture, perfusion with 10 mL of PBS followed by 10 mL of 10% neutral buffered formalin (NBF). Tissues were then stored overnight in 1mL of 10% NBF at 4°C before being transferred to PBS at 4°C for longer term storage. Tissues were then sliced at a 5µm mm thickness by the University of North Carolina at Chapel Hill Histology Research Core and stained with a ZIKV-specific RNA probe (ACDBio, #467871)[118,120,129,343] and a hematoxylin counter-stain. Positive and negative staining controls for RNA-specific staining were confirmed with probes against peptidyl-prolyl cis-isomerase B (PPIB, #321651) and dihydrodicipicolinate reductase (dapB, #320751) as recommended by the manufacturer.

Flow cytometry

Spleens and iliac lymph nodes (iLNs) were mechanically dissociated and red blood cells were lysed using RBC lysis buffer (0.84% NH_4Cl in PBS). Cells were pelleted by centrifugation and resuspended in media (RPMI 1640 with 1% FBS). Cells

were filtered through a 70-μm cell strainer to make a single-cell suspension. Cells were resuspended in media at a concentration of $1x10^7$ cells/mL for flow cytometric analysis.

Murine vaginal tissue was excised, minced with scissors, and digested in HBSS (with Ca^{2+} and Mg^{2+}) containing 1mg/mL collagenase I and 0.05mg/mL DNAse I for 60min at 37°C in a shaking incubator. After incubation, 1mL FBS was added to stop digestion and cells were serially filtered through a 70- and 40-μm cell strainer and washed with HBSS (with Ca^{2+} and Mg^{2+}). Cells were centrifuged and resuspended in media at a concentration of $1x10^7$ cells/mL for flow cytometry analysis.

Isolated cells were stained in PBS with 1% FBS for 20–30 min in the dark on ice. Fc receptor blockade was performed with anti-CD16/32 mAb prior to surface staining. Dead cells were excluded from analysis using Zombie UV (BioLegend). Cells were fixed in 2% paraformaldehyde, and samples were acquired using an LSRII flow cytometer (UNC Flow Cytometry Core Facility) using fluorescence-minus-one compensation controls. Data were analyzed using FlowJo software (Tree Star).

The following markers were used to identify immune cell populations: T cells (CD45+CD3e+), B cells (CD45+CD19+), NK cells (CD45+NK1.1+), dendritic cells (CD45+CD11c+), neutrophils (CD45+CD11b+Ly6G+), and monocytes (CD45+CD11b+Ly6G-Ly6C+/-).

The following antibodies were used in this study: anti-CD16/32 (clone 2.4G2; BD Biosciences), anti-CD45 AF700 (clone 30-F11; BioLegend), anti-CD3e APC-Fire/750 (clone 17A2; BioLegend), anti-CD19 PE-Cy7 (clone 6D5; BioLegend), anti-NK1.1 PE (clone PK136; BioLegend), anti-CD11b APC (clone M1/70; BioLegend), anti-CD11c

BV650 (clone N418; BioLegend), anti-Ly6G FITC (clone IA8; BioLegend), and anti-Ly6C BV605 (clone HK1.4; BioLegend).

Statistical analysis

Statistical tests were performed with Graphpad Prism 9.0. Tests used include unpaired multiple Mann-Whitney analyses with the Holm-*Šídák* method and two-way ANOVA with matched time points where multiple time points of the same mouse were taken, the Geisser-Greenhouse correction for lack of sphericity, comparison to control cell means, and the Dunnett correction for multiple comparisons.

3.4 Results

Evaluating whether ZIKV may be immobilized in human vaginal mucus in an IgG-dependent fashion

To evaluate if ZIKV could be immobilized in vaginal mucus in the presence of binding IgG, we first generated fluorescently-labelled ZIKV virions to use in microscopy assays. We purified ZIKV by density gradient and then covalently labelled with a fluorescent dye. Individual labeled particles were then tracked via inverted epifluorescence microscopy in the presence of monoclonal human antibodies in fresh vaginal mucus from human donors. Mucus donors were North Carolina residents and thus unlikely to have antibodies against ZIKV or closely related flaviviruses, although we did not ascertain the flavivirus immune status of the donors. We observed that in the presence of either of two cross-reactive DENV antibodies (1M7 and C8), ZIKV particles diffused through vaginal mucus at a slower speed than in the presence of a non-binding monoclonal antibody (VRC01 which targets HIV) or no exogenous antibodies (Figure 3.1A). The percentage of fast-moving particles was determined, defining fast-moving as

capable of diffusing through a 50μm mucus layer in 30 minutes (Figure 3.1B), the same expected thickness of mucus overlying the vaginal epithelium in humans[344]. However, subsequent experiments did not yield similar results and it was too challenging to produce labeled virions without aggregation so we did not continue to pursue this avenue of investigation.

Non-neutralizing IgG do not protect against intravaginal ZIKV infection

Microscopy studies suggested human vaginal mucus could lead to decreased transmissibility of ZIKV in the presence of ZIKV-binding IgG (e.g. from a prior DENV infection). To test this in an animal model, we challenged *Ifnar1*$^{-/-}$ mice intravaginally with ZIKV premixed with either a neutralizing or non-neutralizing monoclonal mouse IgG that bind ZIKV (Figure 3.2A-B). Five days prior to infection, mice were treated with depot medroxyprogesterone acetate (DMPA) by subcutaneous injection, as is standard in infection models for HSV, *Chlamydia*, and ZIKV[128,177,178]. We observed no difference in either the number of mice that become infected or in viral load in vaginal washes or serum in mice treated with the non-neutralizing monoclonal antibody, but a ZIKV-neutralizing antibody did provide protection from infection. These results were in contrast to prior studies showing that a non-neutralizing antibody provided protection from HSV vaginal infection in BALB/c mice[153]. To test this effect in our hands, we infected BALB/c mice intravaginally with HSV-1 that had been pre-incubated with a potently neutralizing monoclonal antibody (DL11) or a non-neutralizing one (MC14) and found that the non-neutralizing antibody provided minimal protection from HSV-1 infection (Figure 3.2C). The difference between our observations and other studies could be due to the HSV-1 strain used, the specific monoclonal antibodies tested, or

other factors. We next considered whether the lack of protection we observed with non-neutralizing antibodies was because the *Ifnar1*$^{-/-}$ mice we used for ZIKV studies were highly susceptible, limiting our ability to observe modest protection phenotypes. To assess whether a protective effect for non-neutralizing antibodies in the vagina might be more apparent in WT mice, we first determined the infectious dose needed to infect WT mice by vaginal inoculation, with the expectation that WT mice would be less susceptible to ZIKV infection (Figure 3.2D)[134]. Unexpectedly, we found robust ZIKV replication in the vaginas of mice inoculated with 1000 FFU (the standard infectious dose used in studies with *Ifnar1*$^{-/-}$ mice) and no significant increase in viral loads when mice were inoculated with 10,000 FFU. We then tested whether non-neutralizing antibodies could protect against intravaginal ZIKV inoculation in WT mice by premixing ZIKV with potently neutralizing (ZV-67) or non-neutralizing (4G2) mouse monoclonal antibodies, but still found that non-neutralizing antibodies did not protect against vaginal ZIKV infection (Figure 3.2E).

ZIKV productively replicates in the vaginas of WT mice

Given the important role for IFN-αβ signaling in controlling ZIKV infection in mice, we were surprised to observe robust ZIKV replication in the vaginas of WT mice. To investigate this further, we pre-treated WT and *Ifnar1*$^{-/-}$ mice with DMPA then 5 days later infected with 1000 FFU of ZIKV via intravaginal instillation. We observed similar ZIKV replication kinetics and RNA burden in the vagina of WT compared to *Ifnar1*$^{-/-}$ mice from 2 days post-infection (dpi) through 8 dpi (Figure 3.3A). Although WT mice supported ZIKV replication in the vagina, they did not support systemic infection as viremia was detected only in *Ifnar1*$^{-/-}$ mice (Figure 3.3B). Likewise, *Ifnar1*$^{-/-}$ mice

supported ascending infection into the upper female reproductive tract (uterus, ovary, and oviduct) whereas ZIKV infection in WT mice was restricted to the lower female reproductive tract (vagina and cervix) (Figure 3.3C). These results show that ZIKV can replicate in the vagina of WT mice, but that IFN-αβ signaling restricts systemic spread.

We found that the amount of ZIKV RNA in vaginal washes increased over time, consistent with productive viral replication, but we were not able to detect infectious ZIKV by FFA directly from vaginal washes collected in PBS. When we instead collected vaginal washes in DMEM with 2% FBS on days 2, 4, 6, and 8 and allowed the virus to amplify on Vero cells prior to titering, we did detect infectious ZIKV (Figure 3.4A) altogether consistent with low but productive ZIKV replication in the vagina. These observations also are consistent with our experience that ZIKV infectivity is not stable in unsupplemented PBS (Figure 3.4B).

To confirm that the ZIKV RNA we detected in vaginal washes represented replicating virus, we inoculated mice with either infectious ZIKV or UV-inactivated virus and measured viral RNA in vaginal washes collected 2 through 8 dpi. No ZIKV RNA was detected in vaginal washes from mice inoculated with UV-inactivated virus, further supporting that the viral RNA detected in vaginal washes results from productive infection (Figure 3.5A). Additionally, we collected serum from mice 14 days after ZIKV inoculation and measured neutralizing activity against ZIKV by focus reduction neutralization assay (Figure 3.5B). In one experiment, 2 of 3 mice inoculated with infectious ZIKV seroconverted but in a second experiment, 0 of 3 mice seroconverted. The mouse that did not seroconvert in the first experiment was the same mouse which had a ZIKV load in the vagina 1 hour post-infection, but did not have detectable ZIKV in

vaginal washes at any other timepoint, potentially indicating that productive replication did not occur in this mouse because ZIKV remained in the vaginal lumen. No mice challenged with UV–inactivated ZIKV had detectable FRNT-50 titers. Altogether, the neutralization assay data indicate that vaginal administration of inactivated ZIKV antigen is not sufficient to induce an antibody response, and that even productive ZIKV replication in the vagina did not consistently induce seroconversion by 14 days post-infection.

It has previously been reported that IFN-λ restricts ZIKV infection in the vagina, in the context of IFN-αβ signaling inhibited by administration of an IFNAR1-blocking antibody[129]. To test whether IFN-λ controls vaginal ZIKV infection in mice with intact IFN-αβ signaling, we treated *Ifnlr1*$^{+/-}$ and *Ifnlr1*$^{-/-}$ mice with DMPA and infected with 1000 FFU of ZIKV by intravaginal instillation. We measured viral loads in vaginal washes by qRT-PCR and found no significant difference between *Ifnlr1*$^{+/-}$ and *Ifnlr1*$^{-/-}$ mice, suggesting that IFN-λ signaling does not restrict ZIKV replication in the vagina in this model system (Figure 3.6).

A high-progesterone state is required for vaginal ZIKV infection.

Since we found that WT mice were susceptible to ZIKV infection via an intravaginal but not a subcutaneous inoculation route, we considered whether DMPA treatment rendered WT mice broadly susceptible to ZIKV infection. We treated WT mice with DMPA or PBS, then 5 days later infected with 1000 FFU of ZIKV via an intravaginal or subcutaneous route and measured viral RNA in vaginal wash and in serum by qRT-PCR. As expected, DMPA treatment increased the permissiveness of WT mice to intravaginal infection: ZIKV RNA was detected in the vaginal wash from 10 of 10 DMPA-

treated mice compared to only 5 of 10 PBS-treated mice (Figure 3.7A-B). DMPA-treated mice also sustained higher viral loads in the vagina than PBS-treated mice with RNA titers (DMPA-treated mice sustained as high as 100-fold higher viral loads in the vagina than PBS-treated mice). Consistent with previous experiments, DMPA-treated WT mice supported ZIKV replication in the vagina but no ZIKV RNA was detected in the serum following intravaginal inoculation. Furthermore, no ZIKV RNA was detected in the serum of mice inoculated by footpad regardless of DMPA treatment indicating that DMPA treatment was not sufficient to render WT mice broadly susceptible to ZIKV infection. Surprisingly, although *Ifnar1*$^{-/-}$ mice are considered to be highly susceptible to ZIKV infection, vaginal infection and systemic dissemination with ZIKV was dependent on DMPA treatment in these mice as well (Figure 3.7 C-D).

To determine if other high progesterone states also confer susceptibility to ZIKV replication in the vagina, we evaluated vaginal ZIKV infection in pregnant mice (without DMPA treatment). We mated 7-to-10-week old WT dams with WT sires and inoculated 7 days post-mating (roughly one-third of gestation) intravaginally with 1000 FFU of ZIKV. We collected vaginal washes and serum and measured ZIKV RNA by qRT-PCR to assess local replication in the vagina and systemic spread, and all mice were harvested at 8 dpi to assess congenital infection. Pregnant mice supported vaginal ZIKV replication (4 of 5 pregnant mice) but ZIKV RNA was not detected in the vaginal lavage of non-pregnant mice (0 of 12 mice) (Figure 3.8A). Consistent with our observations in DMPA treated WT mice, pregnant WT mice did not support systemic ZIKV spread, as ZIKV RNA was not detected in serum, even in the context of robust replication in the vagina (Figure 3.8B). Additionally, ZIKV RNA was detected in only 1 of the 40 placentas

and none of the corresponding fetuses (Figure 3.8C), consistent with the lack of ascending or systemic infection we observed after vaginal ZIKV inoculation in DMPA-treated WT mice. Altogether these data suggest that a high progesterone state (DMPA treatment or pregnancy) is required for vaginal permissiveness to ZIKV infection.

A physically compromised vaginal epithelial barrier is not sufficient to render WT mice susceptible to ZIKV infection.

The vaginal epithelium of mice in diestrus, the high progesterone state of the estrus cycle, is thinned and lacks the keratinized layer protecting the vaginal epithelium during the estrus phase[128,172,345]. Since DMPA induces a diestrus-like state, it has been hypothesized that a thinned epithelial barrier is more easily targeted by ZIKV, explaining the susceptibility of WT mice to vaginal ZIKV infection following DMPA treatment. To test whether an impaired epithelial barrier could overcome the requirement for DMPA treatment, we abraded the vaginal epithelium with an interdental brush prior to intravaginal inoculation with 1000 FFU of ZIKV and measured ZIKV RNA in vaginal washes by qRT-PCR. However, vaginal infection was only detected in mice that were treated with DMPA, regardless of vaginal abrasion (Figure 3.9A) suggesting that physical access to epithelial cells is not sufficient for productive ZIKV infection in the vagina. Vaginal abrasion also did not facilitate ZIKV dissemination as ZIKV RNA was not detected in serum even of abraded mice (Figure 3.9B). In DMPA-treated mice, abrasion did not result in higher viral loads in vaginal washes, altogether suggesting that compromised epithelial barrier integrity is not the mechanism by which DMPA treatment promotes vaginal ZIKV infection.

The vagina is permissive to replication of diverse IFN-αβ-restricted flaviviruses.

ZIKV is unique among flaviviruses in its ability to spread among humans via both vector-borne (mosquito) and vector-independent (sexual) transmission routes. To assess whether this reflects an unusual vaginal tropism of ZIKV, we evaluated vaginal infection with 3 additional flaviviruses, Spondweni virus (SPOV), Usutu virus (USUV), and dengue virus (DENV). SPOV and DENV are closely related with ZIKV, wheras USUV is more distant. These flaviviruses were selected because, like ZIKV, they replicate poorly in WT mice. WT mice were treated with DMPA 5 days prior to intravaginal inoculation with 1000 FFU of ZIKV, SPOV, USUV, or DENV3 and viral RNA was measured by qRT-PCR from vaginal washes on days 2, 4, 6, 8 (Figure 3.10). Viral RNA was detected in vaginal washes after ZIKV, USUV, and SPOV infection, suggesting that these viruses could replicate in the vagina of WT mice and at levels similar to ZIKV. In contrast, DENV3 RNA was not detected. To test whether the vagina is permissive to other RNA viruses that generally are restricted by innate antiviral responses in WT mice[337], we inoculated WT mice intravaginally with 1000 FFU of rubella virus (*Matonaviridae*) or 5µl of mouse liver homogenate containing 5 x 10^8 genome equivalents of hepatitis A virus (*Picornaviridae*), but detected no viral RNA in vaginal washes at any of the time points evaluated through 8 days post-inoculation (data not shown). Altogether, these data show that vaginal infection is not a unique property of ZIKV among flaviviruses. Rather, in WT mice the vagina is more permissive to flavivirus replication compared to other inoculation sites, but does not allow unrestricted replication of all RNA viruses.

DMPA treatment does not inhibit ISG expression

It has previously been reported that the mouse lower female reproductive tract (LFRT, vagina and cervix) expresses lower levels of viral RNA pattern recognition receptors (PRRs) compared to the upper female reproductive tract (UFRT, uterus, ovaries, and ovarian ducts) regardless of DMPA treatment[183]. Therefore this treatment does not explain why DMPA is required for ZIKV infection in the vagina or whether these differences in PRR expression lead to functional differences in downstream IFN-stimulated gene (ISG) expression. To determine for ourselves whether the previously observed decreased expression of viral RNA pattern recognition receptors (PRRs) after DMPA treatment leads to decreased ISG expression, we treated mice with pI:C intravaginally or intraperitoneally with or without DMPA pre-treatment and measured expression of *Ifit1*, an ISG that is highly induced by viral infection and PRR signaling. We did not observe any DMPA-dependent change in *Ifit1* induction in the spleen or LFRT following intravaginal or intraperitoneal pI:C stimulation (Figure 3.11A-B). In the UFRT, DMPA increased *Ifit1* expression at baseline and induction in response to intravaginal pI:C treatment (Figure 3.11C). Additionally, the expression of IFIT1 does not appear to be different between the LFRT, spleen, and UFRT under any condition (Figure 3.11 A-C) Altogether, these results suggest that DMPA treatment does not promote ZIKV vaginal infection by broadly inhibiting ISG expression in the vagina.

ZIKV infection in the vagina is localized to the epithelium

To better define the location of infected cells in the vagina, we harvested vaginal tissue 2 to 10 dpi and detected ZIKV RNA using *in situ* hybridization (RNAscope) (Figure 3.12). ZIKV positive cells were rare and sporadically distributed in the vagina,

but they tended to be clusters of adjacent epithelial cells located along the vaginal lumen although there was some positive staining in the parenchyma as well. 0 of 3 mice contained positive staining at 2 dpi, 1 of 2 at 4 dpi, 3 of 3 at 6 dpi, 2 of 2 at 8 dpi, and 0 of 5 at 10 dpi. The largest clusters of infected cells were detected at 6 dpi. There was no tendency for infected cells to be nearer to the cervix or nearer to the vaginal opening. No sections from infected mice exhibited leukocyte infiltrate into to the vaginal tissue relative to uninfected DMPA treated mice. Altogether, these results indicate that ZIKV infection in the vagina primarily targets epithelial cells (rather than the leukocytes that are the main targets of ZIKV systemic infection) and that infected cells are not associated with a pronounced immune infiltrate.

DMPA does not induce changes in the number of leukocytes in the LFRT or secondary lymphoid tissue

We next determined if the numbers of specific leukocyte populations were changed after DMPA treatment or ZIKV infection in either the LFRT, spleen, or iLN. We treated WT mice with DMPA or PBS and 5 days later some DMPA-treated mice were also infected with ZIKV. At 6 days post-infection, LFRT tissue, iLN, and spleen were collected and leukocytes isolated for immunophenotyping. We found that ZIKV infection caused an increase in the number of B cells in secondary lymphoid tissues relative to mice only treated with DMPA (Fig. 3.13A-B). In the LFRT, greater numbers of dendritic cells were observed after ZIKV infection (Fig. 3.13C). However, DMPA treatment alone caused no change in T cells, NK cells, B cells, dendritic cells, eosinophils, monocytes, or neutrophils in any of these tissues (Fig. 3.13A-C). In the spleen and iLN, These

results suggest that DMPA-induced susceptibility to vaginal ZIKV infection does not result from a dramatic change in the immune milieu of the vagina.

Altogether, our data show that although WT mice generally do not support ZIKV replication, the vagina is an unique site that supports the replication of ZIKV (and other flaviviruses) in WT mice and the immune system is able to clear the localized infection. The ability of ZIKV to replicate in the vagina of WT mice requires a high progesterone state (pregnancy or DMPA treatment) but the mechanism by which progesterone promotes ZIKV vaginal infection remains unclear.

3.5 Discussion

The emergence of ZIKV in Latin America in 2015-2016 not only revealed new severe disease manifestations but also confirmed a prior report of sexual transmission as an additional mode of transmission for ZIKV, making ZIKV the first arbovirus demonstrated to spread between humans through sexual contact. Most ZIKV cases in the Americas are presumed to be due to transmission via mosquitoes, but sexual transmission may still represent a significant transmission mechanism. It is difficult to estimate to the extent to which sexual transmission contributes to ZIKV transmission in areas with frequent and concurrent mosquito-borne transmission. However, a retrospective study of ZIKV serology in Brazil found that cohabitants with a ZIKV seropositive sexual partner had a 4-fold greater risk of also being seropositive compared to cohabitating with a ZIKV-seronegative partner. Cohabitating with a ZIKV-seropositive non-sexual partner was associated with less than a 2-fold greater risk, supporting a role for sexual transmission even in areas with mosquito-borne transmission[346]. Sexual transmission may thus have contributed to the high force of

infection of ZIKV in this epidemic even in Latin America where any ZIKV cases were presumed to have been acquired via mosquito.

IgG-mucin complexes can immobilize sexually transmitted viruses in vaginal mucus and may contribute to protection[153,347]. The significant degree of cross-reactivity between DENV and ZIKV led us to hypothesize that mechanisms of immune protection dependent on antibody binding and the presence of mucins in the vagina may also apply to protection from ZIKV infection. We found preliminary evidence that ZIKV may be immobilized by antibody-mucin interactions in human vaginal mucus, though these experiments were technically challenging and subject to effects of mucus donor variability. Our initial observations were not reproduced in subsequent experiments, which may be attributable to technical considerations, but these studies were not pursued further. Despite the potential interaction of antibodies and mucins *in vitro*, our data in a mouse vaginal infection model did not support a role for non-neutralizing antibodies in protection against vaginal ZIKV infection.

ZIKV infection is often modeled in *Ifnar1*$^{-/-}$ mice to produce consistent disseminated infection, including via vaginal inoculation. Though others have also observed productive ZIKV vaginal infection in WT mice[135,159,182,183], these studies did not specifically investigate the mechanisms that make the vagina an unusually susceptible site for ZIKV replication in WT mice. We found that ZIKV replicates efficiently in the vagina of WT mice as measured by viral genomes detectable in both the vaginal washes and cervix. Additionally, we did not find increased ZIKV replication in the vagina in mice lacking the IFN-λ receptor, contrasting with a prior study reporting that IFN-λ plays a protective role against ZIKV infection in the female reproductive tract[129]. This

previous study involved treating mice with an antibody blocking IFNAR1, so the effect observed for IFN-λ may only be in the context of deficient IFN-αβ signaling though we also found that ZIKV replicated equally well in the vaginas of WT and *Ifnar1*$^{-/-}$ mice. This other study also was done in the context of ovariectomized mice which then need to be supplemented with sex hormones, though our study was performed in mice with exogenous progesterone in addition to sex hormones natively present in the mice. Another key difference is that the strain used in our study (H/PF/2013) is different from the mouse-adapted ZIKV strain used in the previous study (DAKAR 41525)[348]. Further investigation is needed to clarify to what extent IFN-λ can control viral infections in the vagina.

Sexual transmission among humans appears to be an unusual property of ZIKV compared to other flaviviruses, although the incidence and epidemiology of most flaviviruses precludes certainty about the absence of sexual transmission. The most prevalent human flavivirus infection is DENV, with an estimated >100 million infections worldwide annually[349]. The best evidence for ZIKV sexual transmission derives from travel-associated cases in areas without endemic mosquito-borne transmission. By comparison, there have only been 2 recently described cases of sexual transmission of DENV despite tens of thousands of travel-associated DENV cases over the years[350,351]. Our data in mice suggest that the vagina may be a permissive site for flavivirus replication, as we observed replication of other flaviviruses (SPOV and USUV) that do not generally replicate in WT mice. Since human infections with those flaviviruses are rare it is not known whether they may share with ZIKV the ability to spread through sexual transmission. Sexual transmission would also require these viruses to have

tropism for the male reproductive tract as well as secretion into semen. It may be that there exists a subset of flaviviruses capable of sexual transmission that have not yet been observed because of the lack of a large enough outbreak for that to be detected. Interestingly, SPOV has been observed in semen in mice and also can cause fetal pathology in mice, though it has reduced tropism for the male reproductive tract compared to ZIKV[139,140]. A high progesterone state confers susceptibility to vaginal ZIKV infection in both WT and *Ifnar1*$^{-/-}$ mice, including high progesterone induced by pregnancy. It is not clear to what extent sex hormones modulate susceptibility to ZIKV infection in humans, though there is precedent for increased HIV susceptibility following progesterone treatment[174–176]. Likewise, progesterone increases susceptibility to HSV in mice[170,177]. The fact that pregnancy in mice causes susceptibility to vaginal ZIKV infection could be important as in humans, some of the most severe ZIKV outcomes result from congenital defects and congenital transmission after either mosquito or sexual transmission. It also is not known whether infection of the fetus via an ascending route via the uterus could be mechanistically different from hematogenous transmission across the placenta such that fetal outcomes may be different.

The mechanism by which progesterone confers susceptibility to vaginal ZIKV infection in this WT mouse model remains unclear. Vaginal abrasion was not sufficient to permit vaginal ZIKV infection, so a thinned epithelial barrier caused by DMPA treatment is unlikely to be the primary mechanism by which the vagina becomes susceptible to ZIKV infection. Likewise, we did not observe a significant change in the relative proportions of immune cells in vaginal tissue after DMPA treatment though it is possible that there may be more subtle changes in subpopulations or activation

phenotypes. The lack of immune cell infiltrate after DMPA treatment is consistent with prior observations that sex hormones alone do not modulate large changes in immune cell profiles within the LFRT in the absence of infection[171].

The increase in dendritic cells in the vagina and concurrent increase in T and B cells that we observed within the spleen and draining lymph node is consistent with a mechanism where dendritic cells are recruited to the vagina and then migrate to these secondary lymphoid organs to facilitate adaptive immune priming[352], despite the lack of systemic infection or viremia in this ZIKV vaginal infection model. The antibody response induced by systemic ZIKV infection can provide potent protection from vaginal ZIKV infection[159], though it remains to be seen whether the local vaginal ZIKV infection induced in WT mice can also provide protective immunity to a subsequent intravaginal challenge. In one experiment we found that WT mice infected intravaginally with ZIKV developed ZIKV-neutralizing serum titers but in a subsequent vaginal infection experiment, no neutralizing activity was induced. Neutralizing antibody titers may be more consistently detected at later time points than the 14 dpi timepoint we evaluated, as this is a mild viral infection that does not appear to cause significant inflammation by histology and does not spread to other tissues or systemically.

It has also been hypothesized that WT mice are susceptible to intravaginal ZIKV infection because the vagina may be deficient in expression of viral RNA PRRs at baseline and after DMPA treatment[183]. Yet this would not explain why progesterone is required for ZIKV infection. Accordingly, we did not find that DMPA negatively affects expression of *Ifit1*, an antiviral ISG, either in the vagina or the spleen in response to pI:C. We also did not find a difference in the relative expression of *Ifit1* between the

LFRT, UFRT, and spleen. Subtle differences in expression of viral RNA sensors themselves are not necessarily predictive of whether or not cells can mount an antiviral response as measured by expression of downstream ISGs. Further, our results suggest that DMPA does not induce a global downregulation of ISG expression that would promote viral infection.

We found that most ZIKV-infected cells in the vagina were epithelial cells and that there did not appear to be substantial immune infiltrate present near sites of infection. The observation that epithelial cells appear to be infected has been reported before in mice with impaired immune signaling[129]. The fact that epithelial cells appear to be the cells primarily infected in vaginal tissue is surprising because ZIKV has particular tropism for myeloid cells in systemic infection[21,22].

Progesterone controls ZIKV susceptibility in the vagina to an even greater extent than IFN signaling. Though there aren't significant changes in overall leukocyte populations or antiviral signaling, DMPA might be inducing small changes in either the quality or quantity of the leukocyte population that were not observed by flow cytometry. Likewise, there may remain a subtle change in antiviral signaling pathways in subpopulations of epithelial cells that are not actively proliferating that are not discernable from mRNA transcripts in whole tissues.

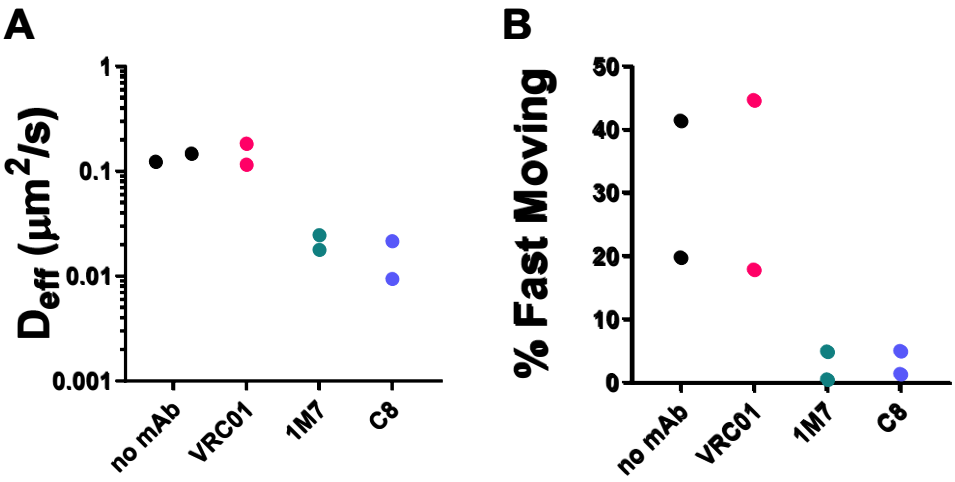

Figure 3.1 ZIKV diffuses slower through human vaginal mucus in the presence of ZIKV-binding IgG. Purified ZIKV was covalently labeled with a succinimidyl ester dye and imaged via inverted epifluorescence microscopy. Each dot represents the mean of 150-900 tracked individual particle paths within 1 human vaginal mucus sample. **A.** The diffusivity of labeled ZIKV particles. **B.** The percentage of particles within a vaginal mucus sample moving more than 50μm in 30 minutes.

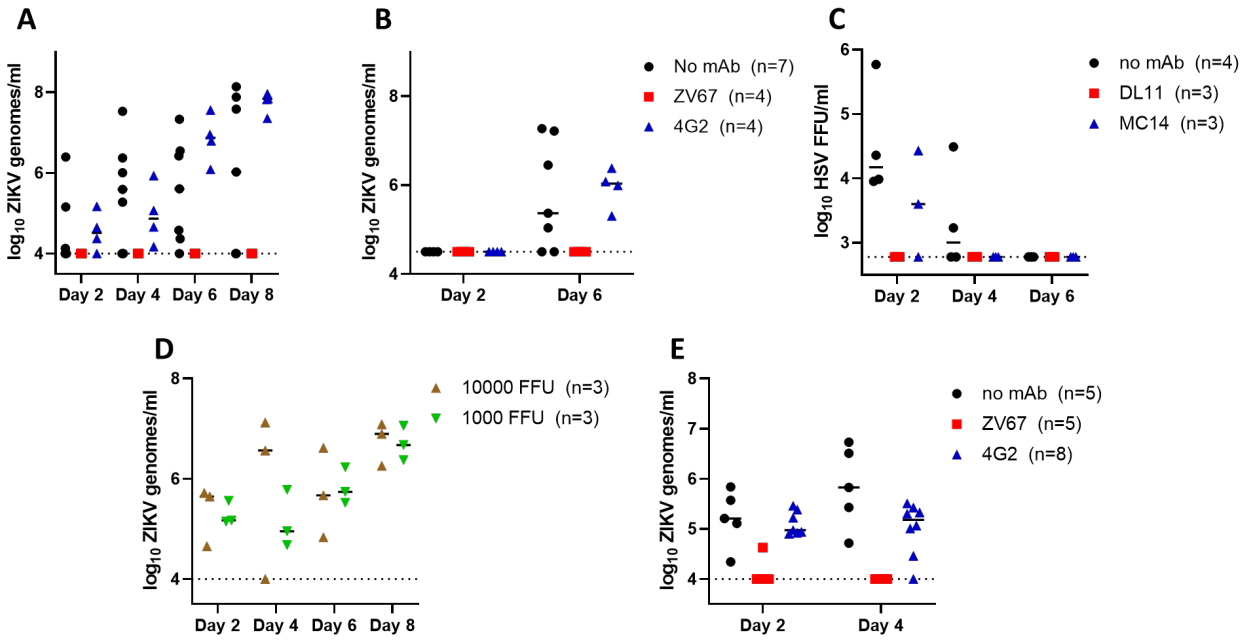

Figure 3.2 Non-neutralizing IgG do not confer protection against intravaginal infection in vivo. A-B. 7 week old *Ifnar1*$^{-/-}$ mice were pre-treated with 2 mg DMPA then infected via vaginal instillation with 100 FFU ZIKV with either a potently neutralizing (ZV67) or weakly neutralizing (4G2) antibody at 5μg/mL. Viral RNA was measured by qRT-PCR in vaginal washes (A) or serum (B). **C.** 7 week old BALBc/J mice were pre-treated with 2 mg DMPA then infected via vaginal instillation with 1000 FFU HSV-1 premixed for 1 hour with either a potently neutralizing (DL11) or weakly neutralizing (MC14) mouse monoclonal antibody. HSV-1 was titered by focus-forming assay directly from vaginal washes. **D-E**. 6-7 week old WT mice were pre-treated with 2 mg DMPA then infected via vaginal instillation with 1000 FFU or 10000 FFU of ZIKV. Viral RNA was measured by qRT-PCR in vaginal washes. In **E**., 1000 FFU of ZIKV was premixed for 1 hour with potently neutralizing (ZV-67) or weakly neutralizing (4G2) mouse monoclonal antibodies.

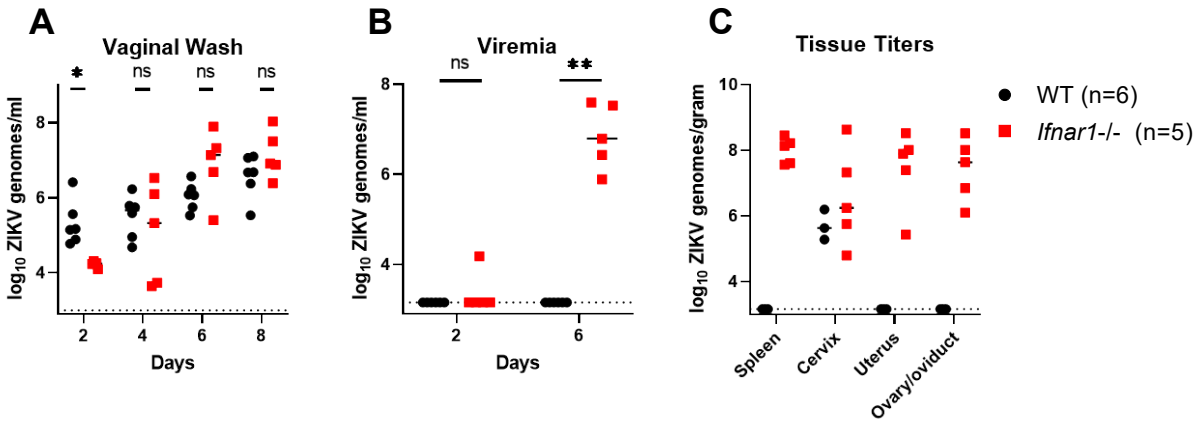

Figure 3.3 WT mice are susceptible to ZIKV vaginal infection. 6 to 7 week-old WT and *Ifnar1*$^{-/-}$ mice were pre-treated with 2 mg DMPA and inoculated with 1000 FFU of ZIKV by intravaginal instillation 5 days later. Viral RNA extracted from vaginal washes (A), serum (B), or tissues (C) was measured by qRT-PCR. Data are combined from 2 independent experiments. WT and *Ifnar1*$^{-/-}$ groups were compared by Mann-Whitney test with adjustment for multiple comparisons (ns, not significant $p>0.05$; *, $p<0.05$; **, $p<0.01$)

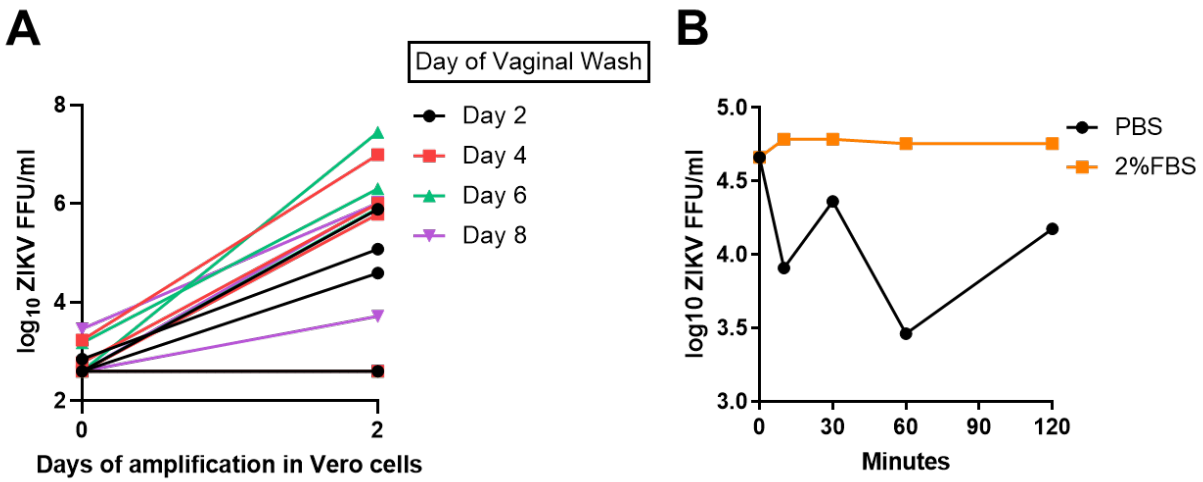

Figure 3.4 ZIKV in vaginal washes is infectious but not stable in unsupplemented PBS. A. 6 week old WT mice pre-treated with 2 mg DMPA were inoculated with 1000 FFU of ZIKV by intravaginal instillation. Vaginal washes were collected 2 to 8 dpi in DMEM supplemented with 2% FBS and HEPES. Vaginal washes were inoculated onto Vero cells and virus amplified for 2 days. Vaginal washes and Vero cell supernatants were titered by focus assay. **B.** 1 x 10^5 FFU/mL ZIKV was diluted in either PBS or PBS supplemented with 2% FBS and incubated for 2 hours on ice for the indicated times then infectious virus was measured by FFA.

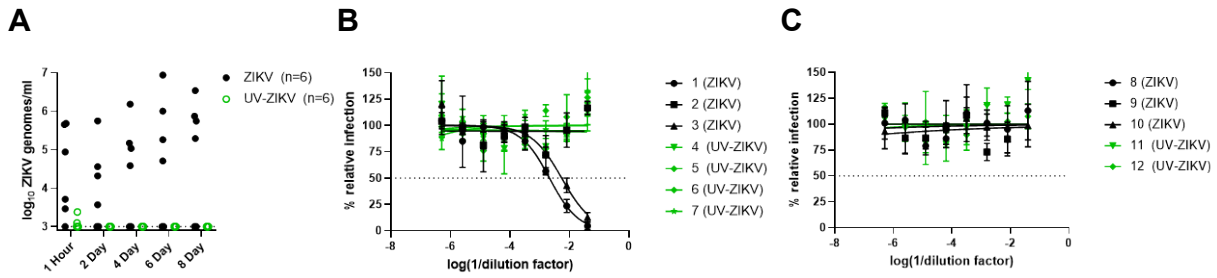

Figure 3.5 ZIKV productively replicates in the vagina of WT mice. 6 to 7 week-old WT mice were pre-treated with 2 mg DMPA and inoculated intravaginally with 1000 FFU of either mock inactivated ZIKV or UV-inactivated ZIKV. **A.** Viral RNA was extracted from vaginal washes and measured by qRT-PCR. Data are combined from 2 independent experiments. Sera were collected 14dpi and ZIKV neutralization measured by FRNT from the first (**B**) and second (**C**) experiment.

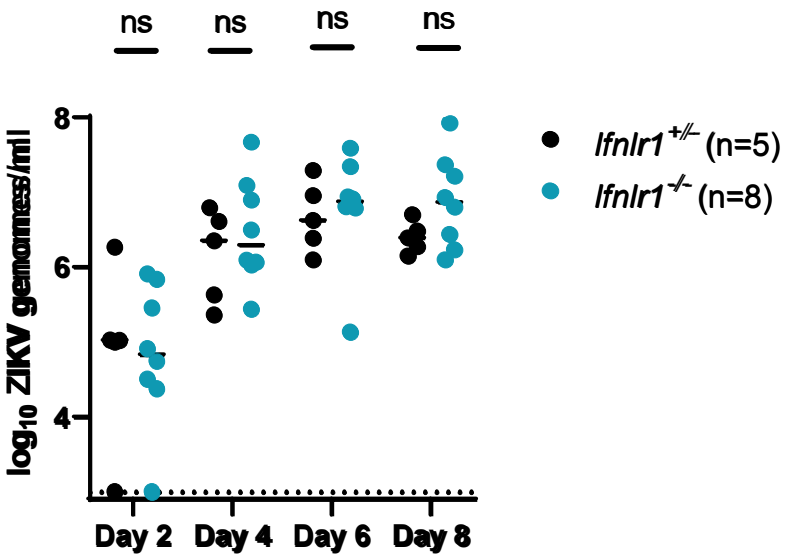

Figure 3.6 IFN-λ does not restrict ZIKV infection in the vagina. 5-6 week old *Ifnlr1*$^{+/-}$ or *Ifnlr1*$^{-/-}$ mice were pre-treated with 2 mg DMPA and inoculated with 1000 FFU of ZIKV by intravaginal instillation 5 days later. Viral RNA was measured by qRT-PCR from vaginal washes. Statistical analysis was performed via Mann-Whitney with adjustment for multiple comparisons (ns, not significant $p>0.05$).

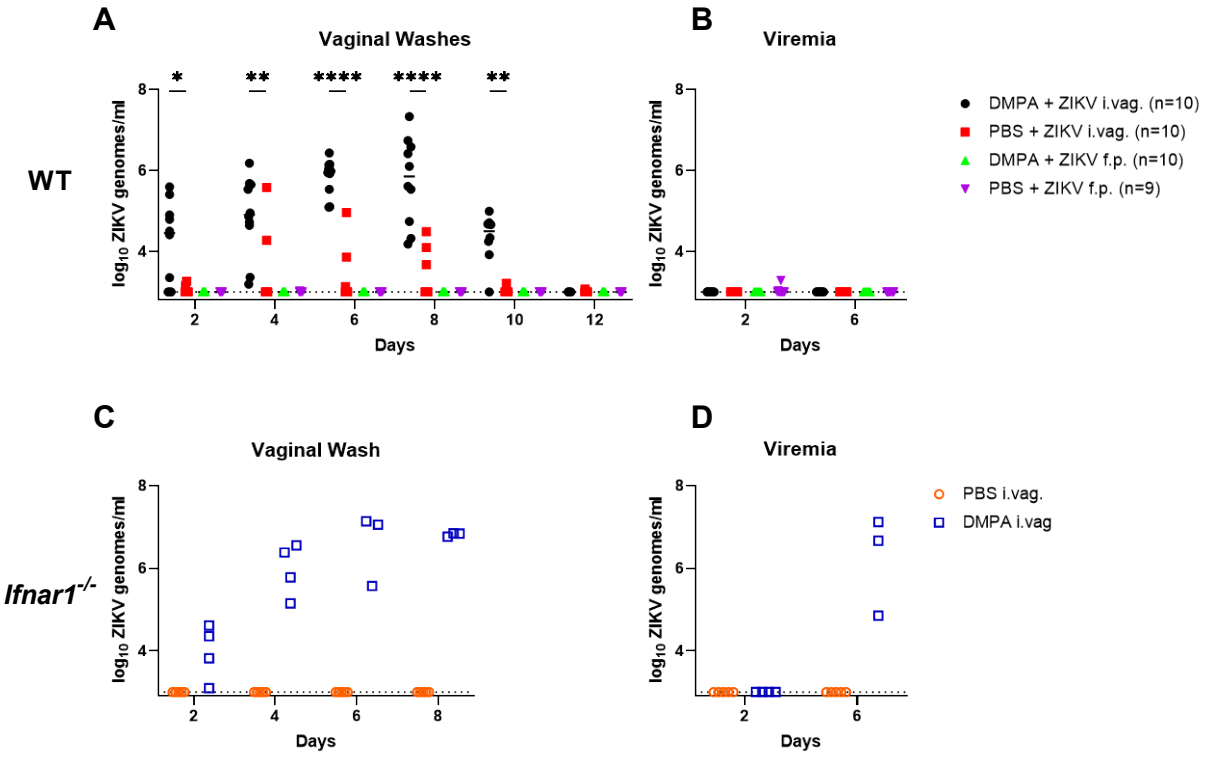

Figure 3.7 DMPA does not sensitize WT mice to ZIKV infection by footpad inoculation. 6 week old WT (**A-B**) or *Ifnar1*$^{-/-}$ mice (**C-D**) were pre-treated with either PBS or 2 mg DMPA then infected with 1000 FFU of ZIKV by intravaginal instillation (**A-D**) or subcutaneous footpad inoculation (**A-B**). Viral RNA was measured by qRT-PCR in vaginal washes (**A, C**) or serum (**B, D**). Data in **A-B** are combined from 2 independent experiments, **C-D** represent a single experiment. Statistical analysis in **A-B** was performed via two-way ANOVA with multiple group correction and time point matching, compared to DMPA only as the control group (ns, not significant $p>0.05$; *, $p<0.05$; **, $p<0.01$) but only comparisons between the two intravaginally infected groups are shown above.

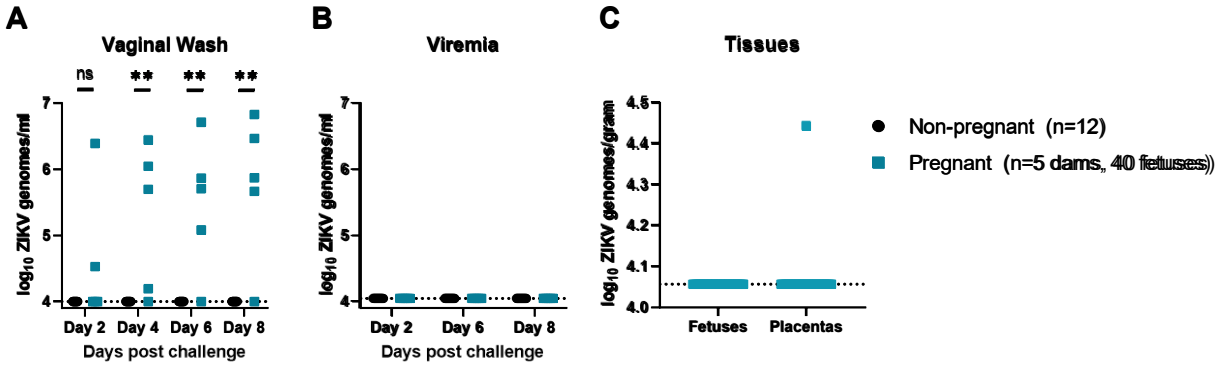

Figure 3.8 Pregnant WT mice are susceptible to intravaginal ZIKV infection. 7-10 week old WT dams were mated with WT sires and inoculated 7 days afterwards intravaginally with 1000 FFU of ZIKV. Viral RNA was measured by qRT-PCR in vaginal washes (**A**), serum (**B**), or fetal tissues harvested at day 8 post-infection (**C**). Data are combined from 2 independent experiments. Statistical analysis was performed via Mann-Whitney with adjustment for multiple comparisons (ns, not significant p>0.05;*, P<0.01)

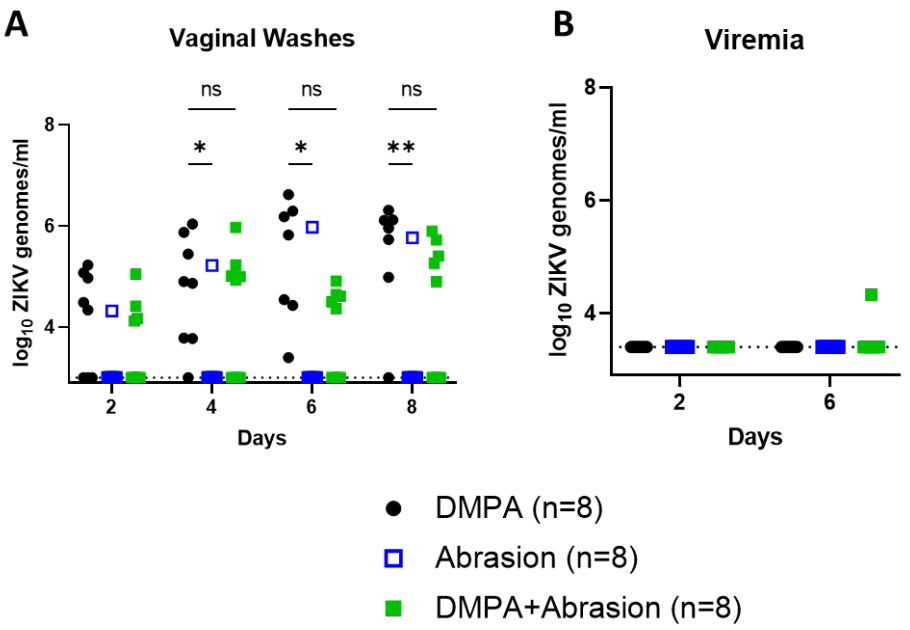

Figure 3.9 Vaginal abrasion is not sufficient to sensitize WT mice to ZIKV intravaginal infection. 6 week old WT mice were treated with 2mg DMPA 5 days prior to challenge, or vaginally abraded with an interdental brush immediately prior to challenge with 1000 FFU ZIKV via vaginal instillation. Viral RNA was measured by qRT-PCR in vaginal washes (A) or serum (B). Data are combined from 2 independent experiments. Statistical analysis was performed via two-way ANOVA with multiple group correction, comparing to DMPA only as the control group (ns, not significant $p>0.05$; *, $p<0.05$; **, $p<0.01$).

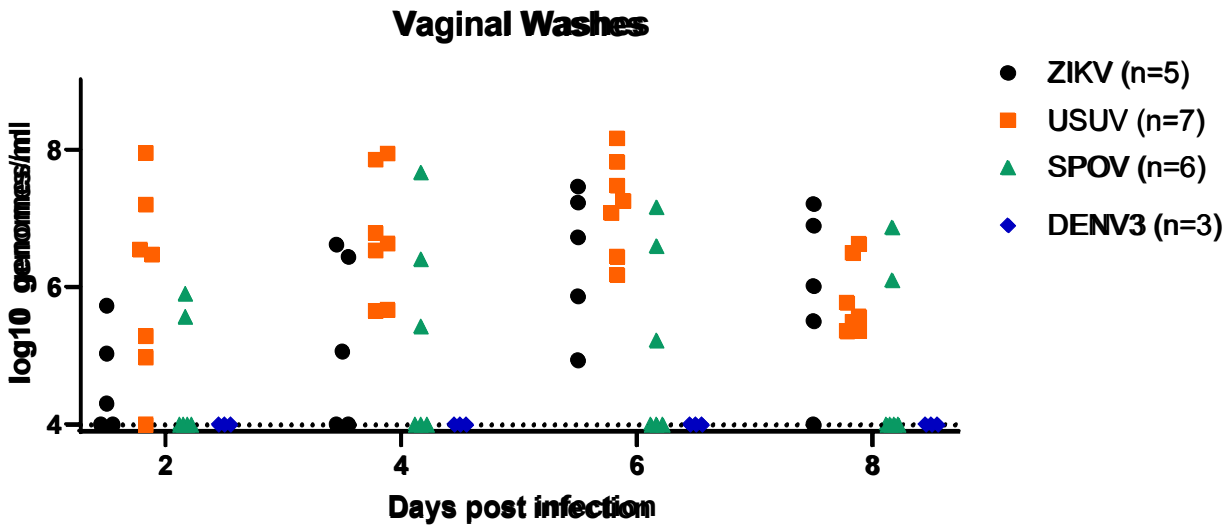

Figure 3.10 Flaviviruses other than ZIKV are able to replicate in the vagina of WT mice. 6 week old WT mice pre-treated with 2mg DMPA were challenged with 1000 FFU of ZIKV, Usutu virus (USUV), Spondweni virus (SPOV), or dengue virus (DENV3). Viral RNA was measured from vaginal washes by qRT-PCR.

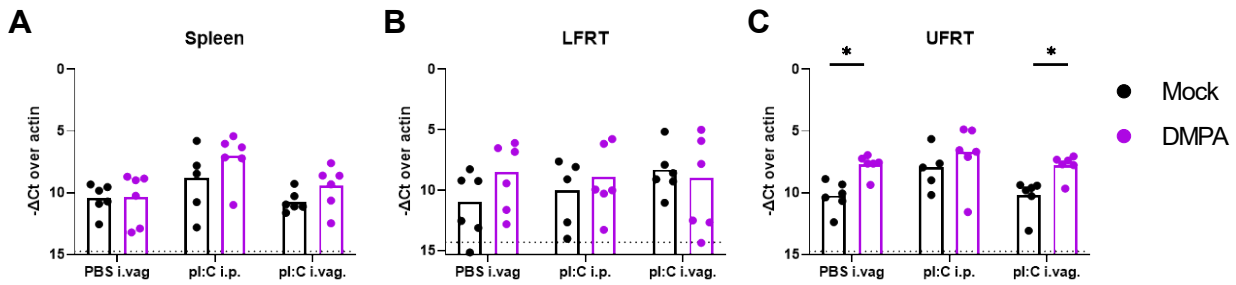

Figure 3.11 DMPA does not downregulate Ifit1 induction in the vagina. 5-6 week old WT mice were either treated with PBS (mock) or DMPA. Four days later, mice were treated with PBS intravaginally (i.vag) or pI:C i.vag. or intraperitoneally (i.p.) and tissues were harvested the next day. Expression of *Ifit1* was measured from RNA extracted from spleen (A), LFRT (B), or UFRT (C) and quantitated as the difference in Ct values between actin in mock-treated mice receiving PBS i.vag and *Ifit1*. Bars represent the geometric mean, and statistical analysis was performed via Mann-Whitney with adjustment for multiple comparisons (*, P<0.5) between mock and DMPA treatment groups for each pI:C or PBS treatment. Only significant associations are indicated.

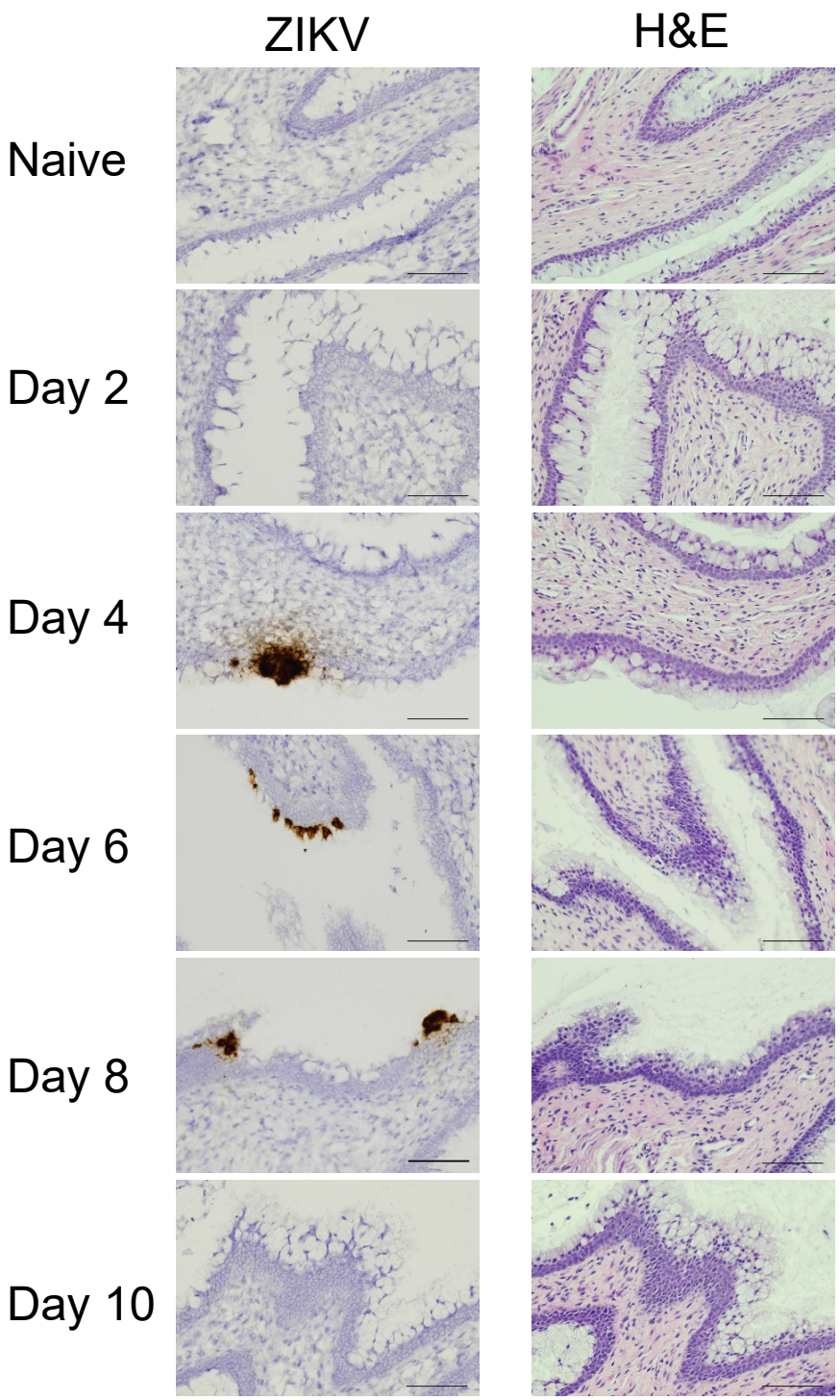

Figure 3.12 ZIKV primarily infects epithelial cells in the vagina. 5-6 week old WT mice were treated with 2mg DMPA and 5 days later, infected with 1000 FFU ZIKV intravaginally. Mice were then harvested 2 to 10 dpi and fixed tissues were H&E stained or labeled for ZIKV RNA via *in situ* hybridization. Pictured is a single field at 20x (scale bars indicate 0.1mm) from 1 mouse from each harvest time point, including an uninfected mouse, prioritizing displaying positive staining.

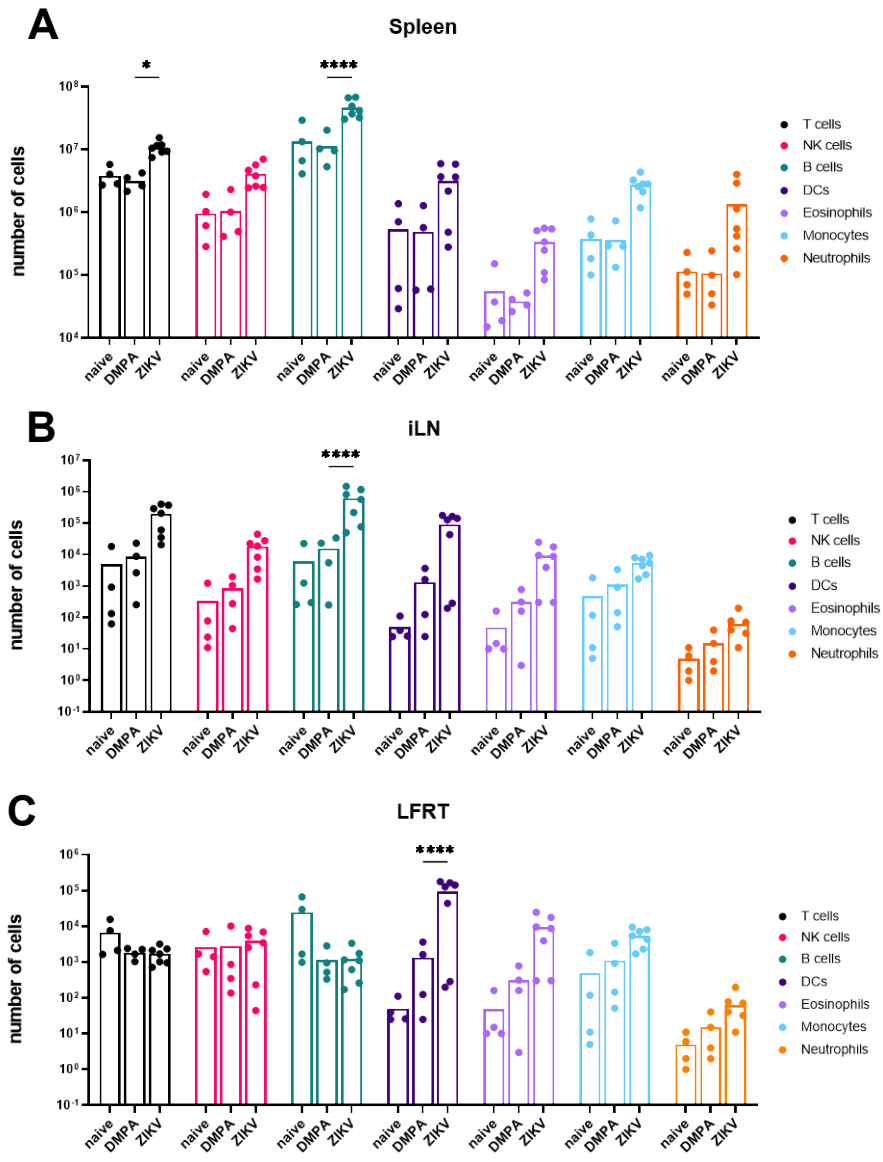

Figure 3.13. Progesterone alone does not alter the immune profile of the lower female reproductive tract. 5-6 week old mice were either left untreated, treated with 2mg of DMPA, or treated with DMPA and 5 days later infected with 1000 FFU of ZIKV intravaginally. All mice were harvested 6 days after ZIKV infection (11 days after DMPA treatment). Cells were isolated from spleens, lymph node, and lower female reproductive tract, and analyzed by flow cytometry. Total cell counts were calculated for T cells, NK cells, B cells, DCs, eosinophils, monocytes, and neutrophils for spleen (A), iLN (B) or LFRT (C). All cells were gated first for live-dead staining and then for CD45 expression. Statistical analysis was performed via two-way ANOVA with multiple group corrections for effects of treatment within each cell type comparing naïve and ZIKV-

infected groups to mice that were only DMPA treated. Only significant results are indicated (*, P<0.05; ****, P<0.00001). Results are combined from 2 independent experiments.

Virus & strain	Accession #	gBlock sequence
Usutu virus (USUV) SA AR 1776	AY453412.1	ACAACTGGGGAGGCCCACAATCCTAAGAGAGCTGAGGACACGTACGTGT GCAAGAGTGGCGTTACTGACAGAGGCTGGGGCAATGGCTGTGGACTATT TGGCAAGGGAAGTATAGACACGTGTGCCAACTTCACCTGCTCCCTGAAAG CGGTGGGCCGAATGATCCAACCGGAAAATGTTAAGTATGAAGTGGGAATC TTCATACATGGTTCCACCAGCTCTGACACTCATGGCAACTATTCTTCACAA CTAGGAGCATCACAAGCTGGGCGGTTTACCATCACTCCCAACTCCCCAGC CATCACTGTGAAGATGGGTGACTATGGAGAAATATCAGTTGAGTGTGAAC CAAGAAATGGGTTGAACACTGAGGCATACTACATCATGTCAGTGGGCACC A
Spondweni virus (SPOV) SA AR 94	KX227370.1	TCACCTTCGCTCGCACCCCCTCTGAAACAATTCACGGCACCGCCACAGTG GAGCTGCAATATGCAGGTGAAGATGGGCCGTGCAAAGTTCCCATAGTAAT TACCAGTGACACCAATAGCATGGCCTCGACAGGCAGGCTGATCACAGCG AATCCGGTGGTCACGGAAAGTGGAGCAAACTCAAAGATGATGGTCGAGAT TGACCCTCCGTTTGGTGATTCTTACATTATTGTGGGCACTGGCACAACAAA AATTACCCACCATTGGCACAGAGCCGGTAGTTCAATTGGACGTGCATTTG AGGCTACCATGAGAGGAGCAAAACGGATGGCGGTCCTCGGCGACACCGC TTGGGACTTTGGCTCTGTTGGGGGCATGTTCAACTCCGTTGGAAAGTTTG TCCACCAGGTGTTTGGATCAGCATTTAAGGCATTGTTTGGAGGCATGTCCT GGTTCACACAGCTCCTGATAGGATTTCT
Dengue virus serotype 3 (DENV3) CH53489	DQ863638.1	CTACGTATGTAAGCATACATACGTGGATAGAGGCTGGGGAAACGGTTGTG GTTTGTTTGGAAAAGGAAGCTTGGTGACATGCGCGAAATTTCAATGCTTAG AATCAATAGAGGGAAAAGTGGTGCAACATGAGAACCTCAAATACACTGTC ATCATTACAGTGCACACAGGAGACCAACACCAGGTGGGAAATGAAACGCA GGGAGTCACGGCTGAGATAACACCCCAGGCATCAACCGTTGAAGCTATCT TGCCTGAATATGGAACCCTTGGGCTAGAATGCTCACCACGGACAGGTTTG GATTTCAATGAAATGATCTTATTGACAATGAAGAACAAAGCATGGATGGTA CATAGACAATGGTTCTTTGACCTCCCCCTACCATGGACATCAGGAGCT
Rubella virus (RUBV) M33	X72393.1	CAACCGCGTGACTGAGGGCGAACGAGAAGTGCGGTATATGCGCATCTCG CGTCACCTGCTCAACAAGAATCACACCGAGATGCCCGGAACGGAACGCG TTCTCAGTGCCGTTTCGCCGTGCGGCTACCGCGCG
Hepatitis A virus (HAV)	KX343018	GTTTGGAACGTCACCTTGCAGTGTTAACTTGGCTTTCATGAATCTCTTTGA TCTTCCACAAGGGGTAGGCTACGGGTGAAACCTCTTAGGCTAATACTTCT ATGAAGAGATGCCTTGGATAGGGTAACAGCGGCGGATATTGGTGAGTTGT TAAGACAAAAACCATTCAACGCCGGAGGACTGACTCTCATCCAGTGGATG

Table 3.1 gBlock fragments used in this study. Viruses and strains listed along with accession numbers from which the gBlocks were designed.

Virus or gene target	Primer type	Sequence
Usutu virus (USUV) SA AR 1776	Forward	TCACAACTAGGAGCATCACAAG
	Reverse	CCATAGTCACCCATCTTCACAG
	Probe	/56-FAM/TT TAC CAT C/ZEN/A CTC CCA ACT CCC CAG /3IABkFQ/
Spondweni virus (SPOV) SA AR 94	Forward	TGTGCCAATGGTGGGTAAT
	Reverse	GGAAAGTGGAGCAAACTCAAAG
	Probe	/56-FAM/CGAGATTGA/ZEN/CCCTCCGTTTGGTGA/3IABkFQ/
Dengue virus serotype 3 (DENV3) CH53489	Forward	ATTACAGTGCACACAGGAGAC
	Reverse	CTAGCCCAAGGGTTCCATATTC
	Probe	/56-FAM/TGGGAAATG/ZEN/AAACGCAGGGAGTCA/3IABkFQ/
Rubella virus (RUBV) M33	Forward	CGAACGAGAAGTGCGGTATATG
	Reverse	GCGAAACGGCACTGAGAA
	Probe	/56-FAM/ACCTGCTCA/ZEN/ACAAGAATCACACCGA/3IABkFQ/
Hepatitis A virus (HAV)	Forward	GGTAGGCTACGGGTGAAAC
	Reverse	AACAACTCACCAATATCCGC
	Probe	/56-FAM/AGATGCCTT/ZEN/GGATAGGGTAACAGCG/3IABkFQ/
ActB	Forward	GACTCATCGTACTCCTGCTTG
	Reverse	GATTACTGCTCTGGCTCCTAG
	Probe	/56-FAM/CTGGCCTCA/ZEN/CTGTCCACCTTCC/3IABkFQ/
Ifit1	Forward	TGAAGCAGATTCTCCATGACC
	Reverse	GCAAGAGAGCAGAGAGTCAAG
	Probe	/56-FAM/ACAGCTACC/ZEN/ACCTTTACAGCAACCAT/3IABkFQ/

Table 3.2. qRT-PCR primers used in this study.

CHAPTER 4 – DISPARITIES IN SARS-COV-2 SEROPREVALENCE AMONG INDIVIDUALS PRESENTING FOR CARE IN CENTRAL NORTH CAROLINA OVER A SIX-MONTH PERIOD[3]

4.1 Summary

Robust community-level SARS-CoV-2 prevalence estimates have been difficult to obtain in the American South and outside of major metropolitan areas. Furthermore, though some previous studies have investigated the association of demographic factors such as race with SARS-CoV-2 exposure risk, fewer have correlated exposure risk to surrogates for socioeconomic status such as health insurance coverage.

We used a highly specific serological assay utilizing the receptor binding domain of the SARS-CoV-2 spike protein to identify SARS-CoV-2 antibodies in remnant blood samples collected by the University of North Carolina Health system. We estimated the prevalence of SARS-CoV-2 in this cohort with Bayesian regression, as well as the association of critical demographic factors with higher prevalence odds.

Between April 21st and October 3rd of 2020, a total of 9,624 samples from unique individuals were collected from clinical sites in central NC and we observed a seroprevalence increase from 2.9 (95% credible interval, CI, 1.7, 4.3) to 9.1 (95% CI 7.2,

[3]The work presented in this chapter will be published as Lopez CA*, Cunningham CH*, Pugh S, Brandt K, Vanna UP, Delacruz MJ, Guerra Q, Goldstein SJ, Hou YJ, Gearhart M, Wiethorn C, Pope C, Amditis C, Pruitt K, Newberry-Dillon C, Schmitz J, Premkumar L, Adimora AA, Emch M, Boyce R, Aiello AE, Fosdick BK, Larremore DB, de Silva AM, Juliano JJ, Markmann AJ. Disparities in SARS-CoV-2 seroprevalence among individuals presenting for care in central North Carolina over a six-month period. Manuscript resubmission in progress.
I performed a portion of the receptor-binding domain assays for both assay validation and study samples in this chapter as well as decisions on ICD-10 categorization and statistical analysis.

11.1) over the study period. Individuals who identified as Latinx were associated with the highest odds ratio of SARS-CoV-2 exposure at 7.77 overall (95% CI 5.20, 12.10). Increased odds were also observed among Black individuals and individuals without public or private health insurance. Our data suggest that for this care-accessing cohort, SARS-CoV-2 seroprevalence was significantly higher than cumulative total cases reported for the study geographical area six months into the COVID-19 pandemic in North Carolina. The increased odds of seropositivity by ethnoracial grouping as well as by health insurance status highlights the urgent and ongoing need to address underlying health and social disparities in these populations.

4.2 Introduction

In December 2019, a cluster of pneumonia cases in China's Hubei province heralded the beginning of what would become a global pandemic caused by severe acute respiratory syndrome coronavirus 2 (SARS-CoV-2). Despite attempts to contain the virus, SARS-CoV-2 has spread around the world, causing over 100 million infections and 3 million deaths due to the respiratory disease it causes, COVID-19[353]. Serological testing complements molecular testing for evaluating the spread of SARS-CoV-2 and can be deployed efficiently at the population level[218]. Recently, large prevalence studies around the United States using remnant samples from healthcare settings have reported substantial geographic variation in prevalence by state: around 30% in New York state but less than 2% in North Carolina (NC), the focus of the present study[354,355]. Notably, two other studies overlap with the present cohort both temporally and geographically. One study of 4,422 asymptomatic inpatients and outpatients in central NC from April 28-June 19, 2020 found an estimated seroprevalence of 0.7 – 0.8%, and another study of 177,919

remnant clinical laboratory samples from routine screening (3,817 from NC) from July 27-September 24, 2020 found an estimated seroprevalence of 2.5 – 6.8%[226,227]. While overall seroprevalence estimates of a given study depend on sampling method, assay characteristics, geography, temporal factors, and statistical methodology, seroprevalence studies can provide information on the spread of COVID-19 that is missed by looking at the number of confirmed acute cases alone.

Seroprevalence studies are also useful for identifying demographic factors such as racial, ethnic and socioeconomic disparities among those exposed to SARS-CoV-2[355–357]. The COVID-19 pandemic has been shaped by the deep and historic impacts of structural racism on disease disparities in US society as identified by serologic studies as well as hospitalization and mortality rates[198,358]. For example, COVID-19 case and hospitalization rates among Black, Hispanic and Native American populations in the US are 2.5-4.5 times higher than those in white populations[199]. Structural and occupational factors previously identified as drivers of race and ethnic disparities in health include lack of sick leave, inadequate access to infection prevention control, and unequal labor market opportunities as well as higher representation in essential work positions that lack job security and health insurance benefits[235–240]. Here, we confirm the findings of disparate SARS-CoV-2 exposure among racial and ethnic groups in the US by measuring seroprevalence using remnant blood samples from a large health care seeking cohort in the southern United States. By October 3rd, 2020, 52,722 SARS-CoV-2 cases in the study catchment area were diagnosed via cumulative total PCR or antigen test[359,360]. These cases represented 2.7% of the population and resulted in 1,266 confirmed deaths (a 2.4% case fatality rate). We used an in-house enzyme-linked immunosorbent assay (ELISA)

against the receptor-binding domain (RBD) of the spike protein of SARS-CoV-2[361] and applied Bayesian inference[230] to estimate seroprevalence and demographic risk factors of SARS-CoV-2 infection in a healthcare-seeking cohort over a six-month period.

4.3 Materials and Methods

Sampling Strategy and Data Collection.

Remnant plasma and serum samples were collected from four hospital-based clinical laboratories affiliated with the University of North Carolina (UNC) Health system. These laboratories receive and process clinical samples from inpatient units as well as outpatient clinics in NC. Each week, up to 300 remnant samples from individuals 5-99 years of age were arbitrarily selected by the clinical laboratory for testing from each location. Samples were collected between April 21st, 2020 – October 3rd, 2020. Medical record numbers were recorded for each sample and duplicates were discarded. We abstracted the following demographic and clinical data from electronic medical records (EMR, Epic): age, sex, ethnicity, race, address including city, state and ZIP code, insurance coverage, insurance type, inpatient or outpatient status, encounter diagnosis (ICD-10 code), inpatient date of discharge, and whether or not COVID-19 testing was performed within a 30-day window prior to study sample collection. Written informed consent was not required due to the use of routinely collected samples. All data for this study were collected under UNC IRB #20-0791, which is conducted under Good Clinical Research Practices (GCP) and compliant with institutional IRB oversight. De-identified samples used for assay validation were collected under UNC IRBs #20-0913 and #08-0895.

Enzyme-Linked Immunosorbent Assays.

Dr. Premkumar Lakshmanane developed a total Ig ELISA (combined IgG, IgM, and IgA) as well as IgM SARS-CoV-2 RBD ELISA, neither of which cross-reacts with common endemic human coronaviruses; both assays were used in this study as previously described[361]. Briefly, the SARS-CoV-2 RBD (amino acids 331-528, accession: QIS60558.1) containing three purification tags (6x histidine, Halo, and TwinStrep) was cloned into the pαH mammalian expression vector and expressed in Expi293 cells (ThermoFisher) and then purified using nickel-nitrilotriacetic acid agarose.

The spike protein N-terminal domain (NTD) antigen used in another ELISA (amino acids 16–305, Accession: P0DTC2.1) was cloned similarly. All ELISA measurement was conducted in duplicate and duplicate values with variance > 25% and/or one value above assay cutoff were repeated.

To account for plate-to-plate variability (i.e., batch effects) we used P/N ratios, rather than using the raw optical density (OD) values. P/N ratios were defined as $P/N=\frac{average\ OD\ sample}{average\ OD\ negative\ control}$ where the negative control values were those from the same plate as the sample[362]. Accounting for batch effects with a P/N ratio removes the need to define plate specific cutoffs, and instead allowed us to define a single cutoff based on a fold increase of sample OD value compared to the negative control OD value on the same plate.

The CDC recommends selecting cutoffs such that the test has 99.5% specificity[363]. We followed this recommendation, specifying the cutoff to be the standard estimate of the 0.995 quantile (based on the quantile function in R) of the negative lab

samples. Validation sera were collected from 145 PCR-confirmed SARS-CoV-2 positive cases from the laboratories of Dr. Jennifer Dan, Dr. Alessandro Sette, and Dr. Shane Crotty at La Jolla Institute of Immunology and 274 negative controls collected prior to 2020 from UNC IRBs #20-0913 and #08-0895 (Table 4.1). The P/N ratio cutoff was 2.57 with empirical sensitivity of 89.7% and empirical specificity of 99.3%. Therefore, a sample was considered positive if its average OD value was ≥2.57 times larger than the average OD of the corresponding plate negative controls.

Nucleocapsid protein ELISA.

Detection of IgG antibody to SARS-CoV-2 N antigen was performed with the EUA approved Abbott SARS-CoV-2 IgG assay (Abbott Laboratories) on the Abbott Architect i2000SR immunoassay analyzer as previously described[364].

SARS-CoV-2 Neutralization Assays.

To further characterize the SARS-CoV-2 antibody responses of this study, viral neutralization assays were performed for 110 ELISA-positive samples that were selected randomly using the sample_n() function of the dplyr R package. Luciferase-expressing, full-length SARS-CoV-2 isolate WA1 strain (GenBank Accession#: MT020880) was engineered and recovered via reverse genetics and used to titer serially diluted sera on Vero E6 USAMRID cells as described previously[365]. Neutralization titers were calculated with a sigmoidal dose-response (variable slope) curve in Prism 9 (Graphpad), constraining values between 0 and 100%.

Statistical Methods and Analyses.

We fit two statistical models to estimate seroprevalence, previously described but applied and further developed by Sierra Pugh working with Dr. Bailey Fosdick (Colorado

State University)[230]. First, we fit a Bayesian autoregressive logistic model to estimate weekly prevalence across the six-month study period while accounting for uncertainty in the assay specificity and sensitivity due to finite lab validation samples. Second, we fit a Bayesian logistic regression model to estimate prevalence and conditional odds ratios by subpopulation with main effects for sex, race/ethnicity, age, in/out-patient status, and health insurance payor, while again accounting for uncertainty in the assay test characteristics. Each group was compared to females, non-Latinx white, ages 5-17, outpatient, and private payor health insurance status as respective baseline categories. These Bayesian hierarchical models (BHM) simultaneously model study data and validation data to produce prevalence estimates and credible intervals that reflect both uncertainty due to the finite study sample as well as the uncertainty in the sensitivity and specificity of the ELISA, with statistical uncertainty represented by 95% credible intervals.

Demographic data categorization.

To categorize individual clinical encounters associated with the blood draws we sampled, we obtained International Classification of Diseases, 10th revision (ICD-10) codes from any inpatient or outpatient visit at the same location within 14 days of when we received and sampled the blood draw. We prioritized inpatient visits over outpatient visits unless no inpatient visit was available. If there was no visit within the past 14 days of the blood draw, we instead used the visit closest to the most recent specimen collection date within a 30-day period. Individuals with no visit at the same location within 30 days of their blood draw were excluded from analysis. To capture any upper respiratory infection, respiratory disease due to external agents, interstitial lung disease, imaging abnormalities of the lung, cough, fever, and dyspnea, we used the ICD-10 codes J00-

J006, J009-J018, J20-J22, J40-J47, J60-J70, J80-J84, J96-J99, R91, R05, R06.0, and R50. COVID-19 diagnosis was defined as presence of the U07.1 code in the visit nearest the sampled blood draw. Likewise, acute or trauma cases were defined as any of the following ICD-10 codes: O00, O01, O02, O03, O04, O07, O08, O015.1, all S codes, all T codes (except T36-T39, T41, T46, T50, T80-T88), all V codes, all W codes, all X codes, all Y codes (except Y62-Y84 and Y-90-99).

Insurance status was determined from the most recent clinical encounter prior to the sampled blood draw. “Private Insurance” was classified as any of the following listed for a patient’s visit: Blue Cross/Blue Shield, private health insurance, or state government insurance. “Public Insurance” was classified as any of these following: Medicaid applicant, Medicaid, Medicare, Department of Veteran’s Affairs, Tricare, and Corrections State insurance. “Self-pay” includes anyone paying out of pocket. “Unknown/Other” consists of individuals for whom the health insurance payor was left blank or otherwise unidentifiable, as well as listed insurance that read “Legal Liability / Liability Insurance”, “Other specified but not otherwise classifiable (includes Hospice - Unspecified plan)”, and “Other”.

Race and ethnicity identity was ascertained from that listed in the EMR for each patient. The categories listed under Epic’s EMR that we received included “American Indian or Alaska Native”, “Asian”, “Black or African American”, “Native Hawaiian or other Pacific Islander”, “Other Race”, “Patient Refused”, “Unknown” or “White or Caucasian”. For ethnicity, we received information on whether patients self-identified as “Hispanic or Latino”, or were listed as “Patient Refused” or “Unknown”. In our report, we collapse race and ethnicity from separate variables into a single variable in order to investigate the impact of systemic racism on SARS-COV-2 seroprevalence by both race and ethnicity at

the same time, though the constructs of race and ethnicity are inherently surrogate measures of racism and other forms of marginalization[366].

We therefore binned individuals into the following groups: Any Black or African American individuals that indicated “Non-Hispanic or Latino,” “Patient Refused,” or “Unknown” were binned as “Non-Latinx Black”. The same was done for White or Caucasian individuals, binning them into “Non-Latinx White” and similarly for all other groups as “Non-Latinx Other”. Any Hispanic or Latino individuals were binned as “Latinx”, and therefore could self-identify as any of the above race categories. We did not further separate out other intersections of race and ethnicity because the number of individuals was too small to make conclusive claims on odds of seropositivity. We here opt to use Latinx in place of “Hispanic”, though neither is the only way to refer to this grouping of individuals that often share cultural characteristics, language, religion, and ancestral geography and history[367]. We also compared racial, ethnic, and age demographics in the study population to the demographics of the 6-county area where most of the study population resided using US Census Data[359].

4.4 Results

Cohort Characteristics.

From April 21, 2020 – October 3, 2020, after excluding duplicate samples, 9,624 remnant samples were analyzed from four UNC Health hospitals in central North Carolina. The six counties most heavily sampled were Orange, Johnson, Chatham, Wake, Durham and Alamance, with 6,946 (72.2%) of individuals residing in these counties. The study consisted of 5,417 females (56.3%) and 4,206 males (43.7%) which is similar to the demographics of this region (Table 4.2). Less than 6% of individuals were

in the youngest age group (5-17 years old), though this age group represents over 18% of the study area's population. Approximately 90% of study individuals were insured, with 8% falling into the self-pay category, but we do not know whether this is representative of the area. The majority of sampled individuals were seen at UNC Memorial Hospital, ~3% were acute or trauma cases, and ~5% had a visit diagnosis of fever or respiratory symptoms. Overall, approximately 1% of patients had an associated COVID-19 visit diagnosis, most of which were inpatients (2.8% compared to 0.3% outpatients) (Chi-squared test; $p<0.0001$).

Seroprevalence in central North Carolina

The six-month period of the study was divided into three, two-month cohorts. The Bayesian Hierarchical Model (BHM)-derived seroprevalence estimates increased from around 3% in April/May to around 9% in August/September (Table 4.3). Raw seroprevalence estimates also showed a similar increasing trend over the study period, but because this does not take into account assay performance uncertainty, they are slightly higher at ~5% and ~11%. Furthermore, seroprevalence estimates peaked in early August following a hospitalization peak in mid-July (Figure 4.1A, 4.1C). The most rapid accumulation of cases occurring from June to August (Figure 4.1B). Unexpectedly, seroprevalence peaked and was followed by a slight decrease in the final weeks of the study. This pattern was related to raw seroprevalence estimates at Johnston County hospital which surged from 7.8% in the first two months to 18.0% in the second two months, then declined to 14.8 in the final two-month period. The surge and then decline in seroprevalence at Johnston County hospital is associated with a peak in PCR-confirmed cases in the region (Table 4.4). This peak and decline was not affected by the

removal of cases with ICD-10 visit codes for “COVID-19” or those we identify as “respiratory disease”.

Clinical and demographic differences in seroprevalence estimates

Latinx-identifying individuals had higher SARS-CoV-2 seroprevalence increased from 15 to 33% compared to non-Latinx individuals which increased from 1-11% seroprevalence over the study period (Table 4.3). Individuals with “Other/Unknown” or “Self-pay” insurance status had a higher estimated seroprevalence (increasing from 20-40% or ~1-18%, respectively) than those with private or public health insurance (increasing from 3-9%). Approximately 30% of Latinx individuals in this study were in the other/unknown or self-pay health categories, disproportionately comprising ~27% of these two categories but only accounting for ~8% of our study population (Table 4.5).

We calculated conditional odds ratios for each variable we collected using the BHM (Table 4.6). Latinx individuals had the highest odds of SARS-CoV-2 seropositivity throughout the study period compared to non-Latinx white individuals, OR 7.77 overall (95% credible interval 5.20, 12.10), ranging from 14.53 (6.47, 36.72) in the first two months to 4.34 (2.61, 7.41) in the last two months of the study. Individuals with unknown insurance status also had an elevated odds ratio of seropositivity at 3.81 (2.23, 6.54) compared to those with private insurance status. Over the entire period of the study, non-Latinx Black individuals, individuals aged 50-64 years, and inpatients, also had increased odds ratios of approximately two-fold compared to non-Latinx white individuals, individuals aged 0-17, and outpatients, respectively. The overall difference in odds ratios by age appears to be driven primarily by increased odds ratios in the first two months.

SARS-CoV-2 RBD positive subset analysis.

To determine the SARS-CoV-2 antibody repertoire in a subset of RBD Ig seropositive individuals, 110 randomly selected RBD Ig positive sera were tested for RBD IgM, NTD IgG, and SARS-CoV-2 neutralizing antibodies. About 75% of these individuals were positive for RBD IgM, 60% had NTD IgG antibodies, and about 50% had detectable neutralizing antibodies (Figure 4.2A). Of the participants with detectable neutralizing antibodies, 23% had a high titer > 1:1280, 47% had a moderate titer of 1:160-1:1279, and 30% had a lower titer of 1:10-1:159. Furthermore, RBD Ig P/N antibody signal correlated more strongly with functionally neutralizing antibody levels (Figure 4.2B), than NTD IgG signal (Figure 4.2C). We also found that 36% (29/80) of those in this subset with an ICD-10 code binned as “Other” had neutralizing antibodies, while 83% (25/30) of individuals with an ICD-10 code of “COVID-19” or what we identify as “respiratory disease” had neutralizing antibodies (Figure 4.2D). There was substantial agreement between the RBD Ig ELISA results reported here and 150 study individuals for which a clinical SARS-CoV-2 nucleocapsid IgG (Abbott assay) was available (Cohen’s kappa=0.685) (Table 4.10).

4.5 Discussion

Here we describe SARS-CoV-2 seroprevalence in a total of 9,624 unique healthcare-seeking individuals in central North Carolina using clinical remnant samples from four regional hospitals between April and October 2020. Employing a Bayesian framework[230] to capture assay uncertainty in both lab validation data as well as study data, we estimated a significant increase in overall seroprevalence from 2.9% (95% CI 1.7% - 4.3%) at the start of the study period, to 9.1% (95% CI 7.2% - 11.1%) at the end of the study period, approximately six months after the first case in the state. The end-of-

study prevalence identified here is significantly higher than the cumulative number of cases identified by PCR or antigen testing in the same county region at the same date, though determining the degree to which the identified cases undercount true infections requires more representative sampling.

A previous study from central North Carolina that overlaps with the first two months of our study period found seroprevalence in an asymptomatic healthcare-seeking cohort below 1% using the Abbott nucleocapsid IgG assay[226]. This is much lower than the ~3% seropositive estimate in our cohort over this time period, and may be due to under-sampling of Latinx individuals in that study and/or preferential sampling of asymptomatic individuals, as that study excluded individuals reporting symptoms consistent with SARS-CoV-2 infection. There is also growing concern about the use and performance of nucleocapsid IgG assays in individuals with asymptomatic or mild disease because the nucleocapsid assays appear to be less sensitive in asymptomatic disease cohorts but have comparable sensitivity to spike or RBD assays in symptomatic disease cohorts[219,368]. A nationwide CDC study that used remnant clinical samples from inpatients and outpatients found a seroprevalence of 6.8% in NC in September 2020, which is closer to our estimate of 9.1% during the final two months of this analysis.

The conditional odds ratios we calculated assume that all other variables are held constant while estimating the effect of one demographic variable at a time. We found that Latinx individuals had the highest odds of SARS-CoV-2 seropositivity, and that non-Latinx Black individuals also had high odds of SARS-CoV-2 seropositivity, corroborating previous observations[355–357]. The high odds ratios by race and ethnicity decreased over time, consistent with the virus spreading first among individuals with high exposure risk

and later to the rest of the population. Residential segregation, crowded households, socioeconomic disadvantage, mass incarceration, as well as inequities in access to insurance, health care, testing, and vaccination have all been cited as factors that have contributed to the large and sustained racial and ethnic disparities in COVID-19 in the US[236,238,369–371]. We also observed that individuals who fell into the "self-pay" category for their healthcare or otherwise had unknown health insurance status had higher SARS-CoV-2 seropositivity and odds ratios. The significant overlap in the Latinx population and these insurance categories is concerning because the high odds ratios and seroprevalence in these categories can lead to much higher exposure risk among the significant number of underinsured Latinx individuals[372].

Studies of PCR-positive symptomatic COVID-19 cases have reported detectable neutralizing antibody responses in these individuals[373]. Thus, it was surprising that we observed 51% of individuals in our RBD-positive subset analysis did not have detectable neutralizing antibodies. Though we do not know what proportion of individuals in our study had asymptomatic infections, low neutralizing antibody titers may be explained by short duration of viral replication in respiratory compartments and low to no viral replication in the serum or blood of those with mild or asymptomatic disease. Not surprisingly, when we looked at our neutralizing antibody results by ICD-10 code, the majority of individuals with a "respiratory disease" or "COVID-19" diagnosis had developed neutralizing antibodies. Reports from mild disease COVID-19 cohorts support the idea that detectable neutralizing antibody titers are not necessarily identified after mild COVID-19[216,219,364]. In this subset analysis we also found that 75% had RBD IgM antibodies, indicating that their infections likely occurred within the past three months[364]. Furthermore, a majority of

individuals in this subset had detectable NTD IgG antibodies; the NTD has recently been found to be an important target for the B.1.1.7, B.1.351, and B.1.1.28.1 SARS-CoV-2 variants[374].

The primary limitation of this study is that the study population, composed of individuals accessing care at UNC area hospitals and clinics may differ from the overall population in central North Carolina in ways that are not captured in demographic data (e.g., overall health status). Accordingly, we have chosen to not weight our dataset to county demographics and therefore do not provide overall estimates of seroprevalence in the six-county area as that would require more representative sampling methodology[228]. Furthermore, many clinics and hospital elective procedures were closed or only seeing patients virtually during the first few months of the study period.

The unexpected seroprevalence peak observed at the Johnston County hospital suggests that the population accessing care at these clinical sites did not have consistent exposure risk over time. As expected, seroprevalence estimates in this cohort track closely with COVID-19 hospitalizations in the four hospitals in this study with a two-week lag which could be due to time to seroconvert. Declining antibody over this time period to undetectable levels is unlikely, as the length of the study is shorter than it takes for antibodies to decline to undetectable levels, although little is known about antibody levels over time in the asymptomatic population[373].

Other limitations of the study include that we could not disaggregate odds ratios by all races and/or by race and ethnicity at the same time, or by multiracial categories because the number of individuals became too small to allow robust interpretation. Finally, though the “self-pay” insurance category includes the uninsured, we cannot

confidently state that everyone in this category was uninsured because lack of insurance is not a specific category that is captured in the EMR. Although SARS-CoV-2 seroprevalence of healthcare-seeking individuals is an imperfect comparison to the general population, we maintain that it is a useful sentinel population to understand overall trends, especially when attempting to surveil rural populations residing in areas without strong public health systems and spread over a large geographic area.

Based on our estimates of seroprevalence in the population accessing healthcare, cumulative case numbers confirmed by molecular diagnostics are likely under-representing the true number of cases. Public health distancing measures, mask wearing, and vaccination should continue to be prioritized in order to lower the transmission of SARS-CoV-2 and subsequent loss of lives while transmission remains high and vaccine coverage remains incomplete. Our findings of a significantly higher odds of SARS CoV-2 seropositivity among Latinx and non-Latinx Black populations corroborate numerous studies describing large racial and ethnic disparities in SARS-CoV-2 infection, morbidity and mortality in the US[355–357]. Vaccination programs should address structural and occupational factors that drive race and ethnic disparities in health outcomes in the US to ensure that individuals at particularly high exposure risk of SARS-CoV-2 have timely access to SARS-CoV-2 vaccination.

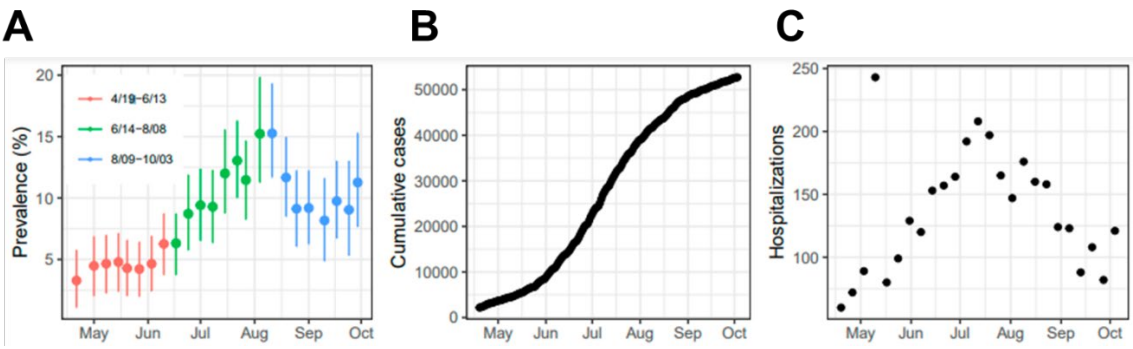

Figure 4.1. Trends in seroprevalence estimates. (A) Weekly posterior mean seroprevalence estimates by ELISA and 95% credible intervals of the hospital samples plotted over time over the course of the study period. (B) Cumulative daily COVID-19 PCR+ cases from the six-county area 4/19-10/3, and (C) weekly COVID-19 hospitalizations in the six-county area 4/19-10/3 from NC Department of Health and Human Services.

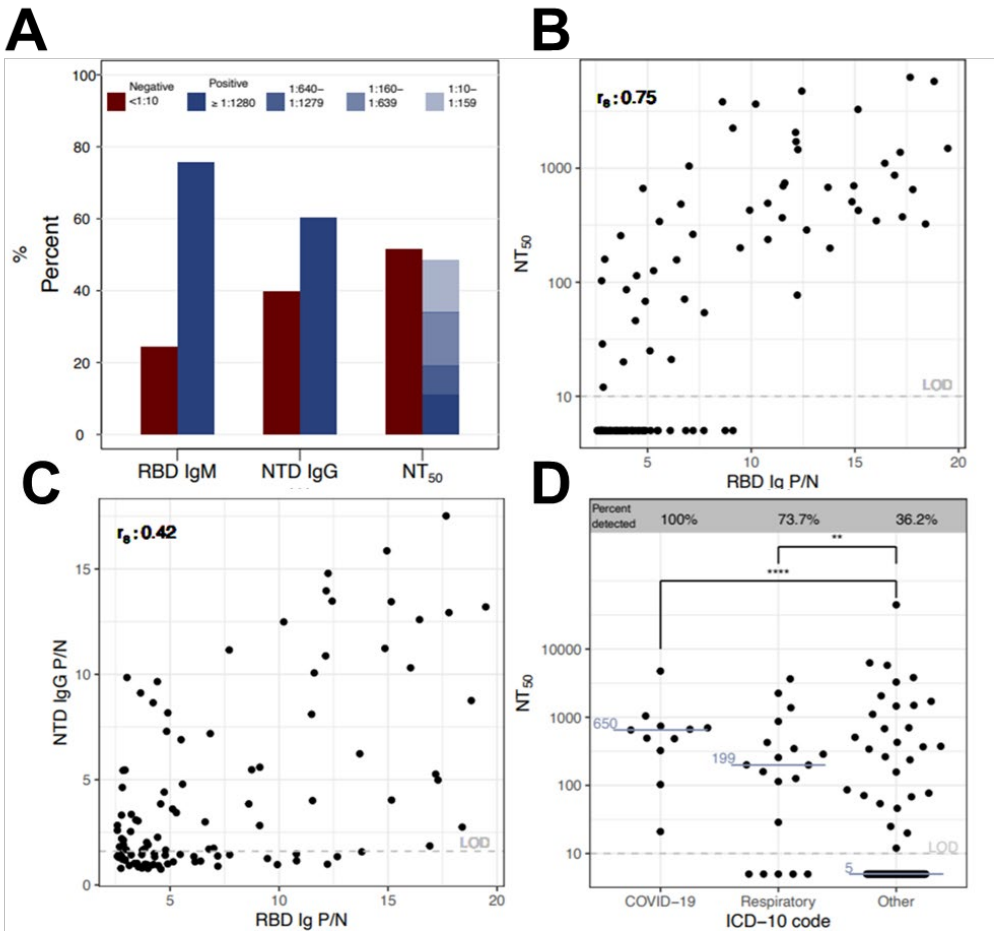

Figure 4.2 Antibody repertoires in an RBD Ig positive subset. 110 RBD Ig positive samples were chosen at random to undergo SARS-2 antibody repertoire analysis. (A) Percent of individuals with RBD IgM, NTD IgG and functionally neutralizing antibodies (NT50). (B) Correlation plot of NT50 and RBD Ig. (C) Correlation plot of NTD IgG and RBD Ig, r_s = Spearman correlation coefficient displayed in the top left of panels (B) and (C). (D) NT50 values for each diagnosis binning category based on ICD-10 codes. Line indicates the median. Two-tailed Mann-Whitney, ****p<0.0001, **p=0.0078.

Table 4.1. ELISA Validation Data		
	% Sensitivity (95% CI)	**% Specificity (95% CI)**
RBD total Ig ELISA (≥ 9 days post symptom onset)	89.7% (130/145) (84.7, 94.6)	99.3% (272/274) (98.3, 100.0)
PCR+ controls (n = 145)	N = 32 (Crotty Lab, La Jolla)	
	N = 113 (UNC convalescent plasma donor cohort)	
Negative controls (n = 274)	N = 122 (UNC pre-2019 healthy adults)	
	N = 48 (UNC pre-COVID-19 arboviral samples, tuberculosis endemic region)	
	N = 44 (UNC, clinical pre-organ transplant)	
	N = 28 (UNC, clinical HIV+)	
	N = 16 (healthy adults, Crotty Lab, La Jolla)	
	N = 16 (UNC, respiratory illness samples, COVID-19 negative)	

Table 4.1 RBD Ig ELISA Validation Data. Serum from PCR-confirmed COVID-19 patients and from individuals prior to 2020 were obtained from the University of North Carolina (UNC) and La Jolla Institute of Immunology. CI, confidence interval; PCR, polymerase chain reaction.

Table 4.2 **Study participant demographics**							
	4/19-6/13		6/14-8/08		8/09-10/03		6-county Demographics (%)
	N	(%)	N	(%)	N	(%)	
Sex							
Female	1947	56.2	2020	57.3	1450	55.1	51.8
Male	1515	43.7	1508	42.7	1183	44.9	48.2
Unreported	1	0.0	0	0.0	0	0.0	—
Age							
5-17	259	7.5	163	4.6	150	5.7	18.4
18-49	1311	37.9	1052	29.8	830	31.5	48.7
50-64	926	26.7	1030	29.2	725	27.5	19.7
65-99	967	27.9	1283	36.4	928	35.2	13.1
Race/Ethnicity							
NL White	2113	61.0	2267	64.3	1628	61.8	59.7
NL Black	845	24.4	803	22.8	603	22.9	21.0
NL Other	210	6.1	195	5.5	194	7.4	8.2
Latinx	295	8.5	263	7.5	208	7.9	11.1
In/Out patient							
Inpatient	1057	30.5	961	27.2	839	31.9	—
Outpatient	2394	69.1	2562	72.6	1792	68.1	—
Unknown	12	0.3	5	0.1	2	0.1	—
Payor							
Public	1825	52.7	2050	58.1	1509	57.3	—
Private	1249	36.1	1172	33.2	920	34.9	—
Self-Pay	326	9.4	254	7.2	181	6.9	—
Other/Unknown	63	1.8	52	1.4	23	0.8	—

Table 4.2 Patients by demographic factors of interest. Note, because of how the NC census reports data, the sex and age breakdowns of the 6-county demographics includes only individuals over the age of 4 (including those over age 99), but the race/ethnicity breakdown includes individuals of all ages. Additionally, the 65-99 age category is actually age 65+ for the 6-county demographics. NL, Non-Latinx

Table 4.3 Cohort prevalence estimates									
	Positivity			**BHM prevalence estimates**					
	4/19-6/13	6/14-8/08	8/09-10/03	4/19-6/13		6/14-8/08		8/09-10/03	
				Estimate	95% CI	Estimate	95% CI	Estimate	95% CI
Overall	5.3	10.5	10.8	2.9	(1.7, 4.3)	8.8	(7.1, 10.6)	9.1	(7.2, 11.1)
Age									
5-17	3.1	9.8	9.3	1.4	(0.3, 3.3)	8.1	(3.9, 13.4)	7.6	(3.5, 13.0)
18-49	6.0	12.6	10.5	3.6	(2.2, 5.4)	11.1	(8.6, 13.8)	8.7	(6.2, 11.5)
50-64	5.9	10.4	13.0	3.7	(1.9, 5.8)	8.7	(6.3, 11.3)	11.5	(8.5, 14.7)
65-99	4.3	9.0	9.6	1.5	(0.2, 3.4)	7.1	(5.0, 9.4)	7.7	(5.2, 10.4)
Sex									
Female	4.5	10.3	10.7	2.1	(1.0, 3.5)	8.5	(6.6, 10.6)	8.9	(6.8, 11.3)
Male	6.3	10.7	10.9	3.9	(2.3, 5.8)	9.2	(7.1, 11.3)	9.2	(6.9, 11.8)
Race/Ethnicity									
NL White	3.7	7.5	8.3	1.4	(0.5, 2.7)	5.4	(3.7, 7.3)	6.3	(4.3, 8.4)
NL Black	5.6	12.0	12.8	2.6	(0.6, 5.0)	10.4	(7.5, 13.4)	11.4	(8.2, 14.8)
NL Other	5.7	10.3	11.3	2.0	(0.1, 5.9)	8.5	(3.9, 13.9)	9.3	(4.5, 14.9)
Latinx	15.9	31.9	24.0	14.8	(10.4, 19.6)	33.2	(26.8, 40.0)	23.9	(17.5, 31.1)
In/out patient									
Outpatient	4.3	9.0	9.1	2.0	(1.0, 3.3)	7.1	(5.4, 9.0)	7.1	(5.1, 9.2)
Inpatient	7.7	14.6	14.4	5.0	(2.9, 7.4)	13.3	(10.5, 16.2)	13.3	(10.3, 16.4)
Payor									
Private	5.2	9.0	8.9	2.9	(1.5, 4.6)	7.3	(5.3, 9.6)	7.1	(4.7, 9.6)
Public	5.0	9.8	10.7	2.5	(1.2, 4.2)	7.9	(5.9, 9.9)	8.9	(6.8, 11.2)
Self-Pay	4.0	18.9	17.1	1.3	(0.2, 3.5)	18.3	(13.1, 23.8)	16.3	(10.4, 23.1)
Other/ Unknown	22.2	30.8	43.5	21.1	(11.8, 31.7)	31.2	(19.4, 44.5)	40.4	(22.4, 60.6)

Table 4.3 Cohort prevalence estimates. Raw seropositivity (%) and posterior mean seroprevalence estimates (%) from BHM with 95% credible intervals (lower bound, upper bound) by different demographics and over time. NL, Non-Latinx.

Table 4.4 Raw antibody test positivity by hospital			
	4/19-6/13	**6/14-8/08**	**8/09-10/03**
Johnston Hospital	7.81	18.00	14.80
Chatham Hospital	7.45	8.69	12.08
UNC Hospitals	4.03	9.93	10.38
Rex Hospital	4.04	5.93	7.71

Table 4.4 Raw antibody test positivity (percent) by hospital. Unadjusted percentage of samples testing positive by RBD Ig ELISA

Table 4.5 Insurance category by race/ethnicity								
	Private		Public		Self-Pay		Other/Unknown	
	N	(%)	N	(%)	N	(%)	N	(%)
NL White	2173	36.2	3439	57.2	347	5.8	49	0.8
NL Black	641	28.5	1402	62.3	177	7.9	31	1.4
NL Other	323	53.9	223	37.2	42	7.0	11	1.8
Latinx	204	26.6	320	41.8	195	25.5	47	6.1
TOTAL	3341	34.7	5384	55.9	761	7.9	138	1.4

Table 4.5 Insurance category by race/ethnicity. Numbers and percentage of individuals within each ethnoracial grouping in the study and insurance payor type.

Table 4.6 Conditional odds ratios of being SARS-CoV-2 seropositivity over the study period.								
	4/19-6/13		**6/14-8/08**		**8/09-10/03**		**4/19-10/03 (overall)**	
	Estimate	95% CI	Estimate	95% CI	Estimate	95% CI	Estimate	95% CI
Sex								
Female	—	—	—	—	—	—	—	—
Male	**2.05**	**(1.08, 4.25)**	1.10	(0.80, 1.51)	0.91	(0.64, 1.29)	1.27	(0.98, 1.69)
Race/Ethnicity								
NL White	—	—	—	—	—	—	—	—
NL Black	1.66	(0.53, 4.28)	**1.94**	**(1.31, 2.92)**	**1.82**	**(1.20, 2.79)**	**1.80**	**(1.19, 2.65)**
NL Other	1.26	(0.12, 5.74)	1.58	(0.74, 3.19)	1.81	(0.87, 3.57)	1.54	(0.66, 2.84)
Latinx	**14.53**	**(6.47, 36.72)**	**7.43**	**(4.70, 11.97)**	**4.34**	**(2.61, 7.41)**	**7.77**	**(5.20, 12.10)**
Age								
5-17	—	—	—	—	—	—	—	—
18-49	3.09	(0.99, 11.43)	1.38	(0.68, 3.05)	0.89	(0.42, 2.03)	1.56	(0.92, 2.77)
50-64	**3.62**	**(1.13, 13.56)**	1.34	(0.64, 2.99)	1.56	(0.76, 3.54)	**1.96**	**(1.15, 3.55)**
65-99	1.62	(0.28, 6.90)	1.49	(0.71, 3.34)	1.13	(0.52, 2.64)	1.40	(0.71, 2.61)
In/out patient								
Outpatient	—	—	—	—	—	—	—	—
Inpatient	**2.50**	**(1.31, 5.10)**	**1.91**	**(1.38, 2.68)**	**1.92**	**(1.34, 2.80)**	**2.09**	**(1.59, 2.85)**
Payor								
Private	—	—	—	—	—	—	—	—
Public	0.85	(0.41, 1.73)	0.89	(0.58, 1.34)	1.16	(0.74, 1.85)	0.96	(0.70, 1.30)
Self-Pay	**0.18**	**(0.03, 0.64)**	**1.78**	**(1.07, 2.93)**	**1.94**	**(1.03, 3.63)**	0.85	(0.45, 1.41)
Other/ Unknown	**3.08**	**(1.15, 8.23)**	**2.73**	**(1.25, 5.98)**	**6.60**	**(2.29, 18.71)**	**3.81**	**(2.23, 6.54)**

Table 4.6 Conditional odds ratios of SARS-CoV-2 seropositivity over the study period. Data are divided into into three two-month long periods. Odds ratios of seropositivity calculated from the BHM with 95% credible intervals (lower bound, upper bound) are reported where the baseline groups for comparison are female, Non-Latinx white, age 5-17, outpatient, and private insurance. Odds ratios that do not overlap a value of one are bolded.

CHAPTER 5 – DISCUSSION

5.1 Overview of Zika virus vector-independent transmission

Like other vector-borne flaviviruses, ZIKV is capable of transmission between two very different animals (humans and mosquitoes), but ZIKV remains an oddity in that it is capable of being transmitted directly between humans via two distinct mechanisms, sexual and congenital transmission. There is little evidence of significant human-to-human transmission of other flaviviruses, though it may be that other flaviviruses have not emerged in a sufficiently large outbreak to reveal rare transmission mechanisms and outcomes. At the time this dissertation research was initiated, there was little information available about pathogenesis resulting from human-to-human transmission of flaviviruses.

Some of the features of ZIKV transmission and pathogenesis in the female reproductive tract have become clearer during the course of the work detailed here. Though ZIKV infects neural progenitor cells within the developing fetus and may thus cause microcephaly directly[74,375], placental pathology is also observed during gestation and may be the cause of intrauterine growth restriction also observed as a result of ZIKV infection[73,97–99,135,136]. Additionally, in mouse models significant fetal loss can be induced by ZIKV infection in pregnant WT mice despite a lack of infection in the fetuses themselves, suggesting that fetal damage can be caused by immunopathology[267]. Other pathogens such as *Plasmodium falciparum* can cause similar placental damage as

gestational ZIKV and in doing so, results in decreased transplacental IgG transfer to the fetus[103–109]. Transfer of IgG targeting different pathogens can be differentially impaired as has now observed during other inflammatory processes such as SARS-CoV-2 infection during pregnancy[266,304,376,377]. This difference in transfer of IgG targeting different pathogens is likely because transfer is dependent on IgG subclass with particular preference for IgG1 and IgG4[266]. Certain Fc glycosylations such as fucosylation are associated with decreased transplacental transfer, possibly because of decreased binding to FcγRIIIa[266].

IgG received during gestation are crucial for health in early life before infants have a chance to develop their own immunity, so it was critical to determine if ZIKV similarly decreased IgG transfer across the placenta. Initially, it was also thought that cross-reactive DENV antibodies that facilitate worsened DENV disease may also be driving fetal damage in gestational ZIKV but it appears that unlike DENV, ZIKV infection is not enhanced by DENV antibodies[62]. It is likely that the same lack of ZIKV ADE will be observed from infants that receive passively transferred antibodies during gestation. By contrast, ZIKV-targeting antibodies can promote ADE of DENV[60]. Interestingly, ADE preferentially occurs as a result of antibodies with low fucosylation which are thus able to mediate ADE via FcγRIIIa, although they have a lower rate of transfer across the placenta[266,378].

The pathogenic mechanisms surrounding sexual transmission of ZIKV have also become clearer. ZIKV is found in semen[124–126,379,380] and most cases follow ejaculation of infected seminal fluid into the vagina. ZIKV then may be infecting a variety of epithelial and immune cells[128,129]. Most mouse pathogenesis models use mice lacking

type I IFN signaling[128,134] because ZIKV is unable to antagonize mouse STAT2 and STING and is therefore unable to disseminate and cause disease in mice[141,329]. All ZIKV vaginal infection models in non-pregnant mice treat with progesterone, similar to common HSV and *Chlamydia* infection models[128,135,159,182,183]. The reasons progesterone sensitizes mice to vaginal infections remain unclear. Some have hypothesized that susceptibility to infection increases as the keratin barrier to infection becomes thinner in a high progesterone state[128].

Recently, Khan et al have provided evidence that viral RNA PRRs in the LFRT might be expressed at a lower level than in the UFRT or draining lymph node[183]. They found a minimal role for DMPA treatment in regulating PRR expression, though Yao et al found that DMPA treatment increases PRR expression in the vagina[381]. However, both of these studies focused on the expression of PRRs themselves rather than induction of ISGs downstream of PRR signaling so more evidence was needed in order to make this claim that there are functional decreases in downstream ISG signaling. Even immunodeficient mice require some level of progesterone treatment in order for susceptibility to infection, so it is difficult to imagine that small decreases in viral RNA PRRs lead to more severe immunosuppression than already exist in mice lacking both Ifnar1 and Ifngr receptors[128].

5.2 Overview of SARS-CoV-2 prevalence and impact in the United States.

During the course of this dissertation research, SARS-CoV-2 emerged and has caused millions of deaths around the world, over 500,000 of which are in the United States[191]. Multiple efforts have been made to define SARS-CoV-2 seroprevalence in order to assess the total number of infections, identify the hardest hit communities and

target resources accordingly, and to understand how many individuals remain susceptible to infection. Molecular testing via PCR is limited by disparities in access and bottlenecks in reagent availability so the total number of infections needs to be evaluated with serological testing which can assay for history of past infection.

Almost every serology study in the United States is limited by unrepresentative sampling methodology[228], though it is very challenging to overcome this without sufficient funding and support to representatively sample across the nation as has been done elsewhere with government support[219]. Some studies have gone so far as to provide prevalence estimates that overestimate their certainty and are statistically likely to comprise entirely false positives because they did not take into account the sensitivity and specificity of their assay[228]. Furthermore, most studies have been limited by their choice of a nucleocapsid test that is not as sensitive at detecting mild or subclinical infections[219,220], though this test was likely chosen because it is readily available and approved for clinical use.

All three limitations were present in a recent study of SARS-CoV-2 seroprevalence in North Carolina by Barzin et al[226]. This study of healthcare-accessing individuals prioritized sampling from asymptomatic individuals, limiting the study's conclusions. Second, though they do correct for the sensitivity and specificity of the assay, they do so using a calculation that assumes a binomial distribution around the final prevalence estimate when instead it should be skewed because of the large effect of false positives at low seroprevalence[232]. Additionally, their cohort is not representative of the general population's demographics (e.g. significant undersampling of Latinx individuals). Finally, the clinically approved nucleocapsid assay used has

reduced sensitivity in individuals after asymptomatic infection—the very population specifically recruited in the study.

Serologic assays must be chosen for serosurveys based on what the expected seroprevalence is in a given area. High specificity (low false positivity rate) needs to be prioritized when exposure is likely to be low, because there are expected to be very few true positives but many negative samples. The likelihood of drawing a false positive sample is high on a background of many true negative samples. This is true for serology at the start of an outbreak or for a rare exposure, as was the case early in the SARS-CoV-2 outbreak.

The opposite is true for flavivirus serology in endemic areas. Nearly everyone has been exposed by adulthood, so there are very few true negatives. There are many positive samples, a large number of which may be false positives even with a low false positive rate simply because there are so many positive samples. Thus sensitivity (low false negative rate) is critical for serology in flavivirus endemic areas. Unfortunately, tests with high specificity are also difficult to generate for flaviviruses, making flavivirus serology complex on both fronts.

5.3 My contributions to understanding the effect of ZIKV on transplacental antibody transfer.

To determine if ZIKV infection during pregnancy results in similar impairment of placental antibody transfer as *Plasmodium* and HIV, I collaborated with Tulika Singh and Dr. Sallie Permar at Duke University to study a paired cohort of 26 neonates and their gestational parents with febrile illness and rash from which 20 paired blood samples were obtained from each at delivery. I differentiated the ZIKV and DENV

exposure history of the gestational parents by neutralization assay, because ZIKV and DENV exposure were not distinguishable by ELISA due to the antigenic cross-reactivity of these viruses. The algorithm I created to differentiate ZIKV and DENV exposure presumes that ZIKV neutralization titers are higher than DENV neutralization titers by having a more stringent cut-off for ZIKV neutralization than DENV neutralization. This assumption was sufficient for this study because if ZIKV exposure happened during gestation, it would have been very recent. Additionally, by sexual maturity, nearly everyone in DENV-endemic regions has already been exposed to DENV, so DENV infections may not have been as recent as the febrile illness during pregnancy[43].

Differentiating these samples by exposure history was necessary in order to compare pregnancies in ZIKV-naïve individuals to those with gestational ZIKV infection, because ZIKV viremia is brief and may have not been detected[381]. I determined that DENV neutralization titers were highly correlated between gestational parents and infants, regardless of gestational ZIKV infection and the slope of the correlations were significantly overlapping. This suggests that gestational ZIKV infection did not affect neutralizing antibody transfer across the placenta. Roughly half of the placentas had evidence of inflammation despite the lack of evidence for placental infection. Additionally, there was no decrease in transplacental transfer of vaccine-induced antibodies as determined by a similar assessment of correlation between cord blood and gestational parent plasma.

My work in this study has since been corroborated by two other cohort studies of gestational ZIKV infection[269,305]. Though each study suffers independently from small sample size, together they suggest that antibody transfer is maintained despite

gestational ZIKV infection even in the presence of placental inflammation. Intact antibody transfer during gestational ZIKV infection may prove beneficial for protection of the fetus from congenital Zika syndrome and the infant from ZIKV infection. Likewise, transplacental antibody transfer is beneficial for health in early life. However, the cross-reactive non-neutralizing DENV-binding antibodies may pose a risk in early life, leading to more severe disease in infants as maternal antibody titers wane[53,257].

The potently ZIKV-neutralizing IgM isolated from the individual with prolonged viremia during pregnancy, once characterized, will provide fascinating insight into the development of neutralizing IgG when their epitopes are compared. This IgM could provide evidence that highly neutralizing flavivirus antibodies can be generated before entering convalescence after continued affinity maturation. This IgM could also serve as a prophylactic against ZIKV infection during gestation as it will neither be transferred across the placenta nor induce ADE, properties which would require additional Fc modifications to achieve with an IgG. Finally, because this IgM can protect against ZIKV viremia in mice and IgM are not thought to be secreted into the female reproductive tract[146], it potentially could be a useful laboratory reagent to restrict viral infection in mice to the female reproductive tract by allowing *Ifnar1*$^{-/-}$ mice to serve as a model for ascending ZIKV infection distinct from systemic spread; ongoing studies in the Lazear Laboratory are investigating this application.

5.4 My contributions to understanding hormonal regulation of ZIKV infection in the vagina

To determine whether IgG-mucin interactions in the vagina can contribute to protection against ZIKV even in the absence of neutralizing antibodies, I vaginally

inoculated *Ifnar1*$^{-/-}$ mice with ZIKV bound to either neutralizing or non-neutralizing antibodies. Although we had hypothesized that non-neutralizing antibodies would provide protection based on analogous studies with HSV, I found that ZIKV infection was only prevented by a neutralizing monoclonal antibody. These results suggest that cross-reactive non-neutralizing antibodies (such as those elicited by prior DENV infection) are unlikely to contribute to protection against ZIKV vaginal infection

I subsequently performed the same experiment in WT mice, which we expected to be less susceptible to ZIKV infection, but again found that the non-neutralizing monoclonal antibody tested did not provide protection against ZIKV infection. Rather than pursuing additional experiments evaluating antibody-mucin effects, I instead opted to follow up on the unexpected ability of ZIKV to infect WT mice intravaginally despite its inability to replicate systemically in these mice.

In addition to type I IFNs restricting ZIKV from replicating systemically in mice[141,329], type III IFNs are thought to play special roles at barrier sites including the vagina[160]. Caine et al found that in the absence of type III IFN signaling, ZIKV was able to replicate to higher levels in the vagina. However, when I tested this in mice lacking the IFN-λ receptor, I found no difference in viral loads between WT and *Ifnlr1*$^{-/-}$ mice. I did not investigate whether ZIKV is able to ascend the FRT in *Ifnlr1*$^{-/-}$ mice, but in WT mice ZIKV infection was restricted to the vagina and cervix with no evidence of replication in the uterus. In humans sexually-acquired ZIKV results in viremia but in these mice the infection is restricted to the vagina so this model is not suited to study systemic dissemination of ZIKV from the vagina. However, the IFN-αβ impaired mice in which ZIKV dissemination is observed die of neuroinvasion[134], and are thus not

necessarily suited to study pathogenesis as it occurs in adult humans which does not result in neuroinvasion. Infection models need to therefore be selected with a clear purpose to most closely match physiologic relevance in humans. I conclude that WT mice should be the model of choice for studies specifically of ZIKV infection within the vagina itself, rather than mouse models with impaired innate immune signaling.

In order to determine the parameters around which ZIKV is able to replicate in the vagina, I inoculated WT and *Ifnar1*$^{-/-}$ mice with ZIKV both with and without prior DMPA treatment. I found that progesterone is required for consistent vaginal infection, even in *Ifnar1*$^{-/-}$ mice. Thus progesterone rather than IFNs regulate ZIKV susceptibility in the vagina. I even found that pregnant WT mice are susceptible to vaginal ZIKV infection. Pregnancy is a high progesterone state, providing further evidence that progesterone regulates ZIKV susceptibility in the vagina

To understand progesterone-induced susceptibility to ZIKV infection, I investigated three potential mechanisms: epithelial barrier integrity, changes in the leukocytes populations, and decreased innate immune antiviral signaling[128,183]. Vaginal abrasion did not sensitize WT mice to ZIKV infection, indicating that disruption of epithelial barrier integrity is insufficient for ZIKV infection. I also did not find any DMPA-induced changes in vaginal leukocyte populations. Finally, I did not find a DMPA-mediated difference in *Ifit1* expression either at baseline or in response to p:IC, arguing against dampened antiviral signaling as the mechanism of DMPA-induced susceptibility. Though Khan et al. found decreased expression of viral RNA sensing PRRs in the vagina relative to other tissues, I did not find relative expression of *Ifit1* in the vagina to be lower than in the spleen[183]. Measurement of expression of the sensors themselves

as Khan et al performed may be misleading if not coupled with measurements of downstream signaling or effector functions.

I found ZIKV infection predominantly in cells along the vaginal lumen (e.g. epithelial cells), rather than in leukocytes or other cell types in the vaginal stroma. In particular, this infection was localized to small sporadic foci of infected cells. I did not find an influx of leukocytes around these infected cells even though I found ZIKV was cleared from the vagina by 10 days after infection, consistent with a protective adaptive immune response. By flow cytometry, I did find an increase in the number of dendritic cells in vaginal tissue at 6 days post-infection, coinciding with the peak of viral load as measured by qRT-PCR of vaginal wash. Concurrently, there was an increase in the number of B cells and T cells in secondary lymphoid tissues (spleen and iLN), which may be the result of expansion indicative of a germinal center reaction and development of an adaptive immune response from dendritic cells sampling antigen at the site of infection. To date no studies have compared immunity resulting from ZIKV vaginal infection or mosquito-borne infection, but vaginal infection may also result in a germinal center reaction even in these mice with a strictly localized infection to the vaginal epithelium. A systemic vaccine response is also likely to protect against vaginal infection, as passively transferred plasma in mice provides potent protection against vaginal ZIKV infection[159].

Despite the prior suggestion that sensing of viral RNA is deficient in the vagina, I did not find a broad ability of other RNA viruses to replicate in the vagina of WT mice. Instead, I observed that some but not all flaviviruses replicated in the vagina even though they do not replicate well in WT mice (SPOV and USUV), though DENV was

unable to. My data suggest that a subset of flaviviruses are capable of replication in the vagina and should be evaluated for their potential to be sexually transmitted in the case of their broader emergence.

5.5 My contributions to understanding SARS-CoV-2 seroprevalence in central North Carolina

To determine to what extent SARS-CoV-2 has been spreading locally and identify the communities bearing the burden of infection, I worked with Dr. Alena Markmann to assay hospital remnant samples by a SARS-CoV-2 RBD-binding ELISA. Though hospital remnant samples are not representative of the general population[228], this is still more representative of the population in central NC than another study by Barzin et al. in the same population center and time frame that prioritized asymptomatic individuals and undersampled by race and ethnicity[226]. Additionally, to avoid common pitfalls of other seroprevalence studies including Barzin et al., I decided the best statistical techniques to employ for this study would require Bayesian inference and recruited the team that developed a state-of-the-art model that estimates assay sensitivity and specificity and simultaneously incorporates that uncertainty into prevalence estimates and credible intervals. Finally and possibly most importantly, this study uses an RBD-binding ELISA that likely has better sensitivity for asymptomatic SARS-CoV-2 infections and therefore can better assess population seroprevalence rather than only seroprevalence among individuals with respiratory infection symptoms[219,220,382]. Prevalence in this cohort of individuals accessing healthcare in central NC rose from 3.9% (1.7, 4.3) to 9.1% (7.2, 11.1) from April to October 2020.

I also decided to analyze seroprevalence by different demographic factors. I collapsed both race and ethnicity into a single ethnoracial variable as an imperfect measure of racism[198] and found that non-Latinx individuals were the group at highest risk of infection over this time frame compared to non-Latinx white individuals. I also included insurance type as a variable in the analysis and decided how to categorize insurance types. Behind Latinx individuals, individuals with undefined health insurance and those self-paying for healthcare were the next most likely to be SARS-CoV-2 seropositive compared to those with private health insurance. Black individuals were at the next greatest risk when compared to non-Latinx white individuals. Interestingly, there was no difference in risk of exposure by age or sex that persisted beyond the first two months despite schools being closed. In general, the increased odds for all of these groups decreased, trending towards baseline risk suggesting that the observed risk is the result of SARS-CoV-2 first spreading among individuals with high exposure risk and later to the rest of the population. The high odds of seropositivity in Latinx and Black populations are indicative of the systemic racism that has been driving the burden of SARS-CoV-2 to largely fall on these communities[198,236,238,239].

Finally, I defined ICD-10 codes that overlap with SARS-CoV-2 respiratory signs, symptoms, and disease. I determined that individuals with documented COVID-19 or symptomatic respiratory disease had increased odds of developing neutralizing antibody titers, consistent with the hypothesis that asymptomatic individuals develop lower titers of neutralizing antibodies to SARS-CoV-2[373]. It is impossible to conclude from neutralization titers the extent to which neutralizing antibodies are necessary to protect against severe disease.

My work on this study allowed for an estimation of SARS-CoV-2 seroprevalence that is more representative and accurate than previous efforts and is one of few seroprevalence studies outside of a major metropolitan region. I further found that there was exceptionally high SARS-CoV-2 exposure risk in Latinx individuals as well as in potentially underinsured individuals in central North Carolina. The driving risk factors for exposure of this infection are both racism and socioeconomic access to infection prevention, not race as a biological factor (race is an imperfect measure of racism and underinsurance is an imperfect measure of socioeconomic discrimination)[358]. Additionally, individuals without SARS-CoV-2 symptoms but who tested positive had lower neutralization titers, consistent with the ideas that asymptomatic infections result in lower neutralization titers.

5.6 Future directions for the study of vector-independent flavivirus infections

The results detailed here demonstrate that even though ZIKV can produce placental damage, it may not necessarily do so via high levels of infection directly within the placenta. Instead, the placental pathology observed may be the result of inflammation. Although this placental damage may resemble that induced in *Plasmodium* infection, it might not result in the same clinical consequences after delivery because transplacental IgG transfer is maintained after gestational ZIKV infection. Other infections such as HIV and SARS-CoV-2 can also cause decreased IgG transfer without necessarily inducing the same degree of placental insufficiency, so much remains to be determined about how some infections can decrease transplacental IgG transfer independent of inflammatory pathology[111,266,376,377].

Intact antibody transfer during gestational ZIKV infection may prove beneficial for protection of the fetus from congenital Zika syndrome and the infant from ZIKV infection. Likewise, transplacental antibody transfer is beneficial for health in infancy. However, we need to remain alert to the possibility that ZIKV antibodies transferred during gestation can negatively impact health in the first year of life because they may enhance DENV infection as is observed in infants born to DENV-immune mothers[257].

Much remains to be learned about ZIKV in the vagina. In particular, we do not yet understand why ZIKV is capable of sexual transmission when other common flaviviruses are not. There is increasing evidence that a subset of other flaviviruses are also capable of either infecting either vaginal tissue or prostate tissues. If any of these were to cause a large outbreak, surveillance of individuals returning from those locations and their sexual partners will help clarify if ZIKV is not so unique after all.

We also do not understand why progesterone has such a strong effect of ZIKV infection in mice, or whether this impacts human health. Sex hormones can affect rates of transmission of other viruses in humans. However, this is no reason to cease sex hormone-based contraceptives if the goal is to prevent CZS. It is possible that increased ZIKV sexual transmission could result a greater number of infectious hosts for mosquitoes to feed on, but the benefits of contraception likely still outweigh this theoretical risk. Potential mechanisms to explore include progesterone-induced innate immune signaling changes or changes to cellular metabolism specifically in epithelial cells , which appear to be the target cells of ZIKV in the vagina. Additionally, we still need to determine whether local ZIKV replication in the vagina is sufficient to induce protective immunity against subsequent vaginal or systemic infection. We also will need

to determine to what extent these observations carry over in sexually mature animals rather than the 5 week old mice I studied.

It also remains to be seen how well the model for vaginal infection in mice I've characterized correlates with vaginal infection in humans. I observe limited replication beyond the superficial layer of epithelial cells in the LFRT without ascension to the uterus. Pregnant non-human primates similarly have replication within epithelial cells in the LFRT with inconsistent ascension to the uterus, though in that model ZIKV is capable of causing viremia[133]. Other non-human primate models demonstrate that the viremia that results from vaginal inoculation is delayed relative to subcutaneous infection[132]. Also, non-human primates inconsistently seroconvert after vaginal ZIKV infection[133,383].

5.7 Future directions for the prevalence of immunity to SARS-CoV-2 and other emerging pathogens

SARS-CoV-2 is likely to become an endemic human pathogen. It is likely we will continue to see emerging β-coronaviruses, so we need to prepare to best estimate the prevalence of novel coronaviruses before the next outbreak. SARS-CoV-2 asymptomatic infections are not accurately detected by the existing nucleocapsid assay in clinical use, and these assays will not detect antibodies to S-based vaccines. However, the limitation to RBD-based assays is that they cannot differentiate between natural infection-induced and vaccine-induced immunity. This is an important distinction for many reasons, including if vaccination proves to provide a different degree of protection from disease than natural infection, as well as defining if some populations are not being reached for vaccination. When combined in the same study, these assays

can therefore have complementary roles to discern infection-vs-vaccine-induced immunity.

Disparities in vaccination unfortunately appear to be along the same ethnoracial groupings that placed Black and Latinx individuals at greater risk of infection. Eliminating the racism that places these groups at risk requires societal change as well as economic investments. Mass incarceration must be eliminated, paid protected sick leave needs to be provided including for essential work positions, and financial inequality leading to overcrowded housing needs to be addressed. Many of the worst impacted areas during the ZIKV epidemic had such a high force of infection as a result of poverty and a lack of infrastructure leading to high numbers of *Aedes aegypti* mosquitoes[384]. The most severe ZIKV outcome, congenital disease, results in high healthcare costs and requires substantial care during and after pregnancy, and pregnant individuals already face difficulties in healthcare access. We must also correct inequities in access to health insurance, care, testing, vaccination, and treatments. Many of the worst impacted areas during the ZIKV epidemic had such a high force of infection as a result of poverty and a lack of infrastructure leading to high numbers of *Aedes aegypti* mosquitoes[384]. Whether global or local, hoarding of supplies drives the burden of disease and disability. These are important considerations for Zika and SARS-CoV-2 today as well as future emerging pathogens.

REFERENCES

1. Fagbami AH. Zika virus infections in Nigeria: Virological and seroepidemiological investigations in Oyo State. *J Hyg (Lond)* 1979; **83**: 213–9.

2. Moore DL, Causey OR, Carey DE, Reddy S, Cooke AR, Akinkugbe FM, David-West TS, Kemp GE. Arthropod-borne viral infections of man in nigeria, 1964-1970. *Ann Trop Med Parasitol* 1975; **69**: 49–64.

3. Olson JG, Ksiazek TG, Suhandiman, Triwibowo. Zika virus, a cause of fever in Central Java, Indonesia. *Trans R Soc Trop Med Hyg* 1981; **75**: 389–93.

4. Simpson DIH. Zika virus infection in man. *Trans R Soc Trop Med Hyg* 1964; **58**: 339–48.

5. Petersen LR, Jamieson DJ, Powers AM, Honein MA. Zika Virus. *N Engl J Med* 2016; **374**: 1552–63.

6. Cao-Lormeau VM, Blake A, Mons S, Lastère S, Roche C, Vanhomwegen J, Dub T, Baudouin L, Teissier A, Larre P, Vial AL, Decam C, Choumet V, Halstead SK, Willison HJ, Musset L, Manuguerra JC, Despres P, Fournier E, Mallet HP, Musso D, Fontanet A, Neil J, Ghawché F. Guillain-Barré Syndrome outbreak associated with Zika virus infection in French Polynesia: A case-control study. *Lancet* 2016; **387**: 1531–9.

7. Oehler E, Watrin L, Larre P, Leparc-Goffart I, Lastãre S, Valour F, Baudouin L, Mallet HP, Musso D, Ghawche F. Zika virus infection complicated by guillain-barré syndrome â€"case report, French Polynesia, December 2013. *Eurosurveillance* 2014; **19**. DOI:10.2807/1560-7917.es2014.19.9.20720.

8. Pan American Health Organization; World Health Organization. Zika suspected and confirmed cases reported by countries and territories in the Americas, Cumulative cases, 2015-2017. .

9. Netto EM, Moreira-Soto A, Pedroso C, Höser C, Funk S, Kucharski AJ, Rockstroh A, Kümmerer BM, Sampaio GS, Luz E, Vaz SN, Dias JP, Bastos FA, Cabral R, Kistemann T, Ulbert S, De Lamballerie X, Jaenisch T, Brady OJ, Drosten C, Sarno M, Brites C, Drexlerc JF. High Zika virus seroprevalence in Salvador, northeastern Brazil limits the potential for further outbreaks. *MBio* 2017; **8**. DOI:10.1128/mBio.01390-17.

10. Zambrana JV, Carrillo FB, Burger-Calderon R, Collado D, Sanchez N, Ojeda S, Monterrey JC, Plazaola M, Lopez B, Arguello S, Elizondo D, Aviles W, Coloma J, Kuan G, Balmaseda A, Gordon A, Harris E. Seroprevalence, risk factor, and spatial analyses of Zika virus infection after the 2016 epidemic in Managua, Nicaragua. *Proc Natl Acad Sci U S A* 2018; **115**: 9294–9.

11. Pierson TC, Diamond MS. The emergence of Zika virus and its new clinical syndromes. *Nature* 2018; **560**: 573–81.

12. Coyne CB, Lazear HM. Zika virus — reigniting the TORCH. *Nat Rev Microbiol* 2016; **14**: 707–15.

13. Pacheco O, Beltrán M, Nelson CA, Valencia D, Tolosa N, Farr SL, Padilla A V., Tong VT, Cuevas EL, Espinosa-Bode A, Pardo L, Rico A, Reefhuis J, González M, Mercado M, Chaparro P, Martínez Duran M, Rao CY, Muñoz MM, Powers AM, Cuéllar C, Helfand R, Huguett C, Jamieson DJ, Honein MA, Ospina Martínez ML. Zika Virus Disease in Colombia — Preliminary Report. *N Engl J Med* 2020; **383**: e44.

14. dos Santos T, Rodriguez A, Almiron M, Sanhueza A, Ramon P, de Oliveira WK, Coelho GE, Badaró R, Cortez J, Ospina M, Pimentel R, Masis R, Hernandez F, Lara B, Montoya R, Jubithana B, Melchor A, Alvarez A, Aldighieri S, Dye C, Espinal MA. Zika Virus and the Guillain–Barré Syndrome — Case Series from Seven Countries. *N Engl J Med* 2016; **375**: 1598–601.

15. Counotte MJ, Kim CR, Wang J, Bernstein K, Deal CD, Broutet NJN, Low N. Sexual transmission of Zika virus and other flaviviruses: A living systematic review. *PLoS Med* 2018; **15**. DOI:10.1371/journal.pmed.1002611.

16. Arsuaga M, Bujalance SG, Díaz-Menéndez M, Vázquez A, Arribas JR. Probable sexual transmission of Zika virus from a vasectomised man. *Lancet Infect Dis* 2016; **16**: 1107.

17. Hills SL, Russell K, Hennessey M, Williams C, Oster AM, Fischer M, Mead P. Transmission of Zika Virus Through Sexual Contact with Travelers to Areas of Ongoing Transmission - Continental United States, 2016. *MMWR Morb Mortal Wkly Rep* 2016; **65**: 215–6.

18. Deckard DT, Chung WM, Brooks JT, Smith JC, Woldai S, Hennessey M, Kwit N, Mead P. Male-to-Male Sexual Transmission of Zika Virus — Texas, January 2016. *MMWR Morb Mortal Wkly Rep* 2016; **65**: 372–4.

19. Russell K, Hills SL, Oster AM, Porse CC, Danyluk G, Cone M, Brooks R, Scotland S, Schiffman E, Fredette C, White JL, Ellingson K, Hubbard A, Cohn A, Fischer M, Mead P, Powers AM, Brooks JT. Male-to-female sexual transmission of zika virus-United States, January-April 2016. *Clin Infect Dis* 2017; **64**: 211–3.

20. Pham AM, Langlois RA, tenOever BR. Replication in Cells of Hematopoietic Origin Is Necessary for Dengue Virus Dissemination. *PLoS Pathog* 2012; **8**: e1002465.

21. Yi G, Xu X, Abraham S, Petersen S, Guo H, Ortega N, Shankar P, Manjunath N. A DNA Vaccine Protects Human Immune Cells against Zika Virus Infection in Humanized Mice. *EBioMedicine* 2017; **25**: 87–94.

22. McDonald EM, Anderson J, Wilusz J, Ebel GD, Brault AC. Zika Virus Replication in Myeloid Cells during Acute Infection Is Vital to Viral Dissemination and Pathogenesis in a Mouse Model. *J Virol* 2020; **94**. DOI:10.1128/jvi.00838-20.

23. Welsch S, Miller S, Romero-Brey I, Merz A, Bleck CKE, Walther P, Fuller SD, Antony C, Krijnse-Locker J, Bartenschlager R. Composition and Three-Dimensional Architecture of the Dengue Virus Replication and Assembly Sites. *Cell Host Microbe* 2009; **5**: 365–75.

24. Mukhopadhyay S, Kuhn RJ, Rossmann MG. A structural perspective of the flavivirus life cycle. *Nat Rev Microbiol* 2005; **3**: 13–22.

25. Neufeldt CJ, Cortese M, Acosta EG, Bartenschlager R. Rewiring cellular networks by members of the Flaviviridae family. Nat. Rev. Microbiol. 2018; **16**: 125–42.

26. Sirohi D, Chen Z, Sun L, Klose T, Pierson TC, Rossmann MG, Kuhn RJ. The 3.8 Å resolution cryo-EM structure of Zika virus. *Science (80-)* 2016; **352**: 467–70.

27. Raut R, Corbett KS, Tennekoon RN, Premawansa S, Wijewickrama A, Premawansa G, Mieczkowski P, Rückert C, Ebel GD, De Silva AD, De Silva AM. Dengue type 1 viruses circulating in humans are highly infectious and poorly neutralized by human antibodies. *Proc Natl Acad Sci U S A* 2019; **116**: 227–32.

28. Rey FA, Heinz FX, Mandl C, Kunz C, Harrison SC. The envelope glycoprotein from tick-borne encephalitis virus at 2 Å resolution. *Nature* 1995; **375**: 291–8.

29. Zhang Y, Zhang W, Ogata S, Clements D, Strauss JH, Baker TS, Kuhn RJ, Rossmann MG. Conformational changes of the flavivirus E glycoprotein. *Structure* 2004; **12**: 1607–18.

30. Smith SA, de Alwis AR, Kose N, Harris E, Ibarra KD, Kahle KM, Pfaf JM, Xiang X, Doranz BJ, de Silva AM, Austin SK, Sukupolvi-Petty S, Diamond MS, Crowe JE. The potent and broadly neutralizing human dengue virus-specific monoclonal antibody 1C19 reveals a unique cross-reactive epitope on the bc loop of domain II of the envelope protein. *MBio* 2013; **4**. DOI:10.1128/mBio.00873-13.

31. Beltramello M, Williams KL, Simmons CP, MacAgno A, Simonelli L, Quyen NTH, Sukupolvi-Petty S, Navarro-Sanchez E, Young PR, De Silva AM, Rey FA, Varani L, Whitehead SS, Diamond MS, Harris E, Lanzavecchia A, Sallusto F. The human immune response to dengue virus is dominated by highly cross-reactive antibodies endowed with neutralizing and enhancing activity. *Cell Host Microbe* 2010; **8**: 271–83.

32. Lai C-Y, Tsai W-Y, Lin S-R, Kao C-L, Hu H-P, King C-C, Wu H-C, Chang G-J, Wang W-K. Antibodies to Envelope Glycoprotein of Dengue Virus during the Natural Course of Infection Are Predominantly Cross-Reactive and Recognize Epitopes Containing Highly Conserved Residues at the Fusion Loop of Domain II. *J Virol* 2008; **82**: 6631–43.

33. Dai L, Song J, Lu X, Deng YQ, Musyoki AM, Cheng H, Zhang Y, Yuan Y, Song H, Haywood J, Xiao H, Yan J, Shi Y, Qin CF, Qi J, Gao GF. Structures of the Zika Virus Envelope Protein and Its Complex with a Flavivirus Broadly Protective Antibody. *Cell Host Microbe* 2016; **19**: 696–704.

34. Zhao H, Fernandez E, Dowd KA, Speer SD, Platt DJ, Gorman MJ, Govero J, Nelson CA, Pierson TC, Diamond MS, Fremont DH. Structural Basis of Zika Virus-Specific Antibody Protection. *Cell* 2016; **166**: 1016–27.

35. Bailey MJ, Broecker F, Freyn AW, Choi A, Brown JA, Fedorova N, Simon V, Lim JK, Evans MJ, García-Sastre A, Palese P, Tan GS. Human Monoclonal Antibodies Potently Neutralize Zika Virus and Select for Escape Mutations on the Lateral Ridge of the Envelope Protein. *J Virol* 2019; **93**. DOI:10.1128/jvi.00405-19.

36. Yu L, Wang R, Gao F, Li M, Liu J, Wang J, Hong W, Zhao L, Wen Y, Yin C, Wang H, Zhang Q, Li Y, Zhou P, Zhang R, Liu Y, Tang X, Guan Y, Qin CF, Chen L, Shi X, Jin X, Cheng G, Zhang F, Zhang L. Delineating antibody recognition against Zika virus during natural infection. *J Clin Invest* 2017; **2**. DOI:10.1172/jci.insight.93042.

37. Zhao H, Xu L, Bombardi R, Nargi R, Deng Z, Errico JM, Nelson CA, Dowd KA, Pierson TC, Crowe JE, Diamond MS, Fremont DH. Mechanism of differential Zika and dengue virus neutralization by a public antibody lineage targeting the DIII lateral ridge. *J Exp Med* 2020; **217**. DOI:10.1084/jem.20191792.

38. Sapparapu G, Fernandez E, Kose N, Bin Cao, Fox JM, Bombardi RG, Zhao H, Nelson CA, Bryan AL, Barnes T, Davidson E, Mysorekar IU, Fremont DH, Doranz BJ, Diamond MS, Crowe JE. Neutralizing human antibodies prevent Zika virus replication and fetal disease in mice. *Nature* 2016; **540**: 443–7.

39. Collins MH, Tu HA, Gimblet-Ochieng C, Liou GJA, Jadi RS, Metz SW, Thomas A, McElvany BD, Davidson E, Doranz BJ, Reyes Y, Bowman NM, Becker-Dreps S, Bucardo F, Lazear HM, Diehl SA, De Silva AM. Human antibody response to Zika targets type-specific quaternary structure epitopes. *JCI Insight* 2019; **4**. DOI:10.1172/jci.insight.124588.

40. De Madrid AT, Porterfield JS. The flaviviruses (group B arboviruses): a cross neutralization study. *J Gen Virol* 1974; **23**: 91–6.

41. Baba SS, Fagbami AH, Olaleye OD. Antigenic relatedness of selected flaviviruses: Study with homologous and heterologous immune mouse ascitic fluids. *Rev Inst Med Trop Sao Paulo* 1998; **40**: 343–9.

42. Calisher CH, Karabatsos N, Dalrymple JM, Shope RE, Porterfield JS, Westaway EG, Brandt WE. Antigenic relationships between flaviviruses as determined by cross-neutralization tests with polyclonal antisera. *J Gen Virol* 1989; **70 (Pt 1)**: 37–43.

43. Reller ME, de Silva AM, Miles JJ, Jadi RS, Broadwater A, Walker K, Woods C, Mayorga O, Matute A. Unsuspected Dengue as a Cause of Acute Febrile Illness in Children and Adults in Western Nicaragua. *PLoS Negl Trop Dis* 2016; **10**: e0005026.

44. Nader PR, Horwitz MS, Rousseau J. Atypical exanthem following exposure to natural measles: Eleven cases in children previously inoculated with killed vaccine. *J Pediatr* 1968; **72**: 22–8.

45. Polack FP, Auwaerter PG, Lee SH, Nousari HC, Valsamakis A, Leiferman KM, Diwan A, Adams RJ, Griffin DE. Production of atypical measles in rhesus macaques: Evidence for disease mediated by immune complex formation and eosinophils in the presence of fusion-inhibiting antibody. *Nat Med* 1999; **5**: 629–34.

46. Chin J, Magoffin RL, Shearer LA, Schieble JH, Lennette EH. Field evaluation of a respiratory syncytial virus vaccine and a trivalent parainfluenza virus vaccine in a pediatric population. *Am J Epidemiol* 1969; **89**: 449–63.

47. Takada A, Watanabe S, Okazaki K, Kida H, Kawaoka Y. Infectivity-Enhancing Antibodies to Ebola Virus Glycoprotein. *J Virol* 2001; **75**: 2324–30.

48. Robinson WE, Montefiori DC, Mitchell WM, Prince AM, Alter HJ, Dreesman GR, Eichberg JW. Antibody-dependent enhancement of human immunodeficiency virus type 1 (HIV-1) infection in vitro by serum from HIV-1-infected and passively immunized chimpanzees. *Proc Natl Acad Sci U S A* 1989; **86**: 4710–4.

49. Robinson WE, Montefiori DC, Mitchell WM. ANTIBODY-DEPENDENT ENHANCEMENT OF HUMAN IMMUNODEFICIENCY VIRUS TYPE 1 INFECTION. *Lancet* 1988; **331**: 790–4.

50. Wan Y, Shang J, Sun S, Tai W, Chen J, Geng Q, He L, Chen Y, Wu J, Shi Z, Zhou Y, Du L, Li F. Molecular Mechanism for Antibody-Dependent Enhancement of Coronavirus Entry. *J Virol* 2019; **94**: 2015–34.

51. Ochiai H, Kurokawa M, Matsui S, Yamamoto T, Kuroki Y, Kishimoto C, Shiraki K. Infection enhancement of influenza A NWS virus in primary murine macrophages by anti-hemagglutinin monoclonal antibody. *J Med Virol* 1992; **36**: 217–21.

52. Takada A, Feldmann H, Ksiazek TG, Kawaoka Y. Antibody-Dependent Enhancement of Ebola Virus Infection. *J Virol* 2003; **77**: 7539–44.

53. Katzelnick LC, Gresh L, Halloran ME, Mercado JC, Kuan G, Gordon A, Balmaseda A, Harris E. Antibody-dependent enhancement of severe dengue disease in humans. *Science (80-)* 2017; **358**: 929–32.

54. Pierson TC, Xu Q, Nelson S, Oliphant T, Nybakken GE, Fremont DHH, Diamond MS. The Stoichiometry of Antibody-Mediated Neutralization and Enhancement of

West Nile Virus Infection. *Cell Host Microbe* 2007; **1**: 135–45.

55. Peiris JSM, Porterfield JS. Antibody-mediated enhancement of Flavivirus replication in macrophage-Like cell lines. Nature. 1979; **282**: 509–11.

56. Schlesinger JJ, Brandriss MW. 17D yellow fever virus infection of P388D1 cells mediated by monoclonal antibodies: Properties of the macrophage Fc receptor. *J Gen Virol* 1983; **64**: 1255–62.

57. Gould EA, Buckley A. Antibody-dependent enhancement of yellow fever and Japanese encephalitis virus neurovirulence. *J Gen Virol* 1989; **70**: 1605–8.

58. Garg H, Yeh R, Watts DM, Mehmetoglu-Gurbuz T, Resendes R, Parsons B, Gonzales F, Joshi A. Enhancement of Zika virus infection by antibodies from West Nile virus seropositive individuals with no history of clinical infection. *BMC Immunol* 2021; **22**: 5.

59. Rathore APS, Saron WAA, Lim T, Jahan N, St John AL. Maternal immunity and antibodies to dengue virus promote infection and Zika virus-induced microcephaly in fetuses. *Sci Adv* 2019; **5**: eaav3208.

60. Gordon A, Gresh L, Ojeda S, Katzelnick LC, Sanchez N, Mercado JC, Chowell G, Lopez B, Elizondo D, Coloma J, Burger-Calderon R, Kuan G, Balmaseda A, Harris E. Prior dengue virus infection and risk of Zika: A pediatric cohort in Nicaragua. *PLOS Med* 2019; **16**: e1002726.

61. Castanha PMS, Cordeiro MT, Martelli CMT, Souza W V., Marques ETA, Braga C. Force of infection of dengue serotypes in a population-based study in the northeast of Brazil. *Epidemiol Infect* 2013; **141**: 1080–8.

62. Katzelnick LC, Narvaez C, Arguello S, Mercado BL, Collado D, Ampie O, Elizondo D, Miranda T, Carillo FB, Mercado JC, Latta K, Schiller A, Segovia-Chumbez B, Ojeda S, Sanchez N, Plazaola M, Coloma J, Elizabeth Halloran M, Premkumar L, Gordon A, Narvaez F, de Silva AM, Kuan G, Balmaseda A, Harris E. Zika virus infection enhances future risk of severe dengue disease. *Science (80-)* 2020; **369**: 1123–8.

63. Budasha NH, Gonzalez JP, Sebhatu TT, Arnold E. Rift Valley fever seroprevalence and abortion frequency among livestock of Kisoro district, South Western Uganda (2016): A prerequisite for zoonotic infection. *BMC Vet Res* 2018; **14**. DOI:10.1186/s12917-018-1596-8.

64. Wernike K, Holsteg M, Schirrmeier H, Hoffmann B, Beer M. Natural Infection of Pregnant Cows with Schmallenberg Virus – A Follow-Up Study. *PLoS One* 2014; **9**: e98223.

65. Burns KF. Congenital Japanese B Encephalitis Infection of Swine. *Exp Biol Med* 1950; **75**: 621–5.

66. Chaturvedi UC, Mathur A, Chandra A, Das SK, Tandon HO, Singh UK. Transplacental infection with Japanese encephalitis virus. *J Infect Dis* 1980; **141**: 712–5.

67. Alpert SG, Fergerson J, Noël LP. Intrauterine West Nile virus: Ocular and systemic findings. *Am J Ophthalmol* 2003; **136**: 733–5.

68. Friedman EE, Dallah F, Harville EW, Myers L, Buekens P, Breart G, Carles G. Symptomatic Dengue infection during pregnancy and infant outcomes: a retrospective cohort study. *PLoS Negl Trop Dis* 2014; **8**: e3226.

69. Ribeiro CF, Lopes VGS, Brasil P, Pires ARC, Rohloff R, Nogueira RMR. Dengue infection in pregnancy and its impact on the placenta. *Int J Infect Dis* 2017; **55**: 109–12.

70. Paixao ES, Harron K, Campbell O, Teixeira MG, Costa M da CN, Barreto ML, Rodrigues LC. Dengue in pregnancy and maternal mortality: a cohort analysis using routine data. *Sci Rep* 2018; **8**: 9938.

71. Tan PC, Soe MZ, Si Lay K, Wang SM, Sekaran SD, Omar SZ. Dengue Infection and Miscarriage: A Prospective Case Control Study. *PLoS Negl Trop Dis* 2012; **6**: e1637.

72. Chitra T V, Panicker S. Maternal and fetal outcome of dengue fever in pregnancy. *J Vector Borne Dis* 2011; **48**: 210–3.

73. Schaub B, Gueneret M, Jolivet E, Decatrelle V, Yazza S, Gueye H, Monthieux A, Juve M-L, Gautier M, Najioullah F, Vouga M, Voluménie J-L, Baud D. Ultrasound imaging for identification of cerebral damage in congenital Zika virus syndrome: a case series. *Lancet Child Adolesc Heal* 2017; **1**: 45–55.

74. Mlakar J, Korva M, Tul N, Popović M, Poljšak-Prijatelj M, Mraz J, Kolenc M, Resman Rus K, Vesnaver Vipotnik T, Fabjan Vodušek V, Vizjak A, Pižem J, Petrovec M, Avšič Županc T. Zika Virus Associated with Microcephaly. *N Engl J Med* 2016; **374**: 951–8.

75. Brasil P, Pereira JP, Moreira ME, Ribeiro Nogueira RM, Damasceno L, Wakimoto M, Rabello RS, Valderramos SG, Halai U-A, Salles TS, Zin AA, Horovitz D, Daltro P, Boechat M, Raja Gabaglia C, Carvalho de Sequeira P, Pilotto JH, Medialdea-Carrera R, Cotrim da Cunha D, Abreu de Carvalho LM, Pone M, Machado Siqueira A, Calvet GA, Rodrigues Baião AE, Neves ES, Nassar de Carvalho PR, Hasue RH, Marschik PB, Einspieler C, Janzen C, Cherry JD, Bispo de Filippis AM, Nielsen-Saines K. Zika Virus Infection in Pregnant Women in Rio de Janeiro. *N Engl J Med* 2016; **375**: 2321–34.

76. Melo AS de O, Aguiar RS, Amorim MMR, Arruda MB, Melo F de O, Ribeiro STC, Batista AGM, Ferreira T, dos Santos MP, Sampaio VV, Moura SRM, Rabello LP, Gonzaga CE, Malinger G, Ximenes R, de Oliveira-Szejnfeld PS, Tovar-Moll F,

Chimelli L, Silveira PP, Delvechio R, Higa L, Campanati L, Nogueira RMR, Filippis AMB, Szejnfeld J, Voloch CM, Ferreira OC, Brindeiro RM, Tanuri A. Congenital Zika Virus Infection. *JAMA Neurol* 2016; **73**: 1407.

77. Bhatnagar J, Rabeneck DB, Martines RB, Reagan-Steiner S, Ermias Y, Estetter LBC, Suzuki T, Ritter J, Keating MK, Hale G, Gary J, Muehlenbachs A, Lambert A, Lanciotti R, Oduyebo T, Meaney-Delman D, Bolaños F, Saad EAP, Shieh WJ, Zaki SR. Zika virus RNA replication and persistence in brain and placental tissue. *Emerg Infect Dis* 2017; **23**: 405–14.

78. Driggers RW, Ho C-Y, Korhonen EM, Kuivanen S, Jääskeläinen AJ, Smura T, Rosenberg A, Hill DA, DeBiasi RL, Vezina G, Timofeev J, Rodriguez FJ, Levanov L, Razak J, Iyengar P, Hennenfent A, Kennedy R, Lanciotti R, du Plessis A, Vapalahti O. Zika Virus Infection with Prolonged Maternal Viremia and Fetal Brain Abnormalities. *N Engl J Med* 2016; **374**: 2142–51.

79. Mittal R, Fifer RC, Liu XZ. A possible association between hearing loss and Zika virus infections. JAMA Otolaryngol. - Head Neck Surg. 2018; **144**: 3–4.

80. Meaney-Delman D, Oduyebo T, Polen KND, White JL, Bingham AM, Slavinski SA, Heberlein-Larson L, St. George K, Rakeman JL, Hills S, Olson CK, Adamski A, Culver Barlow L, Lee EH, Likos AM, Muñoz JL, Petersen EE, Dufort EM, Dean AB, Cortese MM, Santiago GA, Bhatnagar J, Powers AM, Zaki S, Petersen LR, Jamieson DJ, Honein MA, U.S. Zika Pregnancy Registry Prolonged Viremia Working Group. Prolonged Detection of Zika Virus RNA in Pregnant Women. *Obstet Gynecol* 2016; **128**: 724–30.

81. Suy A, Sulleiro E, Rodó C, Vázquez É, Bocanegra C, Molina I, Esperalba J, Sánchez-Seco MP, Boix H, Pumarola T, Carreras E. Prolonged Zika Virus Viremia during Pregnancy. *N Engl J Med* 2016; **375**: 2611–3.

82. Paz-Bailey G, Rosenberg ES, Sharp TM. Persistence of Zika Virus in Body Fluids — Final Report. *N Engl J Med* 2019; **380**: 198–9.

83. Fouda GG, Martinez DR, Swamy GK, Permar SR. The Impact of IgG transplacental transfer on early life immunity. *ImmunoHorizons* 2018; **2**: 14–25.

84. Khan AA, Zahidie A, Rabbani F. Interventions to reduce neonatal mortality from neonatal tetanus in low and middle income countries--a systematic review. *BMC Public Health* 2013; **13**: 322.

85. Benowitz I, Esposito DB, Gracey KD, Shapiro ED, Vázquez M. Influenza vaccine given to pregnant women reduces hospitalization due to influenza in their infants. *Clin Infect Dis* 2010; **51**: 1355–61.

86. Tapia MD, Sow SO, Tamboura B, Tégueté I, Pasetti MF, Kodio M, Onwuchekwa U, Tennant SM, Blackwelder WC, Coulibaly F, Traoré A, Keita AM, Haidara FC, Diallo F, Doumbia M, Sanogo D, DeMatt E, Schluterman NH, Buchwald A, Kotloff

KL, Chen WH, Orenstein EW, Orenstein LA V, Villanueva J, Bresee J, Treanor J, Levine MM. Maternal immunisation with trivalent inactivated influenza vaccine for prevention of influenza in infants in Mali: a prospective, active-controlled, observer-blind, randomised phase 4 trial. *Lancet Infect Dis* 2016; **16**: 1026–35.

87. Nunes MC, Cutland CL, Jones S, Hugo A, Madimabe R, Simões EAF, Weinberg A, Madhi SA, Maternal Flu Trial Team. Duration of Infant Protection Against Influenza Illness Conferred by Maternal Immunization: Secondary Analysis of a Randomized Clinical Trial. *JAMA Pediatr* 2016; **170**: 840–7.

88. Robbins JR, Skrzypczynska KM, Zeldovich VB, Kapidzic M, Bakardjiev AI. Placental Syncytiotrophoblast Constitutes a Major Barrier to Vertical Transmission of Listeria monocytogenes. *PLoS Pathog* 2010; **6**: e1000732.

89. Ander SE, Rudzki EN, Arora N, Sadovsky Y, Coyne CB, Boyle JP. Human placental syncytiotrophoblasts restrict toxoplasma gondii attachment and replication and respond to infection by producing immunomodulatory chemokines. *MBio* 2018; **9**. DOI:10.1128/mBio.01678-17.

90. Koi H, Zhang J, Makrigiannakis A, Getsios S, MacCalman CD, Strauss JF, Parry S. Syncytiotrophoblast is a barrier to maternal-fetal transmission of herpes simplex virus. *Biol Reprod* 2002; **67**: 1572–9.

91. Roopenian DC, Akilesh S. FcRn: the neonatal Fc receptor comes of age. *Nat Rev Immunol* 2007; **7**: 715–25.

92. Wood G, Reynard J, Krishnan E, Racela L. Immunobiology of the human placenta. II. Localization of macrophages, in vivo bound IgG and C3. *Cell Immunol* 1978; **35**: 205–16.

93. Khan S, Katabuchi H, Araki M, Nishimura R, Okamura H. Human villous macrophage-conditioned media enhance human trophoblast growth and differentiation in vitro. *Biol Reprod* 2000; **62**: 1075–83.

94. Seval Y, Korgun ET, Demir R. Hofbauer Cells in Early Human Placenta: Possible Implications in Vasculogenesis and Angiogenesis. *Placenta* 2007; **28**: 841–5.

95. Anteby EY, Natanson-Yaron S, Greenfield C, Goldman-Wohl D, Haimov-Kochman R, Holzer H, Yagel S. Human placental Hofbauer cells express sprouty proteins: A possible modulating mechanism of villous branching. *Placenta* 2005; **26**: 476–83.

96. Quicke KM, Bowen JR, Johnson EL, McDonald CE, Ma H, O'Neal JT, Rajakumar A, Wrammert J, Rimawi BH, Pulendran B, Schinazi RF, Chakraborty R, Suthar MS. Zika Virus Infects Human Placental Macrophages. *Cell Host Microbe* 2016; **20**: 83–90.

97. Rosenberg AZ, Yu W, Hill DA, Reyes CA, Schwartz DA. Placental Pathology of

Zika Virus: Viral Infection of the Placenta Induces Villous Stromal Macrophage (Hofbauer Cell) Proliferation and Hyperplasia. *Arch Pathol Lab Med* 2017; **141**: 43–8.

98. Rabelo K, Souza LJ, Salomão NG, Oliveira ERA, Sentinelli L de P, Lacerda MS, Saraquino PB, Rosman FC, Basílio-de-Oliveira R, Carvalho JJ, Paes M V. Placental inflammation and fetal injury in a rare Zika case associated with Guillain-Barré Syndrome and abortion. *Front Microbiol* 2018; **9**: 1018.

99. Yockey LJ, Jurado KA, Arora N, Millet A, Rakib T, Milano KM, Hastings AK, Fikrig E, Kong Y, Horvath TL, Weatherbee S, Kliman HJ, Coyne CB, Iwasaki A. Type I interferons instigate fetal demise after Zika virus infection. *Sci Immunol* 2018; **3**: eaao1680.

100. Jagger BW, Miner JJ, Cao B, Arora N, Smith AM, Kovacs A, Mysorekar IU, Coyne CB, Diamond MS. Gestational Stage and IFN-λ Signaling Regulate ZIKV Infection In Utero. *Cell Host Microbe* 2017; **22**: 366-376.e3.

101. Vouga M, Baud D. Imaging of congenital Zika virus infection: the route to identification of prognostic factors. *Prenat Diagn* 2016; **36**: 799–811.

102. Hirsch AJ, Roberts VHJ, Grigsby PL, Haese N, Schabel MC, Wang X, Lo JO, Liu Z, Kroenke CD, Smith JL, Kelleher M, Broeckel R, Kreklywich CN, Parkins CJ, Denton M, Smith P, DeFilippis V, Messer W, Nelson JA, Hennebold JD, Grafe M, Colgin L, Lewis A, Ducore R, Swanson T, Legasse AW, Axthelm MK, MacAllister R, Moses A V., Morgan TK, Frias AE, Streblow DN. Zika virus infection in pregnant rhesus macaques causes placental dysfunction and immunopathology. *Nat Commun* 2018; **9**: 263.

103. Ismail MR, Ordi J, Menendez C, Ventura PJ, Aponte JJ, Kahigwa E, Hirt R, Cardesa A, Alonso PL. Placental pathology in malaria: A histological, immunohistochemical, and quantitative study. *Hum Pathol* 2000; **31**: 85–93.

104. Ahmed R, Singh N, Ter Kuile FO, Bharti PK, Singh PP, Desai M, Udhayakumar V, Terlouw DJ. Placental infections with histologically confirmed Plasmodium falciparum are associated with adverse birth outcomes in India: A cross-sectional study. *Malar J* 2014; **13**: 232.

105. Obiri D, Erskine IJ, Oduro D, Kusi KA, Amponsah J, Gyan BA, Adu-Bonsaffoh K, Ofori MF. Histopathological lesions and exposure to Plasmodium falciparum infections in the placenta increases the risk of preeclampsia among pregnant women. *Sci Rep* 2020; **10**: 1–10.

106. Agudelo OM, Aristizabal BH, Yanow SK, Arango E, Carmona-Fonseca J, Maestre A. Submicroscopic infection of placenta by Plasmodium produces Th1/Th2 cytokine imbalance, inflammation and hypoxia in women from north-west Colombia. *Malar J* 2014; **13**. DOI:10.1186/1475-2875-13-122.

107. Dechavanne C, Cottrell G, Garcia A, Migot-Nabias F. Placental Malaria: Decreased Transfer of Maternal Antibodies Directed to Plasmodium falciparum and Impact on the Incidence of Febrile Infections in Infants. *PLoS One* 2015; **10**: e0145464.

108. Okoko BJ, Wesumperuma LH, Ota MOC, Pinder M, Banya W, Gomez SF, McAdam KPJ, Hart AC. The Influence of Placental Malaria Infection and Maternal Hypergammaglobulinemia on Transplacental Transfer of Antibodies and IgG Subclasses in a Rural West African Population. *J Infect Dis* 2001; **184**: 627–32.

109. Chaikitgosiyakul S, Rijken MJ, Muehlenbachs A, Lee SJ, Chaisri U, Viriyavejakul P, Turner GD, Pongponratn E, Nosten F, McGready R. A morphometric and histological study of placental malaria shows significant changes to villous architecture in both Plasmodium falciparum and Plasmodium vivax infection. *Malar J* 2014; **13**: 4.

110. de Moraes-Pinto MI, Verhoeff F, Chimsuku L, Milligan PJ, Wesumperuma L, Broadhead RL, Brabin BJ, Johnson PM, Hart CA. Placental antibody transfer: influence of maternal HIV infection and placental malaria. *Arch Dis Child Fetal Neonatal Ed* 1998; **79**: F202-5.

111. Moro L, Bardají A, Nhampossa T, Mandomando I, Serra-Casas E, Sigaúque B, Cisteró P, Chauhan VS, Chitnis CE, Ordi J, Dobaño C, Alonso PL, Menéndez C, Mayor A. Malaria and HIV Infection in Mozambican Pregnant Women Are Associated With Reduced Transfer of Antimalarial Antibodies to Their Newborns. *J Infect Dis* 2015; **211**: 1004–14.

112. Castanha PMS, Braga C, Cordeiro MT, Souza AI, Silva CD, Martelli CMT, van Panhuis WG, Nascimento EJM, Marques ETA. Placental Transfer of Dengue Virus (DENV)–Specific Antibodies and Kinetics of DENV Infection–Enhancing Activity in Brazilian Infants. *J Infect Dis* 2016; **214**: 265–72.

113. Perret C, Chanthavanich P, Pengsaa K, Limkittikul K, Hutajaroen P, Bunn JEG, Brabin BJ. Dengue infection during pregnancy and transplacental antibody transfer in Thai mothers. *J Infect* 2005; **51**: 287–93.

114. D'Ortenzio E, Matheron S, de Lamballerie X, Hubert B, Piorkowski G, Maquart M, Descamps D, Damond F, Yazdanpanah Y, Leparc-Goffart I. Evidence of Sexual Transmission of Zika Virus. *N Engl J Med* 2016; **374**: 2195–8.

115. Deckard DT, Chung WM, Brooks JT, Smith JC, Woldai S, Hennessey M, Kwit N, Mead P. Male-to-Male Sexual Transmission of Zika Virus — Texas, January 2016. *MMWR Morb Mortal Wkly Rep* 2016; **65**: 372–4.

116. Davidson A, Slavinski S, Komoto K, Rakeman J, Weiss D. Suspected Female-to-Male Sexual Transmission of Zika Virus — New York City, 2016. *MMWR Morb Mortal Wkly Rep* 2016; **65**: 716–7.

117. Duggal NK, Ritter JM, Pestorius SE, Zaki SR, Davis BS, Chang G-JJ, Bowen RA, Brault AC. Frequent Zika Virus Sexual Transmission and Prolonged Viral RNA Shedding in an Immunodeficient Mouse Model. *Cell Rep* 2017; **18**: 1751–60.

118. Tsetsarkin KA, Acklin JA, Liu G, Kenney H, Teterina NL, Pletnev AG, Lim JK. Zika virus tropism during early infection of the testicular interstitium and its role in viral pathogenesis in the testes. *PLOS Pathog* 2020; **16**: e1008601.

119. McDonald EM, Duggal NK, Brault AC. Pathogenesis and sexual transmission of Spondweni and Zika viruses. *PLoS Negl Trop Dis* 2017; **11**. DOI:10.1371/journal.pntd.0005990.

120. Govero J, Esakky P, Scheaffer SM, Fernandez E, Drury A, Platt DJ, Gorman MJ, Richner JM, Caine EA, Salazar V, Moley KH, Diamond MS. Zika virus infection damages the testes in mice. *Nature* 2016; **540**: 438–42.

121. Matusali G, Houzet L, Satie AP, Mahé D, Aubry F, Couderc T, Frouard J, Bourgeau S, Bensalah K, Lavoué S, Joguet G, Bujan L, Cabié A, Avelar G, Lecuit M, Le Tortorec A, Dejucq-Rainsford N. Zika virus infects human testicular tissue and germ cells. *J Clin Invest* 2018; **128**: 4697–710.

122. Osuna CE, Lim SY, Deleage C, Griffin BD, Stein D, Schroeder LT, Omange R, Best K, Luo M, Hraber PT, Andersen-Elyard H, Ojeda EFC, Huang S, Vanlandingham DL, Higgs S, Perelson AS, Estes JD, Safronetz D, Lewis MG, Whitney JB. Zika viral dynamics and shedding in rhesus and cynomolgus macaques. *Nat Med* 2016; **22**: 1448–55.

123. Koide F, Goebel S, Snyder B, Walters KB, Gast A, Hagelin K, Kalkeri R, Rayner J. Development of a zika virus infection model in cynomolgus macaques. *Front Microbiol* 2016; **7**. DOI:10.3389/fmicb.2016.02028.

124. Vanegas H, González F, Reyes Y, Centeno E, Palacios J, Zepeda O, Hagbom M, Collins MH, Coward RM, Becker-Dreps S, Bowman N, Bucardo F. Zika RNA and Flavivirus-Like Antigens in the Sperm Cells of Symptomatic and Asymptomatic Subjects. *Viruses* 2021; **13**: 152.

125. Huits R, De Smet B, Ariën KK, Van Esbroeck M, Bottieau E, Cnops L. Zika virus in semen: A prospective cohort study of symptomatic travellers returning to Belgium. *Bull World Health Organ* 2017; **95**: 802–9.

126. Mead PS, Duggal NK, Hook SA, Delorey M, Fischer M, Olzenak McGuire D, Becksted H, Max RJ, Anishchenko M, Schwartz AM, Tzeng W-P, Nelson CA, McDonald EM, Brooks JT, Brault AC, Hinckley AF. Zika Virus Shedding in Semen of Symptomatic Infected Men. *N Engl J Med* 2018; **378**: 1377–85.

127. Spencer JL, Lahon A, Tran LL, Arya RP, Kneubehl AR, Vogt MB, Xavier D, Rowley DR, Kimata JT, Rico-Hesse RR. Replication of Zika virus in human prostate cells: A potential source of sexually transmitted virus. *J Infect Dis* 2018;

217: 538–47.

128. Tang WW, Young MP, Mamidi A, Regla-Nava JA, Kim K, Shresta S. A Mouse Model of Zika Virus Sexual Transmission and Vaginal Viral Replication. *Cell Rep* 2016; **17**: 3091–8.

129. Caine EA, Scheaffer SM, Arora N, Zaitsev K, Artyomov MN, Coyne CB, Moley KH, Diamond MS. Interferon lambda protects the female reproductive tract against Zika virus infection. *Nat Commun* 2019; **10**. DOI:10.1038/s41467-018-07993-2.

130. Brooks RB, Carlos MP, Myers RA, White MG, Bobo-Lenoci T, Aplan D, Blythe D, Feldman KA. Likely Sexual Transmission of Zika Virus from a Man with No Symptoms of Infection — Maryland, 2016. *MMWR Morb Mortal Wkly Rep* 2016; **65**: 915–6.

131. Yarrington CD, Hamer DH, Kuohung W, Lee-Parritz A. Congenital Zika syndrome arising from sexual transmission of Zika virus, a case report. *Fertil Res Pract* 2019; **5**. DOI:10.1186/s40738-018-0053-5.

132. Carroll T, Lo M, Lanteri M, Dutra J, Zarbock K, Silveira P, Rourke T, Ma ZM, Fritts L, O'Connor S, Busch M, Miller CJ. Zika virus preferentially replicates in the female reproductive tract after vaginal inoculation of rhesus macaques. *PLoS Pathog* 2017; **13**. DOI:10.1371/journal.ppat.1006537.

133. Gurung S, Nadeau H, Maxted M, Peregrine J, Reuter D, Norris A, Edwards R, Hyatt K, Singleton K, Papin JF, Myers DA. Maternal Zika Virus (ZIKV) Infection following Vaginal Inoculation with ZIKV-Infected Semen in Timed-Pregnant Olive Baboons. *J Virol* 2020; **94**. DOI:10.1128/jvi.00058-20.

134. Lazear HM, Govero J, Smith AM, Platt DJ, Fernandez E, Miner JJ, Diamond MS. A Mouse Model of Zika Virus Pathogenesis. *Cell Host Microbe* 2016; **19**: 720–30.

135. Yockey LJ, Varela L, Rakib T, Khoury-Hanold W, Fink SL, Stutz B, Szigeti-Buck K, Van den Pol A, Lindenbach BD, Horvath TL, Iwasaki A. Vaginal Exposure to Zika Virus during Pregnancy Leads to Fetal Brain Infection. *Cell* 2016; **166**: 1247-1256.e4.

136. Miner JJ, Cao B, Govero J, Smith AM, Fernandez E, Cabrera OH, Garber C, Noll M, Klein RS, Noguchi KK, Mysorekar IU, Diamond MS. Zika Virus Infection during Pregnancy in Mice Causes Placental Damage and Fetal Demise. *Cell* 2016; **165**: 1081–91.

137. Trus I, Udenze D, Cox B, Berube N, Nordquist RE, Van Der Staay FJ, Huang Y, Kobinger G, Safronetz D, Gerdts V, Karniychuk U. Subclinical in utero Zika virus infection is associated with interferon alpha sequelae and sex-specific molecular brain pathology in asymptomatic porcine offspring. *PLoS Pathog* 2019; **15**. DOI:10.1371/journal.ppat.1008038.

138. Casazza RL, Lazear HM. Maternal interferon lambda signaling limits transplacental transmission and mediates fetal pathology during congenital Zika virus infection in mice. *J Immunol* 2020; **204**.

139. Jaeger AS, Weiler AM, Moriarty R V., Rybarczyk S, O'Connor SL, O'Connor DH, Seelig DM, Fritsch MK, Friedrich TC, Aliota MT. Spondweni virus causes fetal harm in Ifnar1−/− mice and is transmitted by Aedes aegypti mosquitoes. *Virology* 2020; **547**: 35–46.

140. McDonald EM, Duggal NK, Brault AC. Pathogenesis and sexual transmission of Spondweni and Zika viruses. *PLoS Negl Trop Dis* 2017; **11**: e0005990.

141. Grant A, Ponia SS, Tripathi S, Balasubramaniam V, Miorin L, Sourisseau M, Schwarz MC, Sánchez-Seco MP, Evans MJ, Best SM, García-Sastre A. Zika Virus Targets Human STAT2 to Inhibit Type i Interferon Signaling. *Cell Host Microbe* 2016; **19**: 882–90.

142. Carson DD, DeSouza MM, Kardon R, Zhou X, Lagow E, Julian J. Mucin expression and function in the female reproductive tract. *Hum Reprod Update*; **4**: 459–64.

143. Hickey DK, Patel M V, Fahey J V, Wira CR. Innate and adaptive immunity at mucosal surfaces of the female reproductive tract: stratification and integration of immune protection against the transmission of sexually transmitted infections. *J Reprod Immunol* 2011; **88**: 185–94.

144. Bouvet JP, Bélec L, Pirès R, Pillot J. Immunoglobulin G antibodies in human vaginal secretions after parenteral vaccination. *Infect Immun* 1994; **62**: 3957–61.

145. Li Z, Palaniyandi S, Zeng R, Tuo W, Roopenian DC, Zhu X. Transfer of IgG in the female genital tract by MHC class I-related neonatal Fc receptor (FcRn) confers protective immunity to vaginal infection. *Proc Natl Acad Sci* 2011; **108**: 4388–93.

146. Jalanti R, Isliker H. Immunoglobulins in human cervico-vaginal secretions. *Int Arch Allergy Appl Immunol* 1977; **53**: 402–8.

147. Usala SJ, Usala FO, Haciski R, Holt JA, Schumacher GF. IgG and IgA content of vaginal fluid during the menstrual cycle. *J Reprod Med* 1989; **34**: 292–4.

148. Wang Y-Y, Schroeder HA, Nunn KL, Woods K, Anderson DJ, Lai SK, Cone RA. Diffusion of Immunoglobulin G in Shed Vaginal Epithelial Cells and in Cell-Free Regions of Human Cervicovaginal Mucus. *PLoS One* 2016; **11**: e0158338.

149. Fahrbach KM, Malykhina O, Stieh DJ, Hope TJ. Differential binding of IgG and IgA to mucus of the female reproductive tract. *PLoS One* 2013; **8**: e76176.

150. Saltzman WM, Radomsky ML, Whaley KJ, Cone RA. Antibody diffusion in human cervical mucus. *Biophys J* 1994; **66**: 508–15.

151. Olmsted SS, Padgett JL, Yudin AI, Whaley KJ, Moench TR, Cone RA. Diffusion of macromolecules and virus-like particles in human cervical mucus. *Biophys J* 2001; **81**: 1930–7.

152. Chen A, McKinley SA, Wang S, Shi F, Mucha PJ, Forest MG, Lai SK. Transient antibody-mucin interactions produce a dynamic molecular shield against viral invasion. *Biophys J* 2014; **106**: 2028–36.

153. Wang Y-Y, Kannan A, Nunn KL, Murphy MA, Subramani DB, Moench T, Cone R, Lai SK. IgG in cervicovaginal mucus traps HSV and prevents vaginal herpes infections. *Mucosal Immunol* 2014; **7**: 1036–44.

154. Iwasaki A. Mucosal dendritic cells. Annu. Rev. Immunol. 2007; **25**: 381–418.

155. Ashkar AA, Rosenthal KL. Interleukin-15 and Natural Killer and NKT Cells Play a Critical Role in Innate Protection against Genital Herpes Simplex Virus Type 2 Infection. *J Virol* 2003; **77**: 10168–71.

156. Thapa M, Kuziel WA, Carr DJJ. Susceptibility of CCR5-Deficient Mice to Genital Herpes Simplex Virus Type 2 Is Linked to NK Cell Mobilization. *J Virol* 2007; **81**: 3704–13.

157. Milligan GN. Neutrophils Aid in Protection of the Vaginal Mucosae of Immune Mice against Challenge with Herpes Simplex Virus Type 2. *J Virol* 1999; **73**: 6380–6.

158. Givan AL, White HD, Stern JE, Colby E, Guyre PM, Wira CR, Gosselin EJ. Flow Cytometric Analysis of Leukocytes in the Human Female Reproductive Tract: Comparison of Fallopian Tube, Uterus, Cervix, and Vagina. *Am J Reprod Immunol* 1997; **38**: 350–9.

159. Scott JM, Lebratti TJ, Richner JM, Jiang X, Fernandez E, Zhao H, Fremont DH, Diamond MS, Shin H. Cellular and Humoral Immunity Protect against Vaginal Zika Virus Infection in Mice. *J Virol* 2018; **92**. DOI:10.1128/jvi.00038-18.

160. Lazear HM, Nice TJ, Diamond MS. Interferon-λ: Immune Functions at Barrier Surfaces and Beyond. Immunity. 2015; **43**: 15–28.

161. Lazear HM, Schoggins JW, Diamond MS. Shared and Distinct Functions of Type I and Type III Interferons. Immunity. 2019; **50**: 907–23.

162. Ank N, West H, Bartholdy C, Eriksson K, Thomsen AR, Paludan SR. Lambda Interferon (IFN-λ), a Type III IFN, Is Induced by Viruses and IFNs and Displays Potent Antiviral Activity against Select Virus Infections In Vivo. *J Virol* 2006; **80**: 4501–9.

163. Hong K, Choi Y. Role of estrogen and RAS signaling in repeated implantation failure. BMB Rep. 2018; **51**: 225–9.

164. Ajayi AF, Akhigbe RE. Staging of the estrous cycle and induction of estrus in experimental rodents: an update. *Fertil Res Pract* 2020; **6**: 5.

165. Wood GA, Fata JE, Watson KLM, Khokha R. Circulating hormones and estrous stage predict cellular and stromal remodeling in murine uterus. *Reproduction* 2007; **133**: 1035–44.

166. Kutteh WH, Prince SJ, Hammond KR, Kutteh CC, Mestecky J. Variations in immunoglobulins and IgA subclasses of human uterine cervical secretions around the time of ovulation. *Clin Exp Immunol* 1996; **104**: 538–42.

167. Gallichan WS, Rosenthal KL. Effects of the estrous cycle on local humoral immune responses and protection of intranasally immunized female mice against herpes simplex virus type 2 infection in the genital tract. *Virology* 1996; **224**: 487–97.

168. Lü FX, Ma Z, Rourke T, Srinivasan S, Mcchesney M, Miller CJ. Immunoglobulin concentrations and antigen-specific antibody levels in cervicovaginal lavages of rhesus macaques are influenced by the stage of the menstrual cycle. *Infect Immun* 1999; **67**: 6321–8.

169. Yang S, Schumacher GFB. Immune response after vaginal application of antigens in the rhesus monkey. *Fertil Steril* 1979; **32**: 588–98.

170. Kaushic C, Ashkar AA, Reid LA, Rosenthal KL. Progesterone Increases Susceptibility and Decreases Immune Responses to Genital Herpes Infection. *J Virol* 2003; **77**: 4558–65.

171. Patton DL, Thwin SS, Meier A, Hooton TM, Stapleton AE, Eschenbach DA. Epithelial cell layer thickness and immune cell populations in the normal human vagina at different stages of the menstrual cycle. In: American Journal of Obstetrics and Gynecology. Mosby Inc., 2000: 967–73.

172. Quispe Calla NE, Vicetti Miguel RD, Boyaka PN, Hall-Stoodley L, Kaur B, Trout W, Pavelko SD, Cherpes TL. Medroxyprogesterone acetate and levonorgestrel increase genital mucosal permeability and enhance susceptibility to genital herpes simplex virus type 2 infection. *Mucosal Immunol* 2016; **9**: 1571–83.

173. Sjöberg I, Cajander S, Rylander E. Morphometrie characteristics of the vaginal epithelium during the menstrual cycle. *Gynecol Obstet Invest* 1988; **26**: 136–44.

174. Ferreira VH, Dizzell S, Nazli A, Kafka JK, Mueller K, Nguyen P V., Tremblay MJ, Cochrane A, Kaushic C. Medroxyprogesterone acetate regulates HIV-1 uptake and transcytosis but not replication in primary genital epithelial cells, resulting in enhanced T-cell infection. *J Infect Dis* 2015; **211**: 1745–56.

175. Cabrera-Muñoz E, Fuentes-Romero LL, Zamora-Chávez J, Camacho-Arroyo I, Soto-Ramírez LE. Effects of progesterone on the content of CCR5 and CXCR4

coreceptors in PBMCs of seropositive and exposed but uninfected Mexican women to HIV-1. *J Steroid Biochem Mol Biol* 2012; **132**: 66–72.

176. Sciaranghella G, Wang C, Hu H, Anastos K, Merhi Z, Nowicki M, Stanczyk FZ, Greenblatt RM, Cohen M, Golub ET, Watts DH, Alter G, Young MA, Tsibris AMN. CCR5 Expression Levels in HIV-Uninfected Women Receiving Hormonal Contraception. *J Infect Dis* 2015; **212**: 1397–401.

177. Gillgrass AE, Fernandez SA, Rosenthal KL, Kaushic C. Estradiol Regulates Susceptibility following Primary Exposure to Genital Herpes Simplex Virus Type 2, while Progesterone Induces Inflammation. *J Virol* 2005; **79**: 3107–16.

178. Kaushic C, Zhou F, Murdin AD, Wira CR. Effects of estradiol and progesterone on susceptibility and early immune responses to Chlamydia trachomatis infection in the female reproductive tract. *Infect Immun* 2000; **68**: 4207–16.

179. Kyurkchiev D, Ivanova-todorova E, Hayrabedyan S, Altankova I, Kyurkchiev S. Female sex steroid hormones modify some regulatory properties of monocyte-derived dendritic cells. *Am J Reprod Immunol* 2007; **58**: 425–33.

180. Miyaura H, Iwata M. Direct and Indirect Inhibition of Th1 Development by Progesterone and Glucocorticoids. *J Immunol* 2002; **168**: 1087–94.

181. Piccinni MP, Giudizi MG, Biagiotti R, Beloni L, Giannarini L, Sampognaro S, Parronchi P, Manetti R, Annunziato F, Livi C. Progesterone favors the development of human T helper cells producing Th2-type cytokines and promotes both IL-4 production and membrane CD30 expression in established Th1 cell clones. *J Immunol* 1995; **155**.

182. Khan S, Woodruff EM, Trapecar M, Fontaine KA, Ezaki A, Borbet TC, Ott M, Sanjabi S. Dampened antiviral immunity to intravaginal exposure to RNA viral pathogens allows enhanced viral replication. *J Exp Med* 2016; **213**: 2913–29.

183. Khan S, Lew I, Wu F, Fritts L, Fontaine KA, Tomar S, Trapecar M, Shehata HM, Ott M, Miller CJ, Sanjabi S. Low expression of RNA sensors impacts Zika virus infection in the lower female reproductive tract. *Nat Commun* 2019; **10**. DOI:10.1038/s41467-019-12371-7.

184. Wu F, Zhao S, Yu B, Chen YM, Wang W, Song ZG, Hu Y, Tao ZW, Tian JH, Pei YY, Yuan ML, Zhang YL, Dai FH, Liu Y, Wang QM, Zheng JJ, Xu L, Holmes EC, Zhang YZ. A new coronavirus associated with human respiratory disease in China. *Nature* 2020; **579**: 265–9.

185. Zhou P, Yang X Lou, Wang XG, Hu B, Zhang L, Zhang W, Si HR, Zhu Y, Li B, Huang CL, Chen HD, Chen J, Luo Y, Guo H, Jiang R Di, Liu MQ, Chen Y, Shen XR, Wang X, Zheng XS, Zhao K, Chen QJ, Deng F, Liu LL, Yan B, Zhan FX, Wang YY, Xiao GF, Shi ZL. A pneumonia outbreak associated with a new coronavirus of probable bat origin. *Nature* 2020; **579**: 270–3.

186. WHO Timeline - COVID-19. https://www.who.int/news-room/detail/27-04-2020-who-timeline---covid-19 (accessed May 22, 2020).

187. Reusken CBEM, Haagmans BL, Müller MA, Gutierrez C, Godeke GJ, Meyer B, Muth D, Raj VS, Vries LS De, Corman VM, Drexler JF, Smits SL, El Tahir YE, De Sousa R, van Beek J, Nowotny N, van Maanen K, Hidalgo-Hermoso E, Bosch BJ, Rottier P, Osterhaus A, Gortázar-Schmidt C, Drosten C, Koopmans MPG. Middle East respiratory syndrome coronavirus neutralising serum antibodies in dromedary camels: A comparative serological study. *Lancet Infect Dis* 2013; **13**: 859–66.

188. Guan Y, Zheng BJ, He YQ, Liu XL, Zhuang ZX, Cheung CL, Luo SW, Li PH, Zhang LJ, Guan YJ, Butt KM, Wong KL, Chan KW, Lim W, Shortridge KF, Yuen KY, Peiris JSM, Poon LLM. Isolation and characterization of viruses related to the SARS coronavirus from animals in Southern China. *Science (80-)* 2003; **302**: 276–8.

189. Zhou H, Chen X, Hu T, Li J, Song H, Liu Y, Wang P, Liu D, Yang J, Holmes EC, Hughes AC, Bi Y, Shi W. A Novel Bat Coronavirus Closely Related to SARS-CoV-2 Contains Natural Insertions at the S1/S2 Cleavage Site of the Spike Protein. *Curr Biol* 2020; **30**: 2196-2203.e3.

190. Banerjee A, Doxey AC, Mossman K, Irving AT. Unraveling the Zoonotic Origin and Transmission of SARS-CoV-2. Trends Ecol. Evol. 2021; **36**: 180–4.

191. COVID-19 Map - Johns Hopkins Coronavirus Resource Center. https://coronavirus.jhu.edu/map.html (accessed March 31, 2021).

192. Bedford T, Greninger AL, Roychoudhury P, Starita LM, Famulare M, Huang ML, Nalla A, Pepper G, Reinhardt A, Xie H, Shrestha L, Nguyen TN, Adler A, Brandstetter E, Cho S, Giroux D, Han PD, Fay K, Frazar CD, Ilcisin M, Lacombe K, Lee J, Kiavand A, Richardson M, Sibley TR, Truong M, Wolf CR, Nickerson DA, Rieder MJ, Englund JA, Hadfield J, Hodcroft EB, Huddleston J, Moncla LH, Müller NF, Neher RA, Deng X, Gu W, Federman S, Chiu C, Duchin JS, Gautom R, Melly G, Hiatt B, Dykema P, Lindquist S, Queen K, Tao Y, Uehara A, Tong S, MacCannell D, Armstrong GL, Baird GS, Chu HY, Shendure J, Jerome KR. Cryptic transmission of SARS-CoV-2 in Washington state. *Science (80-)* 2020; **370**: 571–5.

193. Chu HY, Englund JA, Starita LM, Famulare M, Brandstetter E, Nickerson DA, Rieder MJ, Adler A, Lacombe K, Kim AE, Graham C, Logue J, Wolf CR, Heimonen J, McCulloch DJ, Han PD, Sibley TR, Lee J, Ilcisin M, Fay K, Burstein R, Martin B, Lockwood CM, Thompson M, Lutz B, Jackson M, Hughes JP, Boeckh M, Shendure J, Bedford T, Seattle Flu Study Investigators. Early Detection of Covid-19 through a Citywide Pandemic Surveillance Platform. *N Engl J Med* 2020; : NEJMc2008646.

194. Deng X, Gu W, Federman S, du Plessis L, Pybus OG, Faria NR, Wang C, Yu G,

Bushnell B, Pan CY, Guevara H, Sotomayor-Gonzalez A, Zorn K, Gopez A, Servellita V, Hsu E, Miller S, Bedford T, Greninger AL, Roychoudhury P, Starita LM, Famulare M, Chu HY, Shendure J, Jerome KR, Anderson C, Gangavarapu K, Zeller M, Spencer E, Andersen KG, MacCannell D, Paden CR, Li Y, Zhang J, Tong S, Armstrong G, Morrow S, Willis M, Matyas BT, Mase S, Kasirye O, Park M, Masinde G, Chan C, Yu AT, Chai SJ, Villarino E, Bonin B, Wadford DA, Chiu CY. Genomic surveillance reveals multiple introductions of SARS-CoV-2 into Northern California. *Science (80-)* 2020; **369**: 582–7.

195. Wiersinga WJ, Rhodes A, Cheng AC, Peacock SJ, Prescott HC. Pathophysiology, Transmission, Diagnosis, and Treatment of Coronavirus Disease 2019 (COVID-19): A Review. JAMA - J. Am. Med. Assoc. 2020; **324**: 782–93.

196. Ng WH, Tipih T, Makoah NA, Vermeulen JG, Goedhals D, Sempa JB, Burt FJ, Taylor A, Mahalingam S. Comorbidities in SARS-CoV-2 patients: A systematic review and meta-analysis. *MBio* 2021; **12**: 1–12.

197. Levin AT, Hanage WP, Owusu-Boaitey N, Cochran KB, Walsh SP, Meyerowitz-Katz G. Assessing the age specificity of infection fatality rates for COVID-19: systematic review, meta-analysis, and public policy implications. Eur. J. Epidemiol. 2020; **35**: 1123–38.

198. Khazanchi R, Evans CT, Marcelin JR. Racism, Not Race, Drives Inequity Across the COVID-19 Continuum. JAMA Netw. open. 2020; **3**: e2019933.

199. Centers for Disease Control. Risk for COVID-19 Infection, Hospitalization, and Death By Race/Ethnicity. 2021; published online Feb 18. https://www.cdc.gov/coronavirus/2019-ncov/covid-data/investigations-discovery/hospitalization-death-by-race-ethnicity.html (accessed Feb 23, 2021).

200. Oudshoorn D, Rijs K, Limpens RWAL, Groen K, Koster AJ, Snijder EJ, Kikkert M, Bárcena M. Expression and cleavage of middle east respiratory syndrome coronavirus nsp3-4 polyprotein induce the formation of double-membrane vesicles that mimic those associated with coronaviral RNA replication. *MBio* 2017; **8**: 1658–75.

201. Stertz S, Reichelt M, Spiegel M, Kuri T, Martínez-Sobrido L, García-Sastre A, Weber F, Kochs G. The intracellular sites of early replication and budding of SARS-coronavirus. *Virology* 2007; **361**: 304–15.

202. Vennema H, Godeke GJ, Rossen JWA, Voorhout WF, Horzinek MC, Opstelten DJE, Rottier PJM. Nucleocapsid-independent assembly of coronavirus-like particles by co-expression of viral envelope protein genes. *EMBO J* 1996; **15**: 2020–8.

203. Ke Z, Oton J, Qu K, Cortese M, Zila V, McKeane L, Nakane T, Zivanov J, Neufeldt CJ, Cerikan B, Lu JM, Peukes J, Xiong X, Kräusslich HG, Scheres SHW, Bartenschlager R, Briggs JAG. Structures and distributions of SARS-CoV-2 spike

proteins on intact virions. *Nature* 2020; **588**: 498–502.

204. Delmas B, Laude H. Assembly of coronavirus spike protein into trimers and its role in epitope expression. *J Virol* 1990; **64**: 5367–75.

205. Beniac DR, Andonov A, Grudeski E, Booth TF. Architecture of the SARS coronavirus prefusion spike. *Nat Struct Mol Biol* 2006; **13**: 751–2.

206. Wrapp D, Wang N, Corbett KS, Goldsmith JA, Hsieh C-L, Abiona O, Graham BS, McLellan JS. Cryo-EM structure of the 2019-nCoV spike in the prefusion conformation. *Science (80-)* 2020; **367**: 1260–3.

207. Walls AC, Park YJ, Tortorici MA, Wall A, McGuire AT, Veesler D. Structure, Function, and Antigenicity of the SARS-CoV-2 Spike Glycoprotein. *Cell* 2020; **181**: 281-292.e6.

208. Tripp RA, Haynes LM, Moore D, Anderson B, Tamin A, Harcourt BH, Jones LP, Yilla M, Babcock GJ, Greenough T, Ambrosino DM, Alvarez R, Callaway J, Cavitt S, Kamrud K, Alterson H, Smith J, Harcourt JL, Miao C, Razdan R, Comer JA, Rollin PE, Ksiazek TG, Sanchez A, Rota PA, Bellini WJ, Anderson LJ. Monoclonal antibodies to SARS-associated coronavirus (SARS-CoV): Identification of neutralizing and antibodies reactive to S, N, M and e viral proteins. *J Virol Methods* 2005; **128**: 21–8.

209. McAndrews KM, Dowlatshahi DP, Dai J, Becker LM, Hensel J, Snowden LM, Leveille JM, Brunner MR, Holden KW, Hopkins NS, Harris AM, Kumpati J, Whitt MA, Jack Lee J, Ostrosky-Zeichner LL, Papanna R, LeBleu VS, Allison JP, Kalluri R. Heterogeneous antibodies against SARS-CoV-2 spike receptor binding domain and nucleocapsid with implications for COVID-19 immunity. *JCI Insight* 2020; **5**. DOI:10.1172/JCI.INSIGHT.142386.

210. Sui J, Li W, Murakami A, Tamin A, Matthews LJ, Wong SK, Moore MJ, Tallarico ASC, Olurinde M, Choe H, Anderson LJ, Bellini WJ, Farzan M, Marasco WA. Potent neutralization of severe acute respiratory syndrome (SARS) coronavirus by a human mAb to S1 protein that blocks receptor association. *Proc Natl Acad Sci U S A* 2004; **101**: 2536–41.

211. Rockx B, Corti D, Donaldson E, Sheahan T, Stadler K, Lanzavecchia A, Baric R. Structural Basis for Potent Cross-Neutralizing Human Monoclonal Antibody Protection against Lethal Human and Zoonotic Severe Acute Respiratory Syndrome Coronavirus Challenge. *J Virol* 2008; **82**: 3220–35.

212. Ying T, Du L, Ju TW, Prabakaran P, Lau CCY, Lu L, Liu Q, Wang L, Feng Y, Wang Y, Zheng B-J, Yuen K-Y, Jiang S, Dimitrov DS. Exceptionally Potent Neutralization of Middle East Respiratory Syndrome Coronavirus by Human Monoclonal Antibodies. *J Virol* 2014; **88**: 7796–805.

213. Wrapp D, De Vlieger D, Corbett KS, Torres GM, Wang N, Van Breedam W,

Roose K, van Schie L, Hoffmann M, Pöhlmann S, Graham BS, Callewaert N, Schepens B, Saelens X, McLellan JS. Structural Basis for Potent Neutralization of Betacoronaviruses by Single-Domain Camelid Antibodies. *Cell* 2020; **181**: 1004-1015.e15.

214. Cao W-C, Liu W, Zhang P-H, Zhang F, Richardus JH. Disappearance of Antibodies to SARS-Associated Coronavirus after Recovery. *N Engl J Med* 2007; **357**: 1162–3.

215. Wu LP, Wang NC, Chang YH, Tian XY, Na DY, Zhang LY, Zheng L, Lan T, Wang LF, Liang GD. Duration of antibody responses after severe acute respiratory syndrome. *Emerg Infect Dis* 2007; **13**: 1562–4.

216. Dan JM, Mateus J, Kato Y, Hastie KM, Yu ED, Faliti CE, Grifoni A, Ramirez SI, Haupt S, Frazier A, Nakao C, Rayaprolu V, Rawlings SA, Peters B, Krammer F, Simon V, Saphire EO, Smith DM, Weiskopf D, Sette A, Crotty S. Immunological memory to SARS-CoV-2 assessed for up to 8 months after infection. *Science (80-)* 2021; **371**. DOI:10.1126/science.abf4063.

217. Long QX, Liu BZ, Deng HJ, Wu GC, Deng K, Chen YK, Liao P, Qiu JF, Lin Y, Cai XF, Wang DQ, Hu Y, Ren JH, Tang N, Xu YY, Yu LH, Mo Z, Gong F, Zhang XL, Tian WG, Hu L, Zhang XX, Xiang JL, Du HX, Liu HW, Lang CH, Luo XH, Wu SB, Cui XP, Zhou Z, Zhu MM, Wang J, Xue CJ, Li XF, Wang L, Li ZJ, Wang K, Niu CC, Yang QJ, Tang XJ, Zhang Y, Liu XM, Li JJ, Zhang DC, Zhang F, Liu P, Yuan J, Li Q, Hu JL, Chen J, Huang AL. Antibody responses to SARS-CoV-2 in patients with COVID-19. *Nat Med* 2020; **26**: 845–8.

218. Population-based age-stratified seroepidemiological investigation protocol for coronavirus 2019 (COVID-19) infection. .

219. Pollán M, Pérez-Gómez B, Pastor-Barriuso R, Oteo J, Hernán MA, Pérez-Olmeda M, Sanmartín JL, Fernández-García A, Cruz I, Fernández de Larrea N, Molina M, Rodríguez-Cabrera F, Martín M, Merino-Amador P, León Paniagua J, Muñoz-Montalvo JF, Blanco F, Yotti R, Gutiérrez Fernández R, Mezcua Navarro S, Muñoz-Montalvo JF, Salinero Hernández M, Sanmartín JL, Cuenca-Estrella M, León Paniagua J, Fernández-Navarro P, Avellón A, Fedele G, Oteo Iglesias J, Pérez Olmeda MT, Fernandez Martinez ME, Rodríguez-Cabrera FD, Hernán MA, Padrones Fernández S, Rumbao Aguirre JM, Navarro Marí JM, Palop Borrás B, Pérez Jiménez AB, Rodríguez-Iglesias M, Calvo Gascón AM, Lou Alcaine ML, Donate Suárez I, Suárez Álvarez O, Rodríguez Pérez M, Cases Sanchís M, Villafáfila Gomila CJ, Carbo Saladrigas L, Hurtado Fernández A, Oliver A, Castro Feliciano E, González Quintana MN, Barrasa Fernández JM, Hernández Betancor MA, Hernández Febles M, Martín Martín L, López López LM, Ugarte Miota T, De Benito Población I, Celada Pérez MS, Vallés Fernández MN, Maté Enríquez T, Villa Arranz M, Domínguez-Gil González M, Fernández-Natal I, Megías Lobón G, Muñoz Bellido JL, Ciruela P, Mas i Casals A, Doladé Botías M, Marcos Maeso MA, Pérez del Campo D, Félix de Castro A, Limón Ramírez R,

Elías Retamosa MF, Rubio González M, Blanco Lobeiras MS, Fuentes Losada A, Aguilera A, Bou G, Caro Y, Marauri N, Soria Blanco LM, del Cura González I, Hernández Pascual M, Alonso Fernández R, Cabrera Castro N, Tomás Lizcano A, Ramírez Almagro C, Segovia Hernández M, Ascunce Elizaga N, Ederra Sanz M, Ezpeleta Baquedano C, Bustinduy Bascaran A, Iglesias Tamayo S, Elorduy Otazua L, Benarroch Benarroch R, Lopera Flores J, Vázquez de la Villa A. Prevalence of SARS-CoV-2 in Spain (ENE-COVID): a nationwide, population-based seroepidemiological study. *Lancet* 2020; **396**: 535–44.

220. Rosadas C, Randell P, Khan M, McClure MO, Tedder RS. Testing for responses to the wrong SARS-CoV-2 antigen? Lancet. 2020; **396**: e23.

221. Wu X, Fu B, Chen L, Feng Y. Serological tests facilitate identification of asymptomatic SARS-CoV-2 infection in Wuhan, China. *J Med Virol* 2020; : jmv.25904.

222. Shakiba M, Nazari SSH, Mehrabian F, Rezvani SM, Ghasempour Z, Heidarzadeh A. Seroprevalence of COVID-19 virus infection in Guilan province, Iran. *medRxiv* 2020; : 2020.04.26.20079244.

223. Fontanet A, Tondeur L, Madec Y, Grant R, Besombes C, Jolly N, Pellerin SF, Ungeheuer M-N, Cailleau I, Kuhmel L, Temmam S, Huon C, Chen K-Y, Crescenzo B, Munier S, Demeret C, Grzelak L, Staropoli I, Bruel T, Gallian P, Cauchemez S, Werf S van der, Schwartz O, Eloit M, Hoen B. Cluster of COVID-19 in northern France: A retrospective closed cohort study. *medRxiv* 2020; : 2020.04.18.20071134.

224. Valenti L, Bergna A, Pelusi S, Facciotti F, Lai A, Tarkowski M, Berzuini A, Caprioli F, Santoro L, Baselli G, Ventura C Della, Erba E, Bosari S, Galli M, Zehender G, Prati D. SARS-CoV-2 seroprevalence trends in healthy blood donors during the COVID-19 Milan outbreak. *medRxiv* 2020; : 2020.05.11.20098442.

225. Stadlbauer D, Tan J, Jiang K, Hernandez MM, Fabre S, Amanat F, Teo C, Arunkumar GA, McMahon M, Capuano C, Twyman K, Jhang J, Nowak MD, Simon V, Sordillo EM, van Bakel H, Krammer F. Repeated cross-sectional sero-monitoring of SARS-CoV-2 in New York City. *Nature* 2021; **590**: 146–50.

226. Barzin A, Schmitz JL, Rosin S, Sirpal R, Almond M, Robinette C, Wells S, Hudgens M, Olshan A, Deen S, Krejci P, Quackenbush E, Chronowski K, Cornaby C, Goins J, Butler L, Aucoin J, Boyer K, Faulk J, Alston-Johnson D, Page C, Zhou Y, Fiscus L, Damania B, Dittmer DP, Peden DB. SARS-CoV-2 seroprevalence among a southern U.S. population indicates limited asymptomatic spread under physical distancing measures. *MBio* 2020; **11**: 1–8.

227. Bajema KL, Wiegand RE, Cuffe K, Patel S V., Iachan R, Lim T, Lee A, Moyse D, Havers FP, Harding L, Fry AM, Hall AJ, Martin K, Biel M, Deng Y, Meyer WA, Mathur M, Kyle T, Gundlapalli A V., Thornburg NJ, Petersen LR, Edens C.

Estimated SARS-CoV-2 Seroprevalence in the US as of September 2020. *JAMA Intern Med* 2020. DOI:10.1001/jamainternmed.2020.7976.

228. Shook-Sa BE, Boyce RM, Aiello AE. Estimation Without Representation: Early Severe Acute Respiratory Syndrome Coronavirus 2 Seroprevalence Studies and the Path Forward. *J Infect Dis* 2020; **222**: 1086–9.

229. Stringhini S, Wisniak A, Piumatti G, Azman AS, Lauer SA, Baysson H, Ridder D De, Petrovic D, Schrempft S, Marcus K, Arm-Vernez I, Yerly S, Keiser O, Hurst S, Posfay-Barbe K, Trono D, Pittet D, Getaz L, Chappuis F, Eckerle I, Vuilleumier N, Meyer B, Flahault A, Kaiser L, Guessous I. Repeated seroprevalence of anti-SARS-CoV-2 IgG antibodies in a population-based sample from Geneva, Switzerland. *medRxiv* 2020; : 2020.05.02.20088898.

230. Larremore DB, Fosdick BK, Bubar KM, Zhang S, Kissler SM, Metcalf CJE, Buckee C, Grad YH. Estimating SARS-CoV-2 seroprevalence and epidemiological parameters with uncertainty from serological surveys. *Elife* 2021; **10**. DOI:10.7554/eLife.64206.

231. Flor M, Weiß M, Selhorst T, Müller-Graf C, Greiner M. Comparison of Bayesian and frequentist methods for prevalence estimation under misclassification. *BMC Public Health* 2020; **20**: 1135.

232. Gelman A, Carpenter B. Bayesian analysis of tests with unknown specificity and sensitivity. *J R Stat Soc Ser C (Applied Stat* 2020; **69**: 1269–83.

233. Rogan WJ, Gladen B. Estimating prevalence from the results of a screening test. *Am J Epidemiol* 1978; **107**: 71–6.

234. Moore JT, Ricaldi JN, Rose CE, Fuld J, Parise M, Kang GJ, Driscoll AK, Norris T, Wilson N, Rainisch G, Valverde E, Beresovsky V, Agnew Brune C, Oussayef NL, Rose DA, Adams LE, Awel S, Villanueva J, Meaney-Delman D, Honein MA, Bautista G, Cowins J, Edge C, Grant G, Gray R, Griffing S, Hayes N, Hughes L, Lavinghouze R, Leonard S, Montierth R, Palipudi K, Rayle V, Ruiz A, Washington M, Davidson S, Dillaha J, Herlihy R, Blackmore C, Troelstrup T, Edison L, Thomas E, Pedati C, Ahmed F, Brown C, Lyon Callo S, Como-Sabetti K, Byers P, Sutton V, Moore Z, de Fijter S, Zhang A, Bell L, Dunn J, Pont S, McCaffrey K, Stephens E, Westergaard R. Disparities in Incidence of COVID-19 Among Underrepresented Racial/Ethnic Groups in Counties Identified as Hotspots During June 5–18, 2020 — 22 States, February–June 2020. *MMWR Morb Mortal Wkly Rep* 2020; **69**: 1122–6.

235. Kerwin D, Nicholson M, Alulema D, Warren R. US Foreign-Born Essential Workers by Status and State, and the Global Pandemic. 2020 DOI:10.14240/cmsrpt0520.

236. Bailey ZD, Robin Moon J. Racism and the political economy of COVID-19: Will we continue to resurrect the past? *J Health Polit Policy Law* 2020; **45**: 937–50.

237. Alberti PM, Lantz PM, Wilkins CH. Equitable Pandemic Preparedness and Rapid Response: Lessons from COVID-19 for Pandemic Health Equity. *J Health Polit Policy Law* 2020; **45**: 921–35.

238. Laster Pirtle WN. Racial Capitalism: A Fundamental Cause of Novel Coronavirus (COVID-19) Pandemic Inequities in the United States. *Heal Educ Behav* 2020; **47**: 504–8.

239. McClure ES, Vasudevan P, Bailey Z, Patel S, Robinson WR. Racial Capitalism Within Public Health—How Occupational Settings Drive COVID-19 Disparities. *Am J Epidemiol* 2020; **189**: 1244–53.

240. Dyal JW, Grant MP, Broadwater K, Bjork A, Waltenburg MA, Gibbins JD, Hale C, Silver M, Fischer M, Steinberg J, Basler CA, Jacobs JR, Kennedy ED, Tomasi S, Trout D, Hornsby-Myers J, Oussayef NL, Delaney LJ, Patel K, Shetty V, Kline KE, Schroeder B, Herlihy RK, House J, Jervis R, Clayton JL, Ortbahn D, Austin C, Berl E, Moore Z, Buss BF, Stover D, Westergaard R, Pray I, DeBolt M, Person A, Gabel J, Kittle TS, Hendren P, Rhea C, Holsinger C, Dunn J, Turabelidze G, Ahmed FS, deFijter S, Pedati CS, Rattay K, Smith EE, Luna-Pinto C, Cooley LA, Saydah S, Preacely ND, Maddox RA, Lundeen E, Goodwin B, Karpathy SE, Griffing S, Jenkins MM, Lowry G, Schwarz RD, Yoder J, Peacock G, Walke HT, Rose DA, Honein MA. COVID-19 Among Workers in Meat and Poultry Processing Facilities — 19 States, April 2020. *MMWR Morb Mortal Wkly Rep* 2020; **69**. DOI:10.15585/mmwr.mm6918e3.

241. Lazear HM, Diamond MS. Zika Virus: New Clinical Syndromes and Its Emergence in the Western Hemisphere. *J Virol* 2016; **90**: 4864–75.

242. Ades AE, Soriano-Arandes A, Alarcon A, Bonfante F, Thorne C, Peckham CS, Giaquinto C. Vertical transmission of Zika virus and its outcomes: a Bayesian synthesis of prospective studies. *Lancet Infect Dis* 2020; **21**: 537–45.

243. Centers for Disease Control and Prevention. Recommended Adult Immunization Schedule for ages 19 years or older. 2019.

244. Recomendações da Sociedade Brasileira de Imunizações. Calendário de vacinação SBIm gestante. 2019.

245. Mansfield KL, Horton DL, Johnson N, Li L, Barrett ADT, Smith DJ, Galbraith SE, Solomon T, Fooks AR. Flavivirus-induced antibody cross-reactivity. *J Gen Virol* 2011; **92**: 2821–9.

246. Murphy BR, Whitehead SS. Immune Response to Dengue Virus and Prospects for a Vaccine. *Annu Rev Immunol* 2011; **29**: 587–619.

247. Vratskikh O, Stiasny K, Zlatkovic J, Tsouchnikas G, Jarmer J, Karrer U, Roggendorf M, Roggendorf H, Allwinn R, Heinz FX. Dissection of Antibody Specificities Induced by Yellow Fever Vaccination. *PLoS Pathog* 2013; **9**:

e1003458.

248. Abbink P, Stephenson KE, Barouch DH. Zika virus vaccines. *Nat Rev Microbiol* 2018; **16**: 594–600.

249. Costa-Carvalho BT, Vieria HM, Dimantas RB, Arslanian C, Naspitz CK, Solé D, Carneiro-Sampaio MM. Transfer of IgG subclasses across placenta in term and preterm newborns. *Brazilian J Med Biol Res = Rev Bras Pesqui medicas e Biol* 1996; **29**: 201–4.

250. Stettler K, Beltramello M, Espinosa DA, Graham V, Cassotta A, Bianchi S, Vanzetta F, Minola A, Jaconi S, Mele F, Foglierini M, Pedotti M, Simonelli L, Dowall S, Atkinson B, Percivalle E, Simmons CP, Varani L, Blum J, Baldanti F, Cameroni E, Hewson R, Harris E, Lanzavecchia A, Sallusto F, Corti D. Specificity, cross-reactivity, and function of antibodies elicited by Zika virus infection. *Science* 2016; **353**: 823–6.

251. Priyamvada L, Quicke KM, Hudson WH, Onlamoon N, Sewatanon J, Edupuganti S, Pattanapanyasat K, Chokephaibulkit K, Mulligan MJ, Wilson PC, Ahmed R, Suthar MS, Wrammert J. Human antibody responses after dengue virus infection are highly cross-reactive to Zika virus. *Proc Natl Acad Sci U S A* 2016; **113**: 7852–7.

252. Premkumar L, Collins M, Graham S, Liou G-JA, Lopez CA, Jadi R, Balmaseda A, Brackbill JA, Dietze R, Camacho E, De Silva AD, Giuberti C, Dos Reis HL, Singh T, Heimsath H, Weiskopf D, Sette A, Osorio JE, Permar SR, Miley MJ, Lazear HM, Harris E, de Silva AM. Development of Envelope Protein Antigens To Serologically Differentiate Zika Virus Infection from Dengue Virus Infection. *J Clin Microbiol* 2018; **56**. DOI:10.1128/JCM.01504-17.

253. Halstead SB. Biologic Evidence Required for Zika Disease Enhancement by Dengue Antibodies. *Emerg Infect Dis* 2017; **23**: 569–73.

254. George J, Valiant WG, Mattapallil MJ, Walker M, Huang Y-JS, Vanlandingham DL, Misamore J, Greenhouse J, Weiss DE, Verthelyi D, Higgs S, Andersen H, Lewis MG, Mattapallil JJ. Prior Exposure to Zika Virus Significantly Enhances Peak Dengue-2 Viremia in Rhesus Macaques. *Sci Rep* 2017; **7**: 10498.

255. Montoya M, Collins M, Dejnirattisai W, Katzelnick LC, Puerta-Guardo H, Jadi R, Schildhauer S, Supasa P, Vasanawathana S, Malasit P, Mongkolsapaya J, de Silva AD, Tissera H, Balmaseda A, Screaton G, de Silva AM, Harris E. Longitudinal Analysis of Antibody Cross-neutralization Following Zika Virus and Dengue Virus Infection in Asia and the Americas. *J Infect Dis* 2018; **218**: 536–45.

256. Collins MH, McGowan E, Jadi R, Young E, Lopez CA, Baric RS, Lazear HM, de Silva AM. Lack of Durable Cross-Neutralizing Antibodies Against Zika Virus from Dengue Virus Infection. *Emerg Infect Dis* 2017; **23**: 773–81.

257. Halstead SB, Lan NT, Myint TT, Shwe TN, Nisalak A, Kalyanarooj S, Nimmannitya S, Soegijanto S, Vaughn DW, Endy TP. Dengue hemorrhagic fever in infants: research opportunities ignored. *Emerg Infect Dis* 2002; **8**: 1474–9.

258. Hammond SN, Balmaseda A, Pérez L, Tellez Y, Saborío SI, Mercado JC, Videa E, Rodriguez Y, Pérez MA, Cuadra R, Solano S, Rocha J, Idiaquez W, Gonzalez A, Harris E. Differences in dengue severity in infants, children, and adults in a 3-year hospital-based study in Nicaragua. *Am J Trop Med Hyg* 2005; **73**: 1063–70.

259. Simmons CP, Chau TNB, Thuy TT, Tuan NM, Hoang DM, Thien NT, Lien LB, Quy NT, Hieu NT, Hien TT, McElnea C, Young P, Whitehead S, Hung NT, Farrar J. Maternal Antibody and Viral Factors in the Pathogenesis of Dengue Virus in Infants. *J Infect Dis* 2007; **196**: 416–24.

260. Rodriguez-Barraquer I, Costa F, Nascimento EJM, Nery N, Castanha PMS, Sacramento GA, Cruz J, Carvalho M, De Olivera D, Hagan JE, Adhikarla H, Wunder EA, Coêlho DF, Azar SR, Rossi SL, Vasilakis N, Weaver SC, Ribeiro GS, Balmaseda A, Harris E, Nogueira ML, Reis MG, Marques ETA, Cummings DAT, Ko AI. Impact of preexisting dengue immunity on Zika virus emergence in a dengue endemic region. *Science* 2019; **363**: 607–10.

261. Kohler PF, Farr RS. Elevation of cord over maternal IgG immunoglobulin: evidence for an active placental IgG transport. *Nature* 1966; **210**: 1070–1.

262. Avanzini MA, Pignatti P, Chirico G, Gasparoni A, Jalil F, Hanson LA. Placental transfer favours high avidity IgG antibodies. *Acta Paediatr* 1998; **87**: 180–5.

263. Garty BZ, Ludomirsky A, Danon YL, Peter JB, Douglas SD. Placental transfer of immunoglobulin G subclasses. *Clin Diagn Lab Immunol* 1994; **1**: 667–9.

264. Martinez DR, Fouda GG, Peng X, Ackerman ME, Permar SR. Noncanonical placental Fc receptors: What is their role in modulating transplacental transfer of maternal IgG? *PLoS Pathog* 2018; **14**. DOI:10.1371/JOURNAL.PPAT.1007161.

265. Abu-Raya B, Smolen KK, Willems F, Kollmann TR, Marchant A. Transfer of Maternal Antimicrobial Immunity to HIV-Exposed Uninfected Newborns. *Front Immunol* 2016; **7**: 338.

266. Martinez DR, Fong Y, Li SH, Yang F, Jennewein MF, Weiner JA, Harrell EA, Mangold JF, Goswami R, Seage GR, Alter G, Ackerman ME, Peng X, Fouda GG, Permar SR. Fc Characteristics Mediate Selective Placental Transfer of IgG in HIV-Infected Women. *Cell* 2019; **178**: 190-201.e11.

267. Szaba FM, Tighe M, Kummer LW, Lanzer KG, Ward JM, Lanthier P, Kim I-J, Kuki A, Blackman MA, Thomas SJ, Lin J-S. Zika virus infection in immunocompetent pregnant mice causes fetal damage and placental pathology in the absence of fetal infection. *PLoS Pathog* 2018; **14**: e1006994.

268. Bhatnagar J, Rabeneck DB, Martines RB, Reagan-Steiner S, Ermias Y, Estetter LBC, Suzuki T, Ritter J, Keating MK, Hale G, Gary J, Muehlenbachs A, Lambert A, Lanciotti R, Oduyebo T, Meaney-Delman D, Bolaños F, Saad EAP, Shieh W-J, Zaki SR. Zika Virus RNA Replication and Persistence in Brain and Placental Tissue. *Emerg Infect Dis* 2017; **23**: 405–14.

269. Castanha PMS, Souza W V., Braga C, Araújo TVB de, Ximenes RAA, Albuquerque M de FPM, Montarroyos UR, Miranda-Filho DB, Cordeiro MT, Dhalia R, Marques ETA, Rodrigues LC, Martelli CMT, Microcephaly Epidemic Research Group. Perinatal analyses of Zika- and dengue virus-specific neutralizing antibodies: A microcephaly case-control study in an area of high dengue endemicity in Brazil. *PLoS Negl Trop Dis* 2019; **13**: e0007246.

270. Conheça cidades e estados do Brasil; Espirito Santo. https://cidades.ibge.gov.br/brasil/es (accessed Aug 20, 2007).

271. Brazilian Ministry of Health Database - DATASUS. http://tabnet.datasus.gov.br/cgi/tabcgi.exe?sinasc/cnv/nvuf.def (accessed July 9, 2018).

272. Secretaria de estado da saúde. Boletim Epidemiológico nº. 1 - 2016. Dengue, Chikungunya e Zika - Semana 13 - 2016. 2016.

273. Secretaria de Estado da Saúde divulga número de casos de Zika. 2015. http://www.saude.es.gov.br/default.asp (accessed Feb 16, 2019).

274. Zanluca C, Melo VCA de, Mosimann ALP, Santos GIV Dos, Santos CND Dos, Luz K. First report of autochthonous transmission of Zika virus in Brazil. *Mem Inst Oswaldo Cruz* 2015; **110**: 569–72.

275. Slon Campos JL, Mongkolsapaya J, Screaton GR. The immune response against flaviviruses. *Nat Immunol* 2018; **19**: 1189–98.

276. World Health Organization. Screening, assessment and management of neonates and infants with complications associated with Zika virus exposure in utero. 2017.

277. Villar J, Cheikh Ismail L, Victora CG, Ohuma EO, Bertino E, Altman DG, Lambert A, Papageorghiou AT, Carvalho M, Jaffer YA, Gravett MG, Purwar M, Frederick IO, Noble AJ, Pang R, Barros FC, Chumlea C, Bhutta ZA, Kennedy SH, International Fetal and Newborn Growth Consortium for the 21st Century (INTERGROWTH-21st). International standards for newborn weight, length, and head circumference by gestational age and sex: the Newborn Cross-Sectional Study of the INTERGROWTH-21st Project. *Lancet (London, England)* 2014; **384**: 857–68.

278. Lanciotti RS, Kosoy OL, Laven JJ, Velez JO, Lambert AJ, Johnson AJ, Stanfield SM, Duffy MR. Genetic and serologic properties of Zika virus associated with an epidemic, Yap State, Micronesia, 2007. *Emerg Infect Dis* 2008; **14**.

DOI:10.3201/eid1408.080287.

279. Martin DA, Muth DA, Brown T, Johnson AJ, Karabatsos N, Roehrig JT. Standardization of immunoglobulin M capture enzyme-linked immunosorbent assays for routine diagnosis of arboviral infections. *J Clin Microbiol* 2000; **38**: 1823–6.

280. Personal correspondence between Helen M. Lazear & Kenneth Plante. 2018.

281. Mayhew TM. Taking tissue samples from the placenta: an illustration of principles and strategies. *Placenta* 2008; **29**: 1–14.

282. Redline RW. Villitis of unknown etiology: noninfectious chronic villitis in the placenta. *Hum Pathol* 2007; **38**: 1439–46.

283. Knox WF, Fox H. Villitis of unknown aetiology: its incidence and significance in placentae from a British population. *Placenta*; **5**: 395–402.

284. Oliphant T, Nybakken GE, Engle M, Xu Q, Nelson CA, Sukupolvi-Petty S, Marri A, Lachmi B-E, Olshevsky U, Fremont DH, Pierson TC, Diamond MS. Antibody Recognition and Neutralization Determinants on Domains I and II of West Nile Virus Envelope Protein. *J Virol* 2006; **80**: 12149–59.

285. Itell HL, McGuire EP, Muresan P, Cunningham CK, McFarland EJ, Borkowsky W, Permar SR, Fouda GG. Development and application of a multiplex assay for the simultaneous measurement of antibody responses elicited by common childhood vaccines. *Vaccine* 2018; published online Aug 4. DOI:10.1016/j.vaccine.2018.07.048.

286. Oduyebo T, Polen KD, Walke HT, Reagan-Steiner S, Lathrop E, Rabe IB, Kuhnert-Tallman WL, Martin SW, Walker AT, Gregory CJ, Ades EW, Carroll DS, Rivera M, Perez-Padilla J, Gould C, Nemhauser JB, Ben Beard C, Harcourt JL, Viens L, Johansson M, Ellington SR, Petersen E, Smith LA, Reichard J, Munoz-Jordan J, Beach MJ, Rose DA, Barzilay E, Noonan-Smith M, Jamieson DJ, Zaki SR, Petersen LR, Honein MA, Meaney-Delman D. Update: Interim Guidance for Health Care Providers Caring for Pregnant Women with Possible Zika Virus Exposure — United States (Including U.S. Territories), July 2017. *MMWR Morb Mortal Wkly Rep* 2017; **66**: 781–93.

287. Wahala WMPB, de Silva AM. The Human Antibody Response to Dengue Virus Infection. *Viruses* 2011; **3**: 2374–95.

288. Liao HX, Levesque MC, Nagel A, Dixon A, Zhang R, Walter E, Parks R, Whitesides J, Marshall DJ, Hwang KK, Yang Y, Chen X, Gao F, Munshaw S, Kepler TB, Denny T, Moody MA, Haynes BF. High-throughput isolation of immunoglobulin genes from single human B cells and expression as monoclonal antibodies. *J Virol Methods* 2009; **158**: 171–9.

289. Kepler TB. Reconstructing a B-cell clonal lineage. I. Statistical inference of unobserved ancestors. *F1000Research* 2013; **2**: 103.

290. Liao HX, Chen X, Munshaw S, Zhang R, Marshall DJ, Vandergrift N, Whitesides JF, Lu X, Yu JS, Hwang KK, Gao F, Markowitz M, Heath SL, Bar KJ, Goepfert PA, Montefiori DC, Shaw GC, Alam SM, Margolis DM, Denny TN, Boyd SD, Marshal E, Egholm M, Simen BB, Hanczaruk B, Fire AZ, Voss G, Kelsoe G, Tomaras GD, Moody MA, Kepler TB, Haynes BF. Initial antibodies binding to HIV-1 gp41 in acutely infected subjects are polyreactive and highly mutated. *J Exp Med* 2011; **208**: 2237–49.

291. Carbaugh DL, Baric RS, Lazear HM. Envelope Protein Glycosylation Mediates Zika Virus Pathogenesis. *J Virol* 2019; **93**. DOI:10.1128/jvi.00113-19.

292. Nivarthi UK, Kose N, Sapparapu G, Widman D, Gallichotte E, Pfaff JM, Doranz BJ, Weiskopf D, Sette A, Durbin AP, Whitehead SS, Baric R, Crowe JE, de Silva AM. Mapping the Human Memory B Cell and Serum Neutralizing Antibody Responses to Dengue Virus Serotype 4 Infection and Vaccination. *J Virol* 2017; **91**: 2041–57.

293. Gallichotte EN, Widman DG, Yount BL, Wahala WM, Durbin A, Whitehead S, Sariol CA, Crowe JE, De Silva AM, Barica RS. A new quaternary structure epitope on dengue virus serotype 2 is the target of durable type-specific neutralizing antibodies. *MBio* 2015; **6**. DOI:10.1128/mBio.01461-15.

294. Patel B, Longo P, Miley MJ, Montoya M, Harris E, de Silva AM. Dissecting the human serum antibody response to secondary dengue virus infections. *PLoS Negl Trop Dis* 2017; **11**. DOI:10.1371/journal.pntd.0005554.

295. World Health Organization. Child Growth Standards. 2018. http://www.who.int/childgrowth/en/ (accessed June 19, 2019).

296. Tamblyn JA, Lissauer DM, Powell R, Cox P, Kilby MD. The immunological basis of villitis of unknown etiology - review. *Placenta* 2013; **34**: 846–55.

297. World Health Organization. Biologicals, Vaccine Standardization. 2019. http://www.who.int/biologicals/vaccines/en/ (accessed June 19, 2019).

298. Oliveira DBL, Almeida FJ, Durigon EL, Mendes ÉA, Braconi CT, Marchetti I, Andreata-Santos R, Cunha MP, Alves RPS, Pereira LR, Melo SR, Neto DFL, Mesquita FS, Araujo DB, Favoretto SR, Sáfadi MAP, Ferreira LCS, Zanotto PMA, Botosso VF, Berezin EN. Prolonged Shedding of Zika Virus Associated with Congenital Infection. *N Engl J Med* 2016; **375**: 1202–4.

299. Nguyen SM, Antony KM, Dudley DM, Kohn S, Simmons HA, Wolfe B, Salamat MS, Teixeira LBC, Wiepz GJ, Thoong TH, Aliota MT, Weiler AM, Barry GL, Weisgrau KL, Vosler LJ, Mohns MS, Breitbach ME, Stewart LM, Rasheed MN, Newman CM, Graham ME, Wieben OE, Turski PA, Johnson KM, Post J, Hayes

JM, Schultz-Darken N, Schotzko ML, Eudailey JA, Permar SR, Rakasz EG, Mohr EL, Capuano S, Tarantal AF, Osorio JE, O'Connor SL, Friedrich TC, O'Connor DH, Golos TG. Highly efficient maternal-fetal Zika virus transmission in pregnant rhesus macaques. *PLOS Pathog* 2017; **13**: e1006378.

300. Magnani DM, Rogers TF, Maness NJ, Grubaugh ND, Beutler N, Bailey VK, Gonzalez-Nieto L, Gutman MJ, Pedreño-Lopez N, Kwal JM, Ricciardi MJ, Myers TA, Julander JG, Bohm RP, Gilbert MH, Schiro F, Aye PP, Blair R V., Martins MA, Falkenstein KP, Kaur A, Curry CL, Kallas EG, Desrosiers RC, Goldschmidt-Clermont PJ, Whitehead SS, Andersen KG, Bonaldo MC, Lackner AA, Panganiban AT, Burton DR, Watkins DI. Fetal demise and failed antibody therapy during Zika virus infection of pregnant macaques. *Nat Commun* 2018; **9**: 1624.

301. Andersen JT, Daba MB, Berntzen G, Michaelsen TE, Sandlie I. Cross-species binding analyses of mouse and human neonatal Fc receptor show dramatic differences in immunoglobulin G and albumin binding. *J Biol Chem* 2010; **285**: 4826–36.

302. Wilcox CR, Holder B, Jones CE. Factors Affecting the FcRn-Mediated Transplacental Transfer of Antibodies and Implications for Vaccination in Pregnancy. *Front Immunol* 2017; **8**: 1294.

303. Palmeira P, Quinello C, Silveira-Lessa AL, Zago CA, Carneiro-Sampaio M. IgG placental transfer in healthy and pathological pregnancies. *Clin Dev Immunol* 2012; **2012**: 985646.

304. Pou C, Nkulikiyimfura D, Henckel E, Olin A, Lakshmikanth T, Mikes J, Wang J, Chen Y, Bernhardsson AK, Gustafsson A, Bohlin K, Brodin P. The repertoire of maternal anti-viral antibodies in human newborns. *Nat Med* 2019; **25**: 591–6.

305. Collier A ris Y, Borducchi EN, Chandrashekar A, Moseley E, Peter L, Teodoro NS, Nkolola J, Abbink P, Barouch DH. Sustained maternal antibody and cellular immune responses in pregnant women infected with Zika virus and mother to infant transfer of Zika-specific antibodies. *Am J Reprod Immunol* 2020; **84**: e13288.

306. Russell P. Inflammatory lesions of the human placenta. III. The histopathology of villitis of unknown aetiology. *Placenta*; **1**: 227–44.

307. Larocca RA, Abbink P, Peron JPS, de A. Zanotto PM, Iampietro MJ, Badamchi-Zadeh A, Boyd M, Ng'ang'a D, Kirilova M, Nityanandam R, Mercado NB, Li Z, Moseley ET, Bricault CA, Borducchi EN, Giglio PB, Jetton D, Neubauer G, Nkolola JP, Maxfield LF, De La Barrera RA, Jarman RG, Eckels KH, Michael NL, Thomas SJ, Barouch DH. Vaccine protection against Zika virus from Brazil. *Nature* 2016; **536**: 474–8.

308. Dowd KA, Ko S-Y, Morabito KM, Yang ES, Pelc RS, DeMaso CR, Castilho LR, Abbink P, Boyd M, Nityanandam R, Gordon DN, Gallagher JR, Chen X, Todd J-P,

Tsybovsky Y, Harris A, Huang Y-JS, Higgs S, Vanlandingham DL, Andersen H, Lewis MG, De La Barrera R, Eckels KH, Jarman RG, Nason MC, Barouch DH, Roederer M, Kong W-P, Mascola JR, Pierson TC, Graham BS. Rapid development of a DNA vaccine for Zika virus. *Science* 2016; **354**: 237–40.

309. Plotkin SA. Correlates of protection induced by vaccination. *Clin Vaccine Immunol* 2010; **17**: 1055–65.

310. Hombach J, Solomon T, Kurane I, Jacobson J, Wood D. Report on a WHO consultation on immunological endpoints for evaluation of new Japanese encephalitis vaccines, WHO, Geneva, 2-3 September, 2004. *Vaccine* 2005; **23**: 5205–11.

311. Mason RA, Tauraso NM, Spertzel RO, Ginn RK. Yellow fever vaccine: direct challenge of monkeys given graded doses of 17D vaccine. *Appl Microbiol* 1973; **25**: 539–44.

312. Kreil TR, Burger I, Bachmann M, Fraiss S, Eibl MM. Antibodies protect mice against challenge with tick-borne encephalitis virus (TBEV)-infected macrophages. *Clin Exp Immunol* 1997; **110**: 358–61.

313. Hermanns K, Göhner C, Kopp A, Schmidt A, Merz WM, Markert UR, Junglen S, Drosten C. Zika virus infection in human placental tissue explants is enhanced in the presence of dengue virus antibodies in-vitro. *Emerg Microbes Infect* 2018; **7**: 1–8.

314. Zimmerman MG, Quicke KM, O'Neal JT, Arora N, Machiah D, Priyamvada L, Kauffman RC, Register E, Adekunle O, Swieboda D, Johnson EL, Cordes S, Haddad L, Chakraborty R, Coyne CB, Wrammert J, Suthar MS. Cross-Reactive Dengue Virus Antibodies Augment Zika Virus Infection of Human Placental Macrophages. *Cell Host Microbe* 2018; **24**: 731-742.e6.

315. Omer SB. Maternal Immunization. *N Engl J Med* 2017; **376**: 1256–67.

316. Paixao ES, Leong W-Y, Rodrigues LC, Wilder-Smith A. Asymptomatic Prenatal Zika Virus Infection and Congenital Zika Syndrome. *Open Forum Infect Dis* 2018; **5**: ofy073.

317. Duffy MR, Chen T-H, Hancock WT, Powers AM, Kool JL, Lanciotti RS, Pretrick M, Marfel M, Holzbauer S, Dubray C, Guillaumot L, Griggs A, Bel M, Lambert AJ, Laven J, Kosoy O, Panella A, Biggerstaff BJ, Fischer M, Hayes EB. Zika Virus Outbreak on Yap Island, Federated States of Micronesia. *N Engl J Med* 2009; **360**: 2536–43.

318. Mitchell PK, Mier-Y-Teran-Romero L, Biggerstaff BJ, Delorey MJ, Aubry M, Cao-Lormeau V-M, Lozier MJ, Cauchemez S, Johansson MA. Reassessing Serosurvey-Based Estimates of the Symptomatic Proportion of Zika Virus Infections. *Am J Epidemiol* 2019; **188**: 206–13.

319. Stapleton NM, Brinkhaus M, Armour KL, Bentlage AEH, de Taeye SW, Temming AR, Mok JY, Brasser G, Maas M, van Esch WJE, Clark MR, Williamson LM, van der Schoot CE, Vidarsson G. Reduced FcRn-mediated transcytosis of IgG2 due to a missing Glycine in its lower hinge. *Sci Rep* 2019; **9**: 1–10.

320. Kim J -K, Tsen M -F, Ghetie V, Ward ES. Localization of the site of the murine IgG1 molecule that is involved in binding to the murine intestinal Fc receptor. *Eur J Immunol* 1994; **24**: 2429–34.

321. Pierson TC, Diamond MS. The continued threat of emerging flaviviruses. Nat. Microbiol. 2020; **5**: 796–812.

322. Blitvich BJ, Magalhaes T, Viridiana Laredo-Tiscareño S, Foy BD. Sexual Transmission of Arboviruses: A Systematic Review. Viruses. 2020; **12**. DOI:10.3390/v12090933.

323. Foy BD, Kobylinski KC, Foy JLC, Blitvich BJ, Travassos da Rosa A, Haddow AD, Lanciotti RS, Tesh RB. Probable Non–Vector-borne Transmission of Zika Virus, Colorado, USA. *Emerg Infect Dis* 2011; **17**: 880–2.

324. Moreira J, Peixoto TM, Siqueira AM, Lamas CC. Sexually acquired Zika virus: a systematic review. Clin. Microbiol. Infect. 2017; **23**: 296–305.

325. Armstrong P, Hennessey M, Adams M, Cherry C, Chiu S, Harrist A, Kwit N, Lewis L, McGuire DO, Oduyebo T, Russell K, Talley P, Tanner M, Williams C. Travel-Associated Zika Virus Disease Cases Among U.S. Residents — United States, January 2015–February 2016. *MMWR Morb Mortal Wkly Rep* 2016; **65**: 286–9.

326. Venturi G, Zammarchi L, Fortuna C, Remoli ME, Benedetti E, Fiorentini C, Trotta M, Rizzo C, Mantella A, Rezza G, Bartoloni A. An autochthonous case of zika due to possible sexual transmission, Florence, Italy, 2014. *Eurosurveillance* 2016; **21**: 1–4.

327. Gregory CJ, Oduyebo T, Brault AC, Brooks JT, Chung KW, Hills S, Kuehnert MJ, Mead P, Meaney-Delman D, Rabe I, Staples E, Petersen LR. Modes of Transmission of Zika Virus. J. Infect. Dis. 2017; **216**: S875–83.

328. 2016 Case Counts in the US | Zika Virus | CDC. https://www.cdc.gov/zika/reporting/2016-case-counts.html (accessed Nov 12, 2020).

329. Ding Q, Gaska JM, Douam F, Wei L, Kim D, Balev M, Heller B, Ploss A. Species-specific disruption of STING-dependent antiviral cellular defenses by the Zika virus NS2B3 protease. *Proc Natl Acad Sci U S A* 2018; **115**: E6310–8.

330. Uraki R, Jurado KA, Hwang J, Szigeti-Buck K, Horvath TL, Iwasaki A, Fikrig E. Fetal Growth Restriction Caused by Sexual Transmission of Zika Virus in Mice. *J Infect Dis* 2017; **215**: 1720–4.

331. Baronti C, Piorkowski G, Charrel RN, Boubis L, Leparc-Goffart I, de Lamballerie X. Complete coding sequence of Zika virus from a French Polynesia outbreak in 2013. *Genome Announc* 2014; **2**: 500–14.

332. Kokernot RH, Smithburn KC, Muspratt J, Hodgson B. Studies on arthropod-borne viruses of Tongaland. VIII. Spondweni virus, an agent previously unknown, isolated from Taeniorhynchus (Mansonioides) uniformis. *S Afr J Med Sci* 1957; **22**: 103–22.

333. Williams MC. The isolation of West Nile virus from man and of Usutu virus from the bird-eating mosquito Mansonia aurites (Theobald) in the Entebbe area of Uganda. *Ann Trop Med Parasitol* 1964; **58**: 367–74.

334. Kraus AA, Messer W, Haymore LB, De Silva AM. Comparison of plaque- and flow cytometry-based methods for measuring dengue virus neutralization. *J Clin Microbiol* 2007; **45**: 3777–80.

335. Osatomi K, Sumiyoshi H. Complete nucleotide sequence of dengue type 3 virus genome RNA. *Virology* 1990; **176**: 643–7.

336. Mangala Prasad V, Klose T, Rossmann MG. Assembly, maturation and three-dimensional helical structure of the teratogenic rubella virus. *PLoS Pathog* 2017; **13**. DOI:10.1371/journal.ppat.1006377.

337. Hirai-Yuki A, Hensley L, McGivern DR, González-López O, Das A, Feng H, Sun L, Wilson JE, Hu F, Feng Z, Lovell W, Misumi I, Ting JPY, Montgomery S, Cullen J, Whitmire JK, Lemon SM. MAVS-dependent host species range and pathogenicity of human hepatitis A virus. *Science (80-)* 2016; **353**: 1541–5.

338. Brien JD, Lazear HM, Diamond MS. Propagation, quantification, detection, and storage of west nile virus. *Curr Protoc Microbiol* 2013; **31**. DOI:10.1002/9780471729259.mc15d03s31.

339. Lazear E, Whitbeck JC, Ponce-de-Leon M, Cairns TM, Willis SH, Zuo Y, Krummenacher C, Cohen GH, Eisenberg RJ. Antibody-Induced Conformational Changes in Herpes Simplex Virus Glycoprotein gD Reveal New Targets for Virus Neutralization. *J Virol* 2012; **86**: 1563–76.

340. Rux JJ, Willis SH, Burnett RM, Cohen GH, Eisenberg RJ. Crystallization and preliminary X-ray analysis of herpes simplex virus neutralizing antibody Fab fragment DL11. *Acta Crystallogr Sect D Biol Crystallogr* 1996; **52**: 583–5.

341. Oh JE, Iijima N, Song E, Lu P, Klein J, Jiang R, Kleinstein SH, Iwasaki A. Migrant memory B cells secrete luminal antibody in the vagina. *Nature* 2019; **571**: 122–6.

342. Singh T, Lopez CA, Giuberti C, Dennis ML, Itell HL, Heimsath HJ, Webster HS, Roark HK, Merçon de Vargas PR, Hall A, Corey RG, Swamy GK, Dietze R, Lazear HM, Permar SR. Efficient transplacental IgG transfer in women infected

with Zika virus during pregnancy. *PLoS Negl Trop Dis* 2019; **13**: e0007648.

343. Cao B, Parnell LA, Diamond MS, Mysorekar IU. Inhibition of autophagy limits vertical transmission of Zika virus in pregnant mice. *J Exp Med* 2017; **214**: 2303–13.

344. McKinley SA, Chen A, Shi F, Wang S, Mucha PJ, Forest MG, Lai SK. Modeling neutralization kinetics of HIV by broadly neutralizing monoclonal antibodies in genital secretions coating the cervicovaginal mucosa. *PLoS One* 2014; **9**. DOI:10.1371/journal.pone.0100598.

345. Pessina MA, Hoyt RF, Goldstein I, Traish AM. Differential Effects of Estradiol, Progesterone, and Testosterone on Vaginal Structural Integrity. *Endocrinology* 2006; **147**: 61–9.

346. Magalhaes T, Morais CNL, Jacques IJAA, Azevedo EAN, Brito AM, Lima P V, Carvalho GMM, Lima ARS, Castanha PMS, Cordeiro MT, Oliveira ALS, Jaenisch T, Lamb MM, Marques ETA, Foy BD. Follow-Up Household Serosurvey in Northeast Brazil for Zika Virus: Sexual Contacts of Index Patients Have the Highest Risk for Seropositivity. *J Infect Dis* 2020; published online Sept 5. DOI:10.1093/infdis/jiaa563.

347. Lai SK, Hida K, Shukair S, Wang Y-Y, Figueiredo A, Cone R, Hope TJ, Hanes J. Human Immunodeficiency Virus Type 1 Is Trapped by Acidic but Not by Neutralized Human Cervicovaginal Mucus. *J Virol* 2009; **83**: 11196–200.

348. Gorman MJ, Caine EA, Zaitsev K, Begley MC, Weger-Lucarelli J, Uccellini MB, Tripathi S, Morrison J, Yount BL, Dinnon KH, Rückert C, Young MC, Zhu Z, Robertson SJ, McNally KL, Ye J, Cao B, Mysorekar IU, Ebel GD, Baric RS, Best SM, Artyomov MN, Garcia-Sastre A, Diamond MS. An Immunocompetent Mouse Model of Zika Virus Infection. *Cell Host Microbe* 2018; **23**: 672-685.e6.

349. Bhatt S, Gething PW, Brady OJ, Messina JP, Farlow AW, Moyes CL, Drake JM, Brownstein JS, Hoen AG, Sankoh O, Myers MF, George DB, Jaenisch T, William Wint GR, Simmons CP, Scott TW, Farrar JJ, Hay SI. The global distribution and burden of dengue. *Nature* 2013; **496**: 504–7.

350. Lee C, Lee H. Probable female to male sexual transmission of dengue virus infection. Infect. Dis. (Auckl). 2019; **51**: 150–2.

351. World Health Organization. Dengue fever –Spain. WHO. 2019; published online Nov 29. https://www.who.int/csr/don/29-november-2019-dengue-spain/en/ (accessed April 26, 2021).

352. Alvarez D, Vollmann EH, von Andrian UH. Mechanisms and Consequences of Dendritic Cell Migration. Immunity. 2008; **29**: 325–42.

353. Home - Johns Hopkins Coronavirus Resource Center. 2020.

https://coronavirus.jhu.edu/ (accessed April 16, 2021).

354. Havers FP, Reed C, Lim T, Montgomery JM, Klena JD, Hall AJ, Fry AM, Cannon DL, Chiang CF, Gibbons A, Krapiunaya I, Morales-Betoulle M, Roguski K, Rasheed MAU, Freeman B, Lester S, Mills L, Carroll DS, Owen SM, Johnson JA, Semenova V, Blackmore C, Blog D, Chai SJ, Dunn A, Hand J, Jain S, Lindquist S, Lynfield R, Pritchard S, Sokol T, Sosa L, Turabelidze G, Watkins SM, Wiesman J, Williams RW, Yendell S, Schiffer J, Thornburg NJ. Seroprevalence of Antibodies to SARS-CoV-2 in 10 Sites in the United States, March 23-May 12, 2020. *JAMA Intern Med* 2020. DOI:10.1001/jamainternmed.2020.4130.

355. Anand S, Montez-Rath M, Han J, Bozeman J, Kerschmann R, Beyer P, Parsonnet J, Chertow GM. Prevalence of SARS-CoV-2 antibodies in a large nationwide sample of patients on dialysis in the USA: a cross-sectional study. *Lancet* 2020; **0**. DOI:10.1016/S0140-6736(20)32009-2.

356. Rogawski McQuade ET, Guertin KA, Becker L, Operario D, Gratz J, Guan D, Khan F, White J, McMurry TL, Shah B, Garofalo S, Southerland M, Bear K, Brush J, Allen C, Frayser A, Vokes R, Pershad R, Peake L, deFilippi C, Barackman K, Bearman G, Bidanset A, Farrell F, Trump D, Houpt ER. Assessment of Seroprevalence of SARS-CoV-2 and Risk Factors Associated With COVID-19 Infection Among Outpatients in Virginia. *JAMA Netw open* 2021; **4**: e2035234.

357. Feehan AK, Velasco C, Fort D, Burton JH, Price-Haywood EG, Katzmarzyk PT, Garcia-Diaz J, Seoane L. Racial and workplace disparities in seroprevalence of SARS-CoV-2, Baton Rouge, Louisiana, USA. *Emerg Infect Dis* 2021; **27**: 314–7.

358. Bailey ZD, Feldman JM, Bassett MT. How Structural Racism Works — Racist Policies as a Root Cause of U.S. Racial Health Inequities. *N Engl J Med* 2020; **384**: 768–73.

359. US Census Bureau. American Community Survey 5-Year Data (2014-2018). 2019.

360. Data Behind the Dashboards: NC DHHS COVID-19. https://covid19.ncdhhs.gov/dashboard/data-behind-dashboards (accessed Feb 13, 2021).

361. Premkumar L, Segovia-Chumbez B, Jadi R, Martinez DR, Raut R, Markmann A, Cornaby C, Bartelt L, Weiss S, Park Y, Edwards CE, Weimer E, Scherer EM, Rouphael N, Edupuganti S, Weiskopf D, Tse L V., Hou YJ, Margolis D, Sette A, Collins MH, Schmitz J, Baric RS, Silva AM de. The receptor binding domain of the viral spike protein is an immunodominant and highly specific target of antibodies in SARS-CoV-2 patients. *Sci Immunol* 2020; **5**: eabc8413.

362. Zhang L, Zhang JJ, Kubiak RJ, Yang H. Statistical methods and tool for cut point analysis in immunogenicity assays. *J Immunol Methods* 2013; **389**: 79–87.

363. Centers for Disease Control and Prevention. Interim Guidelines for COVID-19 Antibody Testing | CDC. 2020; published online Aug 1. https://www.cdc.gov/coronavirus/2019-ncov/lab/resources/antibody-tests-guidelines.html (accessed Feb 26, 2021).

364. Markmann AJ, Giallourou N, Ryan Bhowmik D, Hou YJ, Martinez DR, Premkumar L, Root H, van Duin D, Graham SD, Guerra Q, Raut R, Petropoulos CJ, Wrin T, Cornaby C, Schmitz J, Kuruc J, Weiss S, Park Y, de Silva AM, Margolis DM, Bartelt LA. Sex disparities and neutralizing antibody durability to SARS-CoV-2 infection in convalescent individuals. *medRxiv* 2021; : 2021.02.01.21250493.

365. Hou YJ, Okuda K, Edwards CE, Martinez DR, Asakura T, Dinnon KH, Kato T, Lee RE, Yount BL, Mascenik TM, Chen G, Olivier KN, Ghio A, Tse L V., Leist SR, Gralinski LE, Schäfer A, Dang H, Gilmore R, Nakano S, Sun L, Fulcher ML, Livraghi-Butrico A, Nicely NI, Cameron M, Cameron C, Kelvin DJ, de Silva A, Margolis DM, Markmann A, Bartelt L, Zumwalt R, Martinez FJ, Salvatore SP, Borczuk A, Tata PR, Sontake V, Kimple A, Jaspers I, O'Neal WK, Randell SH, Boucher RC, Baric RS. SARS-CoV-2 Reverse Genetics Reveals a Variable Infection Gradient in the Respiratory Tract. *Cell* 2020; published online May 27. DOI:10.1016/j.cell.2020.05.042.

366. Williams DR, Mohammed SA, Leavell J, Collins C. Race, socioeconomic status, and health: Complexities, ongoing challenges, and research opportunities. *Ann N Y Acad Sci* 2010; **1186**: 69–101.

367. Guidotti-Hernández NM. Affective communities and millennial desires: Latinx, or why my computer won't recognize Latina/o. *Cult Dyn* 2017; **29**: 141–59.

368. Ripperger TJ, Uhrlaub JL, Watanabe M, Wong R, Castaneda Y, Pizzato HA, Thompson MR, Bradshaw C, Weinkauf CC, Bime C, Erickson HL, Knox K, Bixby B, Parthasarathy S, Chaudhary S, Natt B, Cristan E, El Aini T, Rischard F, Campion J, Chopra M, Insel M, Sam A, Knepler JL, Capaldi AP, Spier CM, Dake MD, Edwards T, Kaplan ME, Scott SJ, Hypes C, Mosier J, Harris DT, LaFleur BJ, Sprissler R, Nikolich-Žugich J, Bhattacharya D. Orthogonal SARS-CoV-2 Serological Assays Enable Surveillance of Low-Prevalence Communities and Reveal Durable Humoral Immunity. *Immunity* 2020; **53**: 925-933.e4.

369. Hagan LM, Williams SP, Spaulding AC, Toblin RL, Figlenski J, Ocampo J, Ross T, Bauer H, Hutchinson J, Lucas KD, Zahn M, Chiang C, Collins T, Burakoff A, Bettridge J, Stringer G, Maul R, Waters K, Dewart C, Clayton J, de Fijter S, Sadacharan R, Garcia L, Lockett N, Short K, Sunder L, Handanagic S. Mass Testing for SARS-CoV-2 in 16 Prisons and Jails — Six Jurisdictions, United States, April–May 2020. *MMWR Morb Mortal Wkly Rep* 2020; **69**: 1139–43.

370. Webb Hooper M, Nápoles AM, Pérez-Stable EJ. COVID-19 and Racial/Ethnic Disparities. JAMA - J. Am. Med. Assoc. 2020; **323**: 2466–7.

371. Figueroa JF, Wadhera RK, Lee D, Yeh RW, Sommers BD. Community-Level

Factors Associated With Racial And Ethnic Disparities In COVID-19 Rates In Massachusetts. *Health Aff* 2020; **39**: 1984–92.

372. Berchick ER, Barnett JC, Upton RD. Health Insurance Coverage in the United States: 2018 Current Population Reports. 2019.

373. Long QX, Tang XJ, Shi QL, Li Q, Deng HJ, Yuan J, Hu JL, Xu W, Zhang Y, Lv FJ, Su K, Zhang F, Gong J, Wu B, Liu XM, Li JJ, Qiu JF, Chen J, Huang AL. Clinical and immunological assessment of asymptomatic SARS-CoV-2 infections. *Nat Med* 2020; **26**: 1200–4.

374. Diamond M, Chen R, Xie X, Case J, Zhang X, VanBlargan L, Liu Y, Liu J, Errico J, Winkler E, Suryadevara N, Tahan S, Turner J, Kim W, Schmitz A, Thapa M, Wang D, Boon A, Pinto D, Presti R, Oâ Halloran J, Kim A, Deepak P, Fremont D, Corti D, Virgin H, Crowe J, Droit L, Ellebedy A, Shi P-Y, Gilchuk P. SARS-CoV-2 variants show resistance to neutralization by many monoclonal and serum-derived polyclonal antibodies. *Res Sq* 2021; published online Feb 10. DOI:10.21203/rs.3.rs-228079/v1.

375. Hughes BW, Addanki KC, Sriskanda AN, McLean E, Bagasra O. Infectivity of Immature Neurons to Zika Virus: A Link to Congenital Zika Syndrome. *EBioMedicine* 2016; **10**: 65–70.

376. Edlow AG, Li JZ, Collier ARY, Atyeo C, James KE, Boatin AA, Gray KJ, Bordt EA, Shook LL, Yonker LM, Fasano A, Diouf K, Croul N, Devane S, Yockey LJ, Lima R, Shui J, Matute JD, Lerou PH, Akinwunmi BO, Schmidt A, Feldman J, Hauser BM, Caradonna TM, De la Flor D, D'Avino P, Regan J, Corry H, Coxen K, Fajnzylber J, Pepin D, Seaman MS, Barouch DH, Walker BD, Yu XG, Kaimal AJ, Roberts DJ, Alter G. Assessment of Maternal and Neonatal SARS-CoV-2 Viral Load, Transplacental Antibody Transfer, and Placental Pathology in Pregnancies During the COVID-19 Pandemic. *JAMA Netw open* 2020; **3**: e2030455.

377. Atyeo C, Pullen KM, Bordt EA, Fischinger S, Burke J, Michell A, Slein MD, Loos C, Shook LL, Boatin AA, Yockey LJ, Pepin D, Meinsohn MC, Nguyen NMP, Chauvin M, Roberts D, Goldfarb IT, Matute JD, James KE, Yonker LM, Bebell LM, Kaimal AJ, Gray KJ, Lauffenburger D, Edlow AG, Alter G. Compromised SARS-CoV-2-specific placental antibody transfer. *Cell* 2021; **184**: 628-642.e10.

378. Thulin NK, Brewer RC, Sherwood R, Bournazos S, Edwards KG, Ramadoss NS, Taubenberger JK, Memoli M, Gentles AJ, Jagannathan P, Zhang S, Libraty DH, Wang TT. Maternal Anti-Dengue IgG Fucosylation Predicts Susceptibility to Dengue Disease in Infants. *Cell Rep* 2020; **31**: 107642.

379. Musso D, Roche C, Robin E, Nhan T, Teissier A, Cao-Lormeau VM. Potential sexual transmission of zika virus. *Emerg Infect Dis* 2015; **21**: 359–61.

380. Atkinson B, Hearn P, Afrough B, Lumley S, Carter D, Aarons EJ, Simpson AJ, Brooks TJ, Hewson R. Detection of zika virus in semen. Emerg. Infect. Dis. 2016;

22: 940.

381. Yao XD, Fernandez S, Kelly MM, Kaushic C, Rosenthal KL. Expression of Toll-like receptors in murine vaginal epithelium is affected by the estrous cycle and stromal cells. *J Reprod Immunol* 2007; **75**: 106–19.

382. Premkumar L, Segovia-Chumbez B, Jadi R, Martinez DR, Raut R, Markmann A, Cornaby C, Bartelt L, Weiss S, Park Y, Edwards CE, Weimer E, Scherer EM, Roupael N, Edupuganti S, Weiskopf D, Tse L V., Hou YJ, Margolis D, Sette A, Collins MH, Schmitz J, Baric RS, Silva AM de. The RBD Of The Spike Protein Of SARS-Group Coronaviruses Is A Highly Specific Target Of SARS-CoV-2 Antibodies But Not Other Pathogenic Human and Animal Coronavirus Antibodies. *medRxiv* 2020; : 2020.05.06.20093377.

383. Haddow AD, Nalca A, Rossi FD, Miller LJ, Wiley MR, Perez-Sautu U, Washington SC, Norris SL, Wollen-Roberts SE, Shamblin JD, Kimmel AE, Bloomfield HA, Valdez SM, Sprague TR, Principe LM, Bellanca SA, Cinkovich SS, Lugo-Roman L, Cazares LH, Pratt WD, Palacios GF, Bavari S, Pitt ML, Nasar F. High infection rates for adult macaques after intravaginal or intrarectal inoculation with zika virus. *Emerg Infect Dis* 2017; **23**: 1274–81.

384. Infrastructure inequality is catalyst for Brazil's Zika epidemic | Reuters. https://www.reuters.com/article/us-health-zika-inequality-insight/infrastructure-inequality-is-catalyst-for-brazils-zika-epidemic-idUSKCN0WH0EH (accessed June 3, 2021).